SCT Report No. 4520-280-1

July 1991

APPLICATION OF MODERN CONTROL DESIGN METHODOLOGY TO OBLIQUE WING RESEARCH AIRCRAFT

Prepared by:

James H. Vincent

Prepared for:

NAVAL AIR TEST CENTER
NAS Patuxent River, Maryland 20670

Under Contract No. N00421-85-D-0155
Deliver Order 0028

TABLE OF CONTENTS

TABLE OF CONTENTS (Continued)

FOREWORD

This research program was sponsored by the Naval Air Systems Command through the Naval Air Test Center (NATC), NAS Patuxent River, MD, under Contract No. 00421-D-0155, Delivery Order No. 0028. This program was jointly sponsored by the NASA Dryden Flight Research Facility. The NATC project manager was Mr. William McNamara. Mr. Glenn Gilyard from NASA Dryden provided technical support for this project.

Systems Control Technology, Inc. (SCT) staff supporting this project included Mr. Uri Rabin and Ms. Michael-Clare Walker. Mr. Rabin developed the linear state models which were used for the design and he participated in the early stages of the design process. He developed many of the Ctrl-C® design procedures which were used to automate the design process. Ms Walker provided technical publication support.

I. INTRODUCTION

1.1 PROJECT OVERVIEW

The U.S. Navy in conjunction with the NASA Ames Research Center worked jointly to develop a supersonic oblique wing research aircraft (OWRA). A major requirement of the OWRA research program is the synthesis of flight control laws that stabilize and decouple the oblique wing aircraft with its inherent highly coupled, lightly damped motion. The control laws must also provide acceptable handling qualities throughout the Mach number (subsonic and supersonic), angle of attack, load factor and wing skew flight envelope. A major goal of the OWRA program is to compare various advanced control law design methodologies via analysis and pilot in-the-loop simulation.

The goal of the research program described by this report is to explore the application of multivariable, explicit model-following control system design techniques to the synthesis of control laws for the OWRA. SCT was tasked to investigate the application of these techniques. Major design considerations included: (1) methodology for directly incorporating flying quality criteria into a linear quadratic regulator design, (2) methodology for designing a control law that decouples the aircraft's response to pilot commands and also provides attenuation to disturbances and (3) methodology to provide gain scheduling to accommodate changes in flight Mach number, altitude and wing skew position.

Table 1.1 provides a specification of the nine flight conditions included for the design.

Table 1.1
Flight Control Law Design Points

Flight Cond No	Altitude (ft)	Mach No	Wing Skew (deg)	Load Factor
1	20,000	0.8	45	1
2	20,000	0.8	55	1
3	20,000	0.8	65	1
4	29,000	0.8	55	1
5	29,000	1.2	55	1
6	29,000	1.4	55	1
7	34,000	0.9	65	1
8	34,000	1.2	65	1
9	34,000	1.6	65	1

This design study included a number of specific items:

- Design and evaluation of control laws at each of the nine flight conditions.
- Development of a gain scheduling strategy to combine the nine individual designs into a unified control law that could operate throughout the range of Mach number, altitude and wing skew combinations that comprise the OWRA's operational flight envelope.
- Evaluation of the robustness of the linearized control laws at the nine design conditions.
- Documentation of the strengths and weaknesses of the selected design methodology for incorporating flying quality requirements and for providing decoupled control.

1.2 BACKGROUND

1.2.1 OWRA Flight Demonstrator Program

Oblique-wing airplanes have advantages for many missions, both military and civilian [1]. For missions that require both long subsonic range and endurance and a good supersonic dash capability, an oblique-wing design will have lower wave drag, lower structural weight, and reduced ground storage area when compared with other variable geometry configuration. Analytic studies, wind tunnel tests, and low-speed lightweight aircraft flight tests have been conducted, but as yet no high-performance demonstrator or operational aircraft has been developed due to the high risk inherent in such a departure from conventional designs [2]. Recent advances in composite structural technology make it possible to tailor oblique-wing panels for multiple flight-operating conditions while retaining the weight advantages of new materials.

The NASA Ames Research Center, Moffett Field (Ames-Moffett) and Dryden Flight Research Facility (Ames-Dryden), Edwards, California, in conjunction with the U.S. Navy, developed designs for an oblique wing research airplane (OWRA) demonstrator [3]. NASA's F-8 digital-fly-by-wire airplane was targeted to be modified for the oblique-wing demonstrator. Synthesis of a flight control system that provides both acceptable vehicle stabilization and handling qualities across the Mach number-altitude, angle of attack, and wing skew flight envelope was a major goal of the U.S. Navy / NASA program .

The advantages of an oblique wing cannot be obtained without overcoming many design challenges. Oblique-wing airplanes show large cross-coupling in control response and dynamic behavior which is not present in conventional symmetric airplanes. The open-loop cross-coupling of the OWRA is characterized as a relatively large roll and lateral acceleration coupling with pitch command inputs and pitch coupling with roll command inputs.

1.2.2 OWRA Controls Technology Research

Development of a flight control system that provides excellent flying qualities for an aircraft such as the OWRA represents a significant design challenge. Multivariable synthesis techniques are preferred because the OWRA has significant coupling between the longitudinal and lateral-directional degrees of freedom. This coupling arises from both aerodynamic and inertial cross-coupling sources. Several research studies have been sponsored to look at applying different multivariable synthesis techniques to the task of designing a decoupled flight control system for the OWRA. This section provides a summary of several research programs that addressed flight control design issues for the OWRA. The next section summarizes a simulation study that investigated one of the flight control system designs.

Alag, Kemple and Pahle [8] developed control laws for the OWRA by using an eigensystem synthesis technique. For their method, desired frequency and damping properties, as dictated by the design handling qualities criteria, were used to determine desired eigenvalue locations. Selection of the desired eigenvectors was based on desired modal response characteristics. The task of relating eigenvectors to handling qualities criteria was not presented in referenced paper. The eigensystem synthesis methodology was used to determine a state feedback gain matrix. Feedforward gains for the control law were based on perfect model-following concepts [9 &10]. The designed control law did not include integral error control. Design results were presented for one design flight condition (Case 1 from Table 1.1). Reasonable decoupled results were obtained for aileron and elevator commands for the one flight condition evaluated.

Alag, Kemple, Pahle, Bresina, and Bartoli [11] explored explicit model-following techniques because the design technique presented in Reference 8 produced a control law which required excessive control surface activity. Linear quadratic techniques were used for the methodology presented in Reference 11. Their formulation of the problem did not include integral error control or frequency shaping. The authors showed that explicit model-following, linear quadratic techniques are suitable for designing a control law that decouples the OWRA's response.

Enns [12 &13] used frequency domain based multivariable synthesis techniques to design decoupling control laws for the OWRA. Reference 12 describes the application of a loop shaping approach called LQG/LTR (Linear-Quadratic-Gaussian with Loop Transfer Recovery). LQG/LTR is a modification of the LQG synthesis. The LQG problem is augmented by appending dynamics to the plant model to represent the desired loop recovery shapes for the aircraft's response. The control specification is formulated at the plant output and the multiple loops are designed to satisfy singular value constraints on the loop transfer function. A second frequency domain based multivariable design technique, called H^{∞} , is described in Reference 13. The H^{∞} method is a method that determines the compensator on the basis of meeting various constraints on the sensitivity functions. The desirable feature of H^{∞} synthesis is that it directly addresses the feedback design issues of achieving performance (i.e., tracking of commanded response and disturbance rejection) with with system stability in the presence of various sources of modeling uncertainty.

1.2.3 Piloted Evaluation of OWRA with Decoupling Control Laws

To evaluate a proposed flight control system for the OWRA, the Vertical Motion Simulator (VMS) at NASA Ames-Moffett was used [1]. The goals of this investigation were as follows: obtain preliminary pilot evaluations of a prototype flight control system designed to provide decoupled handling qualities; identify important response variables in the evaluation of this unusual configuration; and develop criteria and requirements for use in future control laws for highly coupled airplanes. The VMS provided a unique capability to investigate the OWRA dynamic characteristics early in the control system design phase in conjunction with realistic large motion and visual simulation systems.

Six pilots participated in the VMS evaluation of the OWRA at five discrete flight conditions ranging from low altitude subsonic Mach numbers to moderate altitude supersonic Mach numbers (note, not all of the five test points match conditions listed in Table 1.1). The control law was a prototype system based on the loop-shaping approach [12] with the specific objectives of decoupling the longitudinal and lateral-directional motions of the aircraft and to satisfy conventional flight control objectives, including gust attenuation, stability augmentation, good command tracking, good handling qualities, and stability robustness with respect to model uncertainty. This control law did not use gain scheduling; therefore, all flights were flown at fixed wing skew and were limited to relatively small variations in Mach number, altitude, and angle of attack about each design point.

1.3 REPORT SUMMARY

This report presents a description of the design and evaluation methodology which has been used to develop an explicit model-following, integrated flight/propulsion control system for the Oblique Wing Research Aircraft. Section II describes the physical, mass and inertial properties that are relevant to the control design task, and it provides background information covering the aerodynamic data base which was used to extract linear state models for the nine flight conditions. Section III presents a functional description of the integrated flight/propulsion control system which has been designed for the OWRA. This description is included in the report as a means to describe the philosophy that underlies the control system design. The design methodology is presented in Section III. The control system is designed to satisfy both mission level operational requirements and handling quality requirements. Mission/operational requirements were established by NASA Dryden for the Oblique Wing Research Airplane. Handling quality requirements are essentially based on interpretations of the MIL-F-8785C. A multistep control system design procedure, originally developed for the DMICS program, was adopted for the OWRA flight control system design task. An evaluation of the explicit model-following control system designed for the Oblique Wing Research Aircraft is presented in Section V. The primary objective of this evaluation centered on demonstrating the model-following performance of the gain scheduled control system. Finally, conclusions based on the design experience derived form this study are presented in Section VI.

II. AIRCRAFT DESCRIPTION

2.1 PHYSICAL CHARACTERISTICS

The oblique-wing research airplane (OWRA) considered for this investigation is based upon a modified version of NASA's F-8 digital-fly-by-wire (DFBW) airplane. Planned modifications include a variable incidence composite wing with a pivot-skew assembly, flight control computers and interfaces, and differential horizontal stabilizer. The skewed wing is designed to pivot from 0° to 65° with the right wing forward. The airplane's aerodynamic controls consist of the following movable surfaces: wing ailerons for roll control, symmetric horizontal tail for pitch control, asymmetric horizontal tail for roll control and rudder for directional control. Trailing edge flaps are used for lift augmentation during low speed flight. A three view drawing of the OWRA is presented in Figure 2-1. Reference geometry for the OWRA is defined as follows:

(S_w = 200 ft^2 , b_w = 542 in , and $\bar{c}_w$ = 57.3 in).

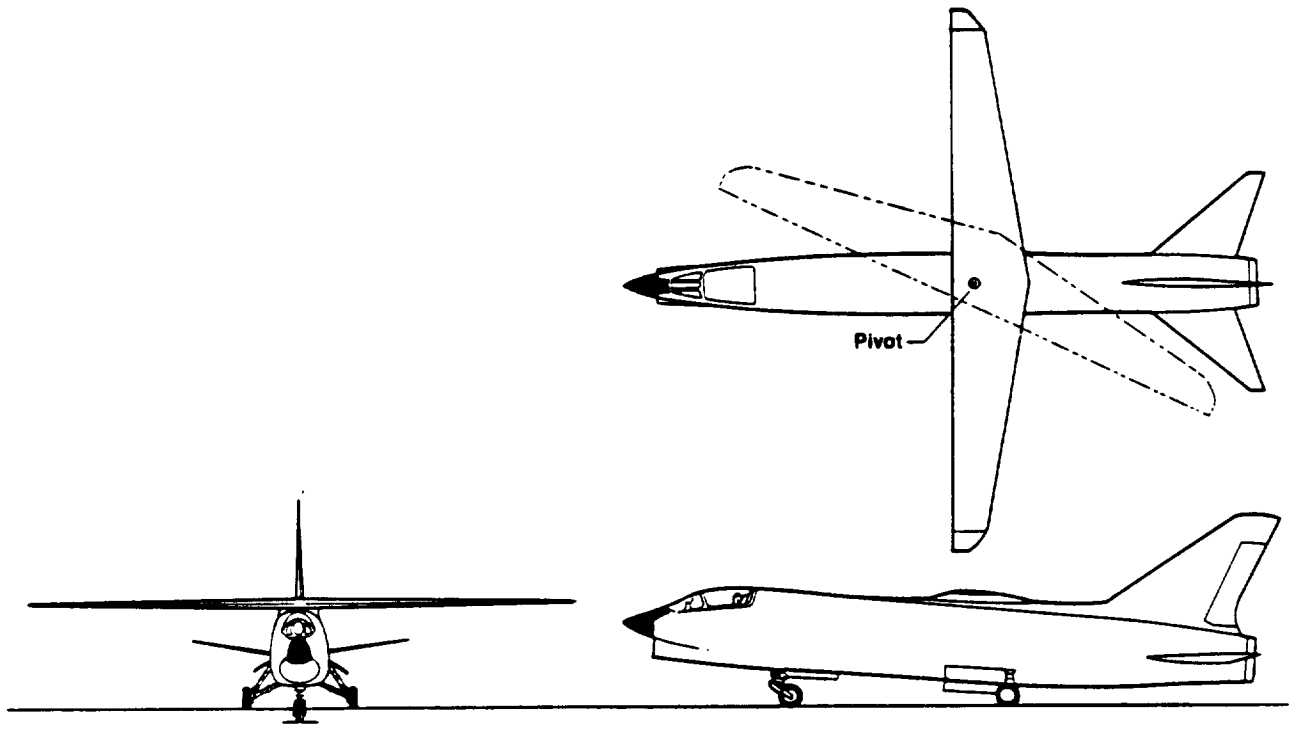

Figure 2-1 OWRA General Arrangement

The weight of the OWRA ranges from 23,500 to an empty weight of 18,800 lb. The weight used for this study was held constant at 21,116 lb which represented 50% fuel loading. The mass and center of gravity characteristics are presented in Figures 2.2 and 2.3, respectively.

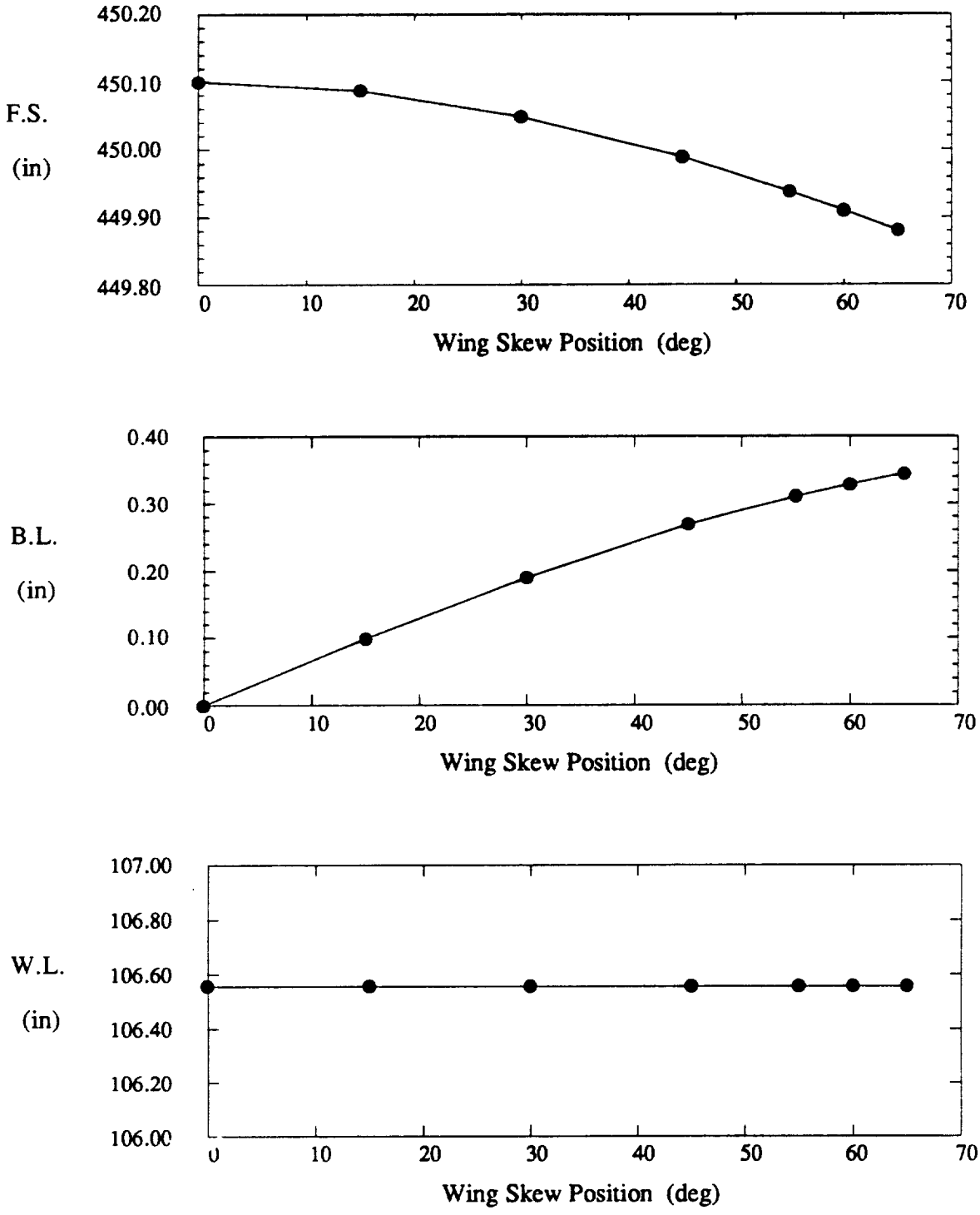

Figure 2-2 Effect of Wing Skew Position on c.g. Location

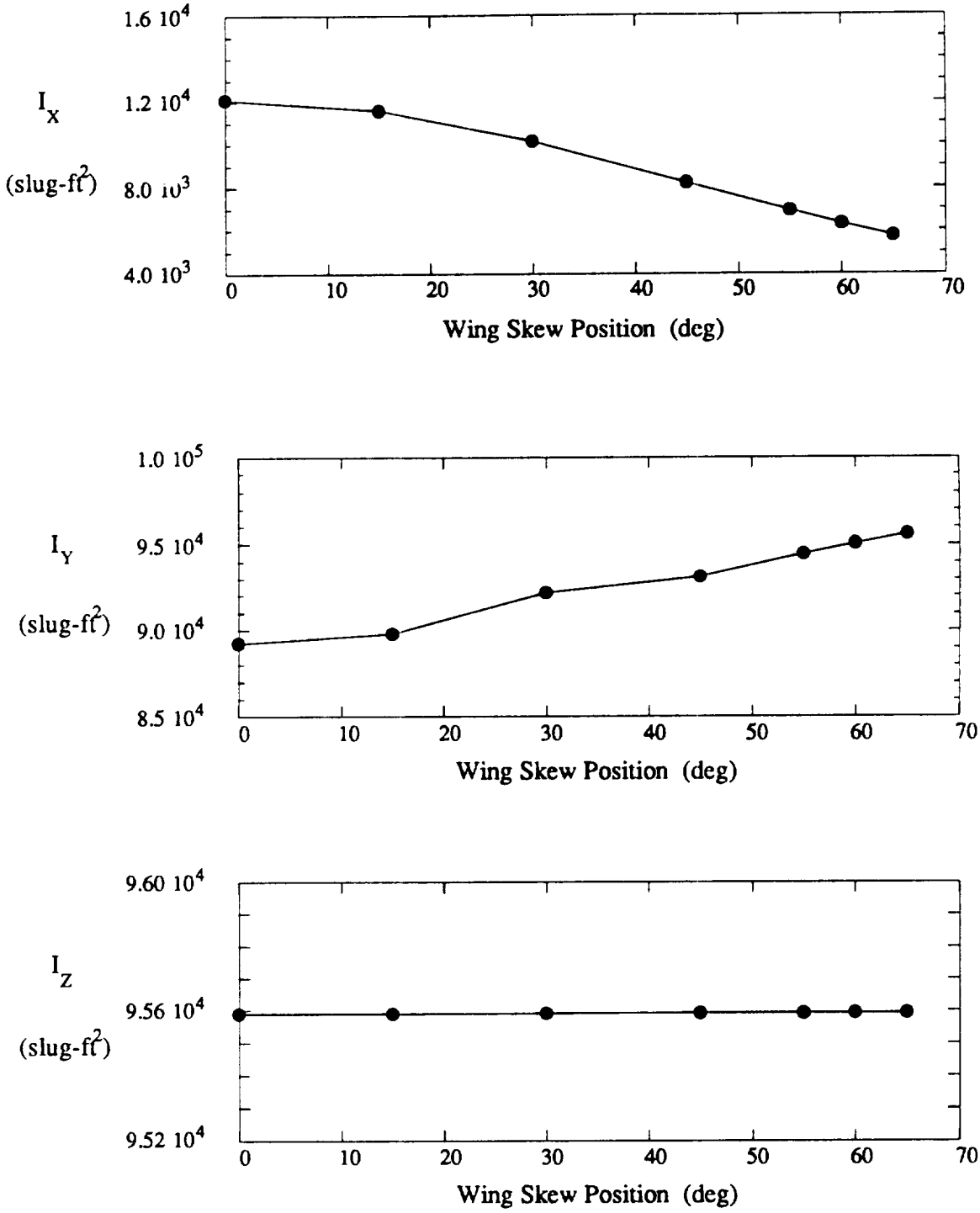

Figure 2-3a Effect of Wing Skew Position on Body Axis Inertias

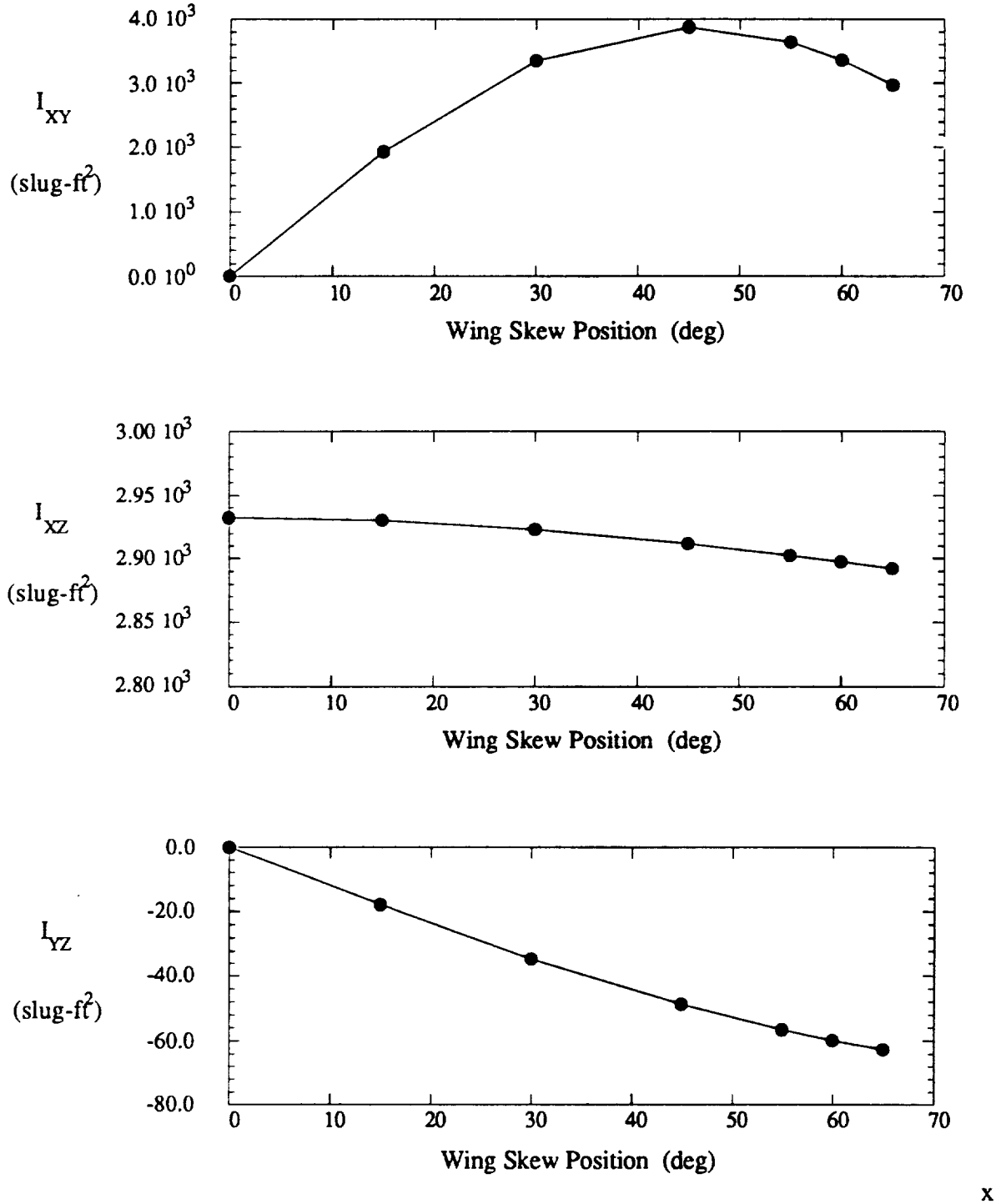

Figure 2-3b Effect of Wing Skew Position on Products of Inertia

2.2 AERODYNAMIC DATA BASE

The aerodynamic data base used in the OWRA was a preliminary nonlinear data set obtained from wind-tunnel tests and augmented with appropriately scaled F-8 data and computed aerodynamic characteristics. The data were nonlinear with angle of attack, Mach number, and wing skew, but not with sideslip. The angle of attack ranged from -4° to 16°. Mach numbers ranged from 0.25 to 1.6, and wing skews were 0°, 45°, 55°, and 65°. The data set did not cover all wing skews at all Mach numbers and was somewhat limited in scope, but was satisfactory for this preliminary study. Linearized state space matrices representing the open loop aerodynamic characteristics for each of the nine flight conditions for 1g trimmed flight were obtained from a NASA Dryden simulation of the OWRA that included this aerodynamic data base. The location of the nine design points relative to the operational limits is shown in Figure 2-4 for wing skew positions of $\Lambda = 45^\circ$, 55°, and 65°.

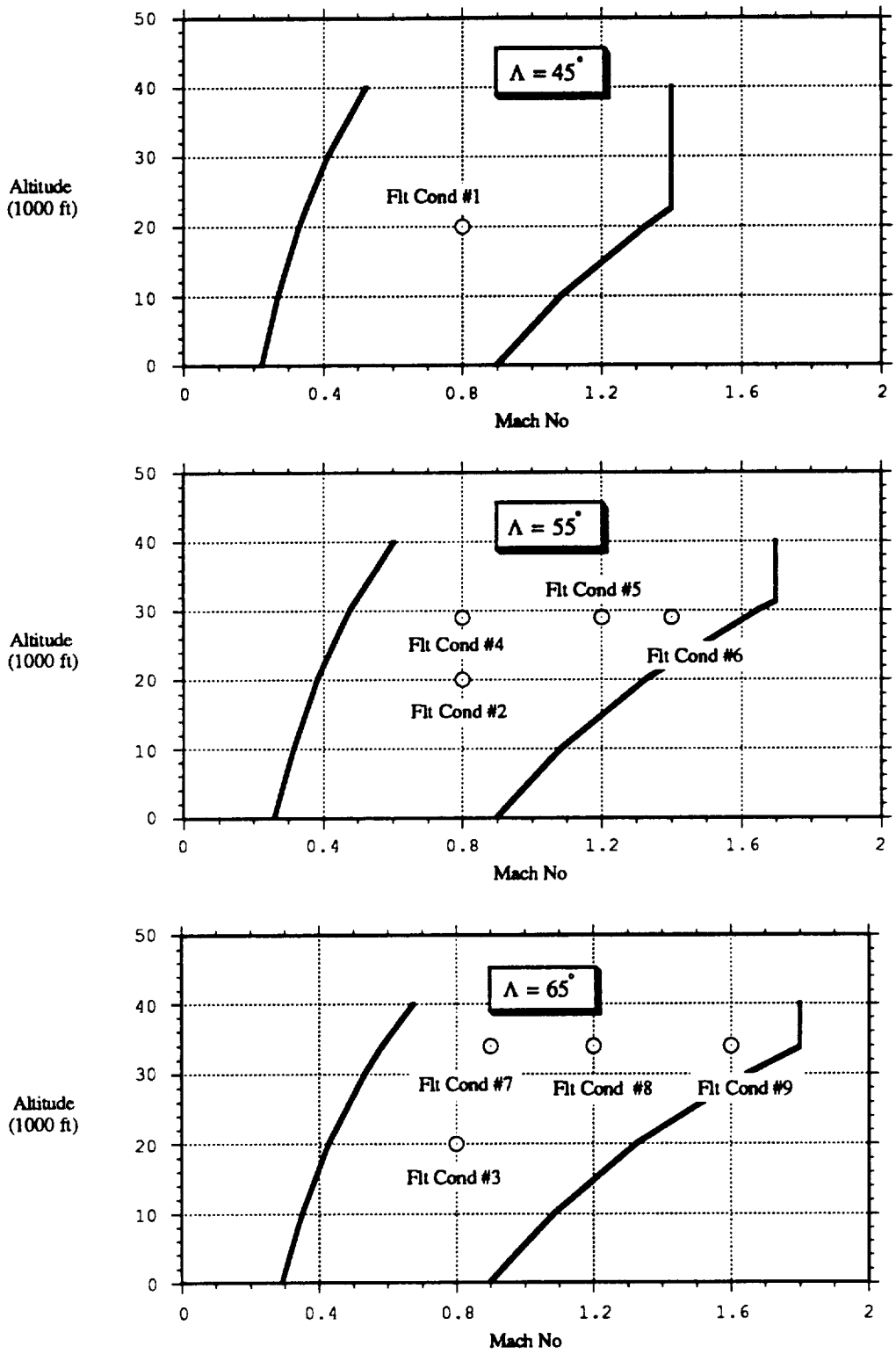

Figure 2-4 Design Flight Condition Summary

III. FLIGHT CONTROL FUNCTIONAL DESCRIPTION

3.1 OVERVIEW

This section presents a brief functional description of the integrated flight/propulsion control system which has been designed for the OWRA. This description is included in the report as a means to describe the philosophy that underlies the control system design. Reference 15 provides a complete description of this control system.

This IFPC structure is based on a *hierarchical* and *decentralized* design philosophy. With this design approach, *mission level* design problems (e.g., flying qualities, tactical combat, etc.) and *function level* problems (e.g., engine surge margin, engine temperature limits, control surface rates, etc.) are approached as separate design tasks. The mission level controller is the flight control system, and the function level controller of the hierarchical design is the propulsion control system. The structure for the flight control and the propulsion control systems is shown in Figure 3-1.

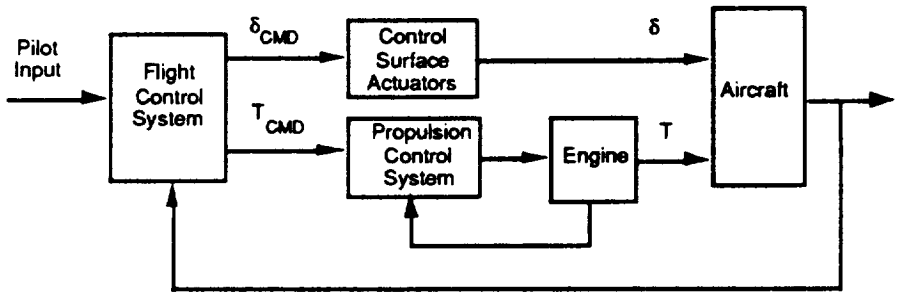

Figure 3-1 IFPC Control System Structure

The OWRA flight control system is based upon an explicit model-following structure. As illustrated in Figure 3-2, the flight control system structure includes three major elements: a maneuver command generator, a proportional-integral-error regulator, and a control selector. The purpose of this section is to describe the design features of these three components that comprise the OWRA flight control system.

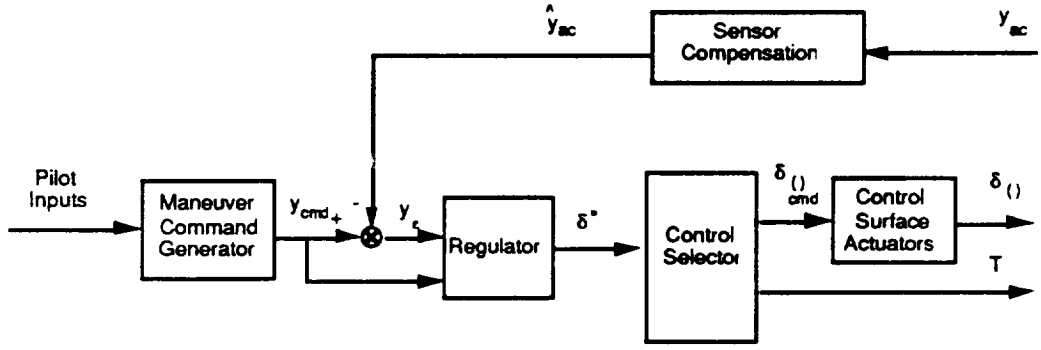

Figure 3-2 Flight Control System Structure

3.2 MANEUVER COMMAND GENERATOR DESCRIPTION

The *maneuver command generator* is the forward path model of the explicit model-following control system. It is designed to directly embody the desired flying qualities characteristics for each mode of flight. The primary inputs for the MCG are the pilot's controller commands (e.g., longitudinal stick force), and the outputs are a vector of commanded flight variables. The commanded response is used to form the error and feedforward terms for the model-following regulator.

The MCG comprises two major sub-elements: a steady state command generator and a response command generator, as indicated in Figure 3-3

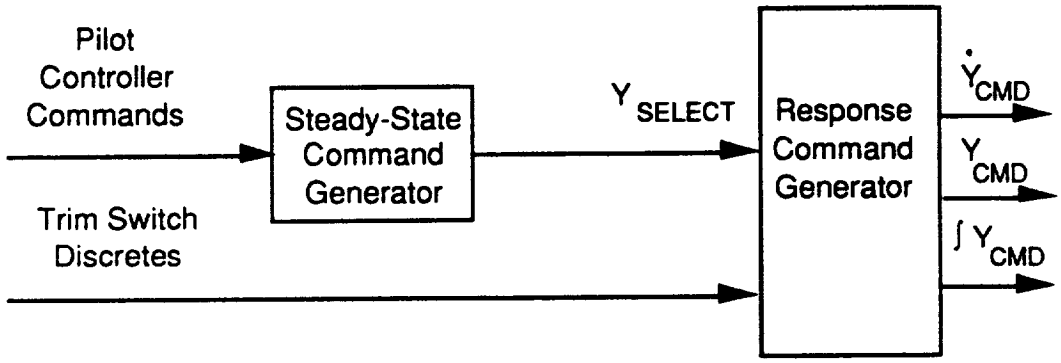

Figure 3-3 MCG Structure

The *steady state command generator* produces the commanded steady state response based on the desired sensitivity for each cockpit controller. Control sensitivity requirements include factors such as the desired stick force per g (F_s/g). The sensitivity terms are programmed as a function of flight condition in order to provide a match between what the pilot can command and what the aircraft can produce. A special form of tuning the control sensitivities to the aircraft's capabilities includes the incorporation of command limiters. For example, limits on commanded longitudinal acceleration or vertical velocity can be used to implement aircraft performance limits. Many of the design features of the *steady state command generator* are illustrated in Figure 3-4, a block diagram of the longitudinal steady state command generator.

The *response command generator* is designed to generate the desired dynamic response and the desired modal coupling/decoupling between various responses. The structure of the response command generator is based on block diagrams that embody the desired transfer function properties for the commanded responses. The OWRA longitudinal command generator is presented in Figure 3-5 to illustrate the structure of a typical response command generator.

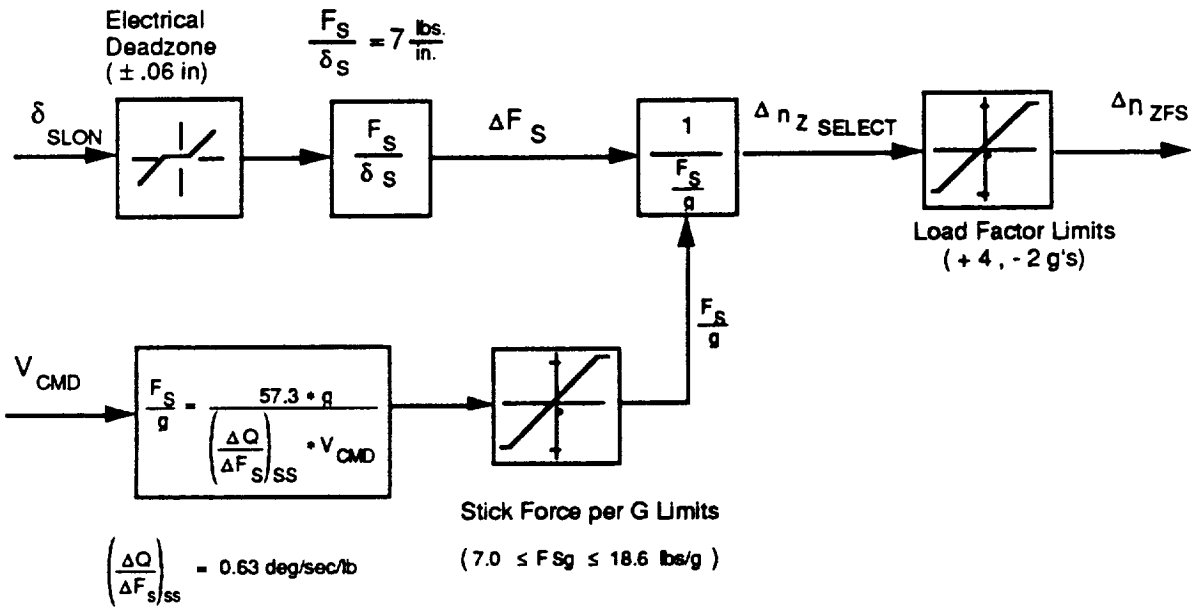

Figure 3-4 Longitudinal Steady State Command Generator

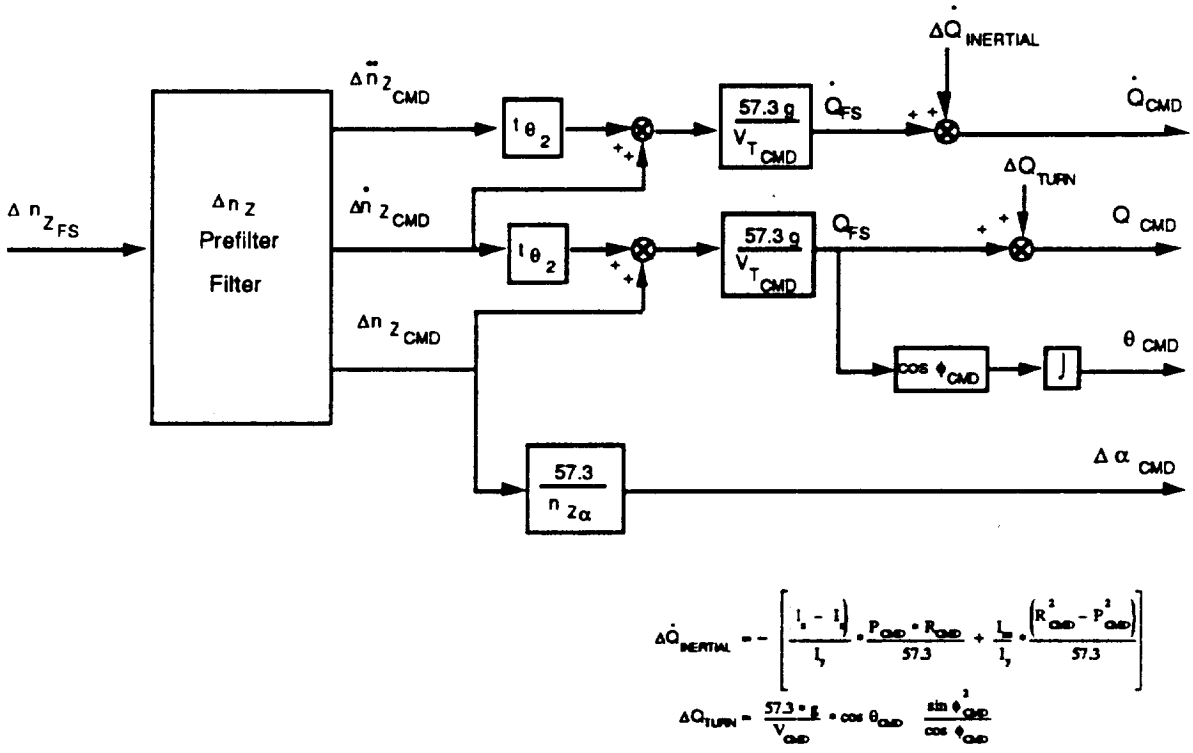

Figure 3-5 Longitudinal Response Command Generator

The desired dynamic response is implemented with a prefilter. The design of the prefilters is based on the following considerations:

- The prefilter provides the commanded response and its first and second derivative. The derivatives are used for feedforward control and modal reconstruction. For example, the load factor filter generates $\ddot{n}_{Z_{CMD}}$ and $\dot{n}_{Z_{CMD}}$ in addition to $n_{Z_{CMD}}$. All three of these quantities are used to reconstruct Q_{CMD} and $\dot{Q}_{CMD}$ as illustrated in Figure 3-6. The pitch acceleration feedforward command signal provides a direct link between the pilot's stick and the control surface. The feedforward signal is important for model following control laws in that it greatly reduces the lag in the aircraft's response to pilot inputs.

- The properties of the prefilter are selected such that they are all related to one design parameter. The selected design parameter for the MCG prefilter is the desired rise time. Two different prefilter forms are used for the MCG models.

  Prefilter Form #1

$$\frac{y_{CMD}}{y_{SELECT}} = \frac{\omega^2\tau\,(s + 1/\tau)}{s^2 + 2\zeta\omega s + \omega^2}$$

  where,

$$\omega = 1.789 / \tau_R \; ; \quad \tau = 0.625 * \tau_R \; ; \quad \zeta = 0.8944\,\tau_R$$

  Prefilter Form #2

$$\frac{y_{CMD}}{y_{SELECT}} = \frac{\omega^2}{s^2 + 2\zeta\omega s + \omega^2}$$

  where,

$$\omega = 3.360 / \tau_R \; ; \quad \zeta = 0.8944\,\tau_R$$

  This set of filter parameters provides a response that is characterized by a minimal overshoot and a rapid settling time. Figure 3-6 illustrates the formulation of a typical prefilter.

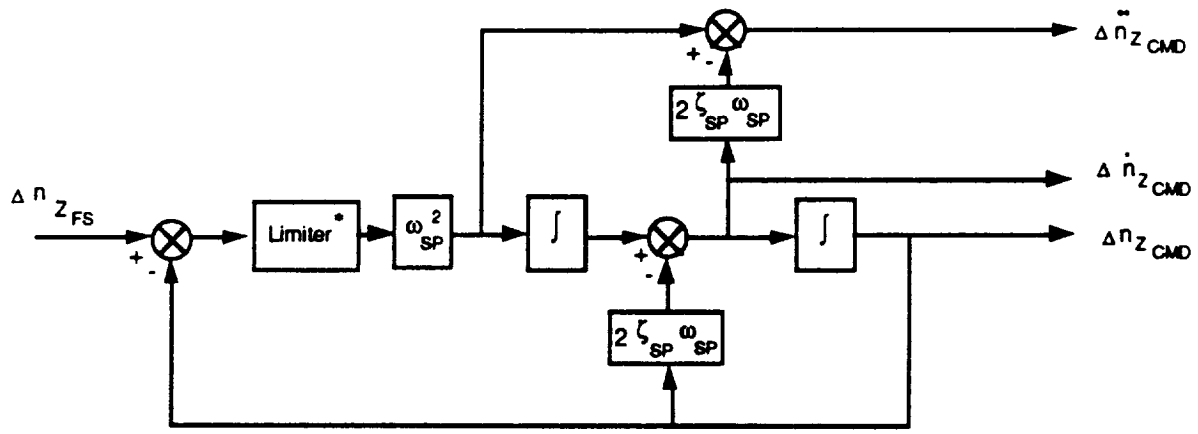

* Limit signal based on the magnitude of $\dot{Q}_{FS}$; e.g.,
  - no limit if $|\dot{Q}_{FS}| \leq 103 \text{ deg/sec}^2$
  - otherwise limit

Figure 3-6 Prefilter Structure

3.3 REGULATOR DESCRIPTION

The flight control system *regulator* is designed to provide stabilization, reference signal tracking (i.e., model-following) and disturbance rejection. The regulator control laws are based on multivariable synthesis techniques, using explicit model-following and a linear quadratic formulations with output error weightings [16]. A special feature of this regulator is that it generates generalized control commands, rather then physical control commands (i.e., pitch rate error produces pitch acceleration, instead of horizontal tail deflection). The use of generalized controls provides a decoupling between the design and implementation of control law gains from the selection of specific controllers for producing the desired control acceleration. Thus, the focus for the regulator design is the achievement of good model-following performance.

The structure for the flight control system regulator is presented in Figure 3-7. This structure is common to both the longitudinal and lateral-directional regulators. Regulator inputs include proportional errors, integral errors and feedforward commands that provide control response quickening. The synchronization logic shown in Figure 3-7 is used to zero proportional error signals, to break inputs to the integral error integrators and to zero integral error signals whenever the control mode is disengaged.

3.4 CONTROL SELECTOR DESCRIPTION

The *control selector* provides the controller mechanization function of the flight control system. Figure 3-8 shows the structure of control selector module. Inputs to the control selector come from the longitudinal and lateral-directional regulators. Control selector outputs include

aerodynamic control surface and thrust commands. The control selector module includes three primary components: control transformation blocks and control surface configuration manager.

The longitudinal and lateral-directional transformation blocks implement a pseudo inverse to convert generalized control commands to physical control commands. The pseudo inverse, which determines the best selection of controls, may be computed on-line, and its solution is based on internal models of the aerodynamic and propulsion controller effectiveness and remaining control power

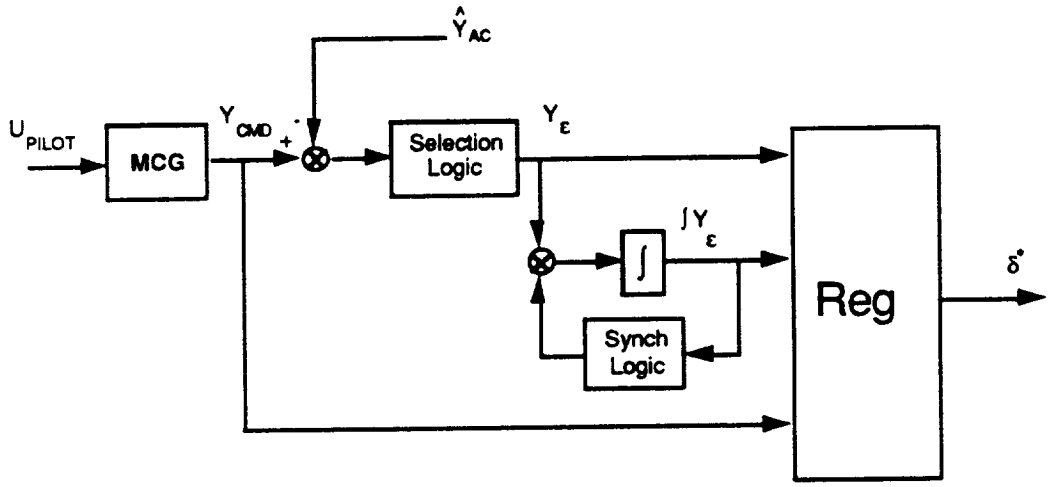

Figure 3-7 Regulator Structure

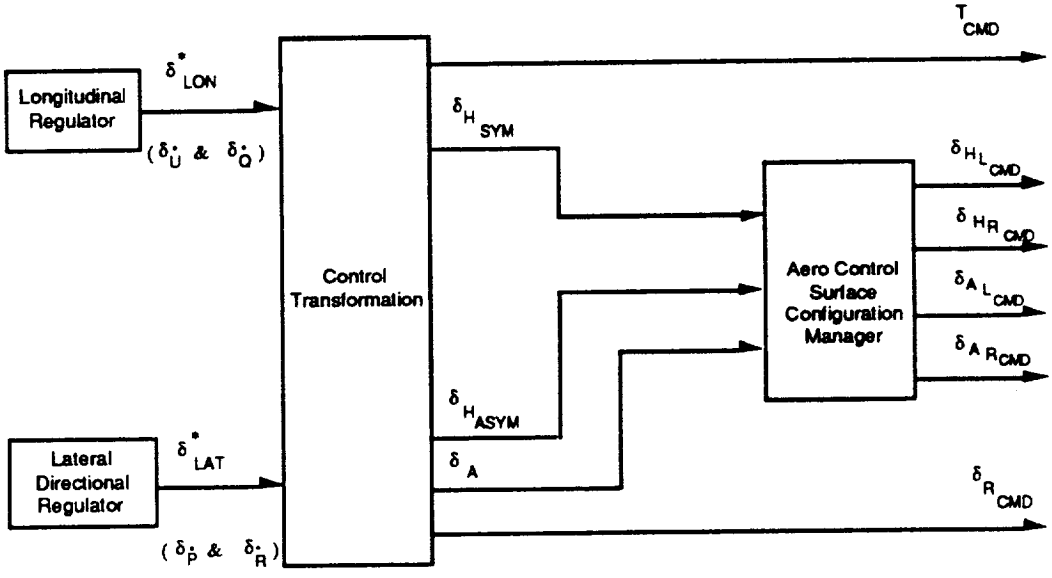

Figure 3-8 Control Selector Block Diagram

IV. DESIGN METHODOLOGY

4.1 OVERVIEW

The purpose of this section is to describes the design methodology for the flight control system. The flight control system is designed to satisfy both mission level operational requirements and handling quality requirements. Mission/operational requirements were established by NASA Dryden for the Oblique Wing Research Airplane. Handling quality requirements are essentially based on interpretations of the MIL-F-8785C.

A multistep flight control system design procedure, which was developed for the DMICS program [14], was adopted for the OWRA flight control system design task, see Figure 4-1. Features of each step are described in this section.

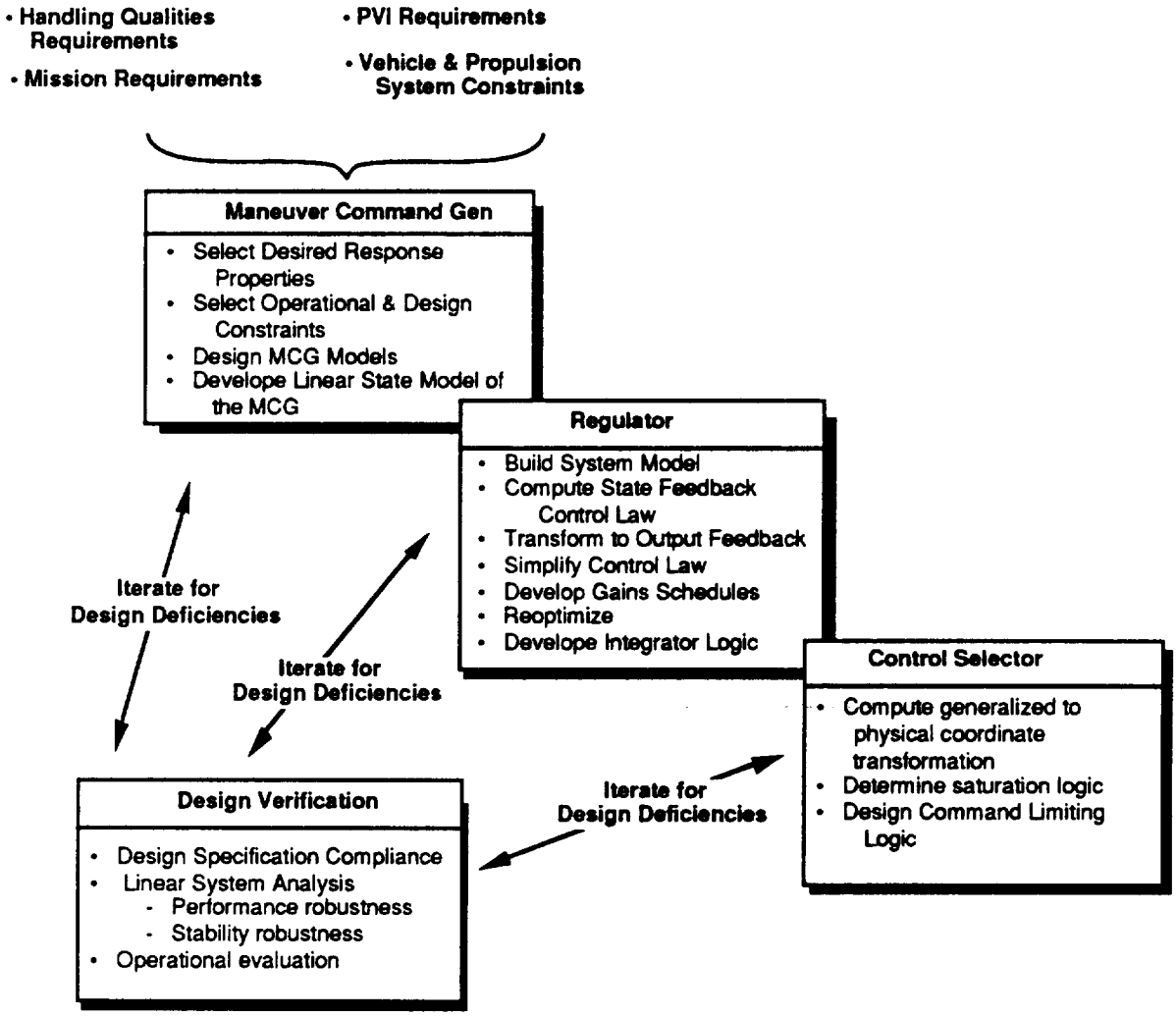

Figure 4-1 Flight Control Design Procedure

Linear math models of the aircraft and functional control design requirements must be available in order to start the flight control design process. The functional control design requirements are used to specify control modes and desired response properties for the flight control system. The initial step for flight control design involves designing the Maneuver Command Generator and the multivariable model-following regulator. The regulator synthesis is based on a Linear Quadratic Regulator (LQR) technique that includes integral error control and frequency shaping. The next step deals with implementation issues such as the development of gain schedules, mode switching logic, integrator logic, etc.. The final steps involve designing the control selector. Detailed evaluations of the design at each stages of the design process represents a key feature of the overall design process.

4.2 MANEUVER COMMAND GENERATOR DESIGN

4.2.1 Design Requirements

The limit load factor for the F-8 OWRA is -2 g's to +4 g's which sets its maneuvering capabilities. For the purposes of this investigation the F-8 OWRA is considered to be a Class IV-L airplane (i.e. a high-maneuverability land-based airplane) as defined by MIL-F-8785C. Level 1 flying qualities are a design goal for the flight control system design. A design objective is to provide the best possible flying qualities across the entire flight envelope.

The flying qualities requirements as specified in MIL-F-8785C are used as a guide for both longitudinal and lateral-directional control. A specific design objective for the flight control system is to minimize all cross-axis coupling and to provide flying qualities similar to a conventional symmetric wing airplane. A preliminary requirement for cross axis coupling is stated in the following:

- For all intended lateral-directional control maneuvers and random disturbances the resulting longitudinal response should be minimized.
- For all intended longitudinal control maneuvers and random disturbances the resulting lateral-directional response should be minimized.
- The pilot's concerns and methods of control shall be the same as they are for a conventional symmetrical airplane. Pilots tend to control the longitudinal or lateral-directional axes independently. An oblique wing airplane should not require unique or unusual piloting control techniques.

4.2.1 Longitudinal MCG Design

The longitudinal Maneuver Command Generator is designed to generate the desired pitch rate, load factor and airspeed responses for the up-and-away flight. A block diagram of the

longitudinal MCG is presented in Figure 4-2. The longitudinal MCG is designed to decouple the airspeed and load factor (i.e., flight path) responses. The interconnection between commanded longitudinal acceleration and pitch rate is included to change the commanded angle-of-attack as airspeed varies such that 1g flight is maintained.

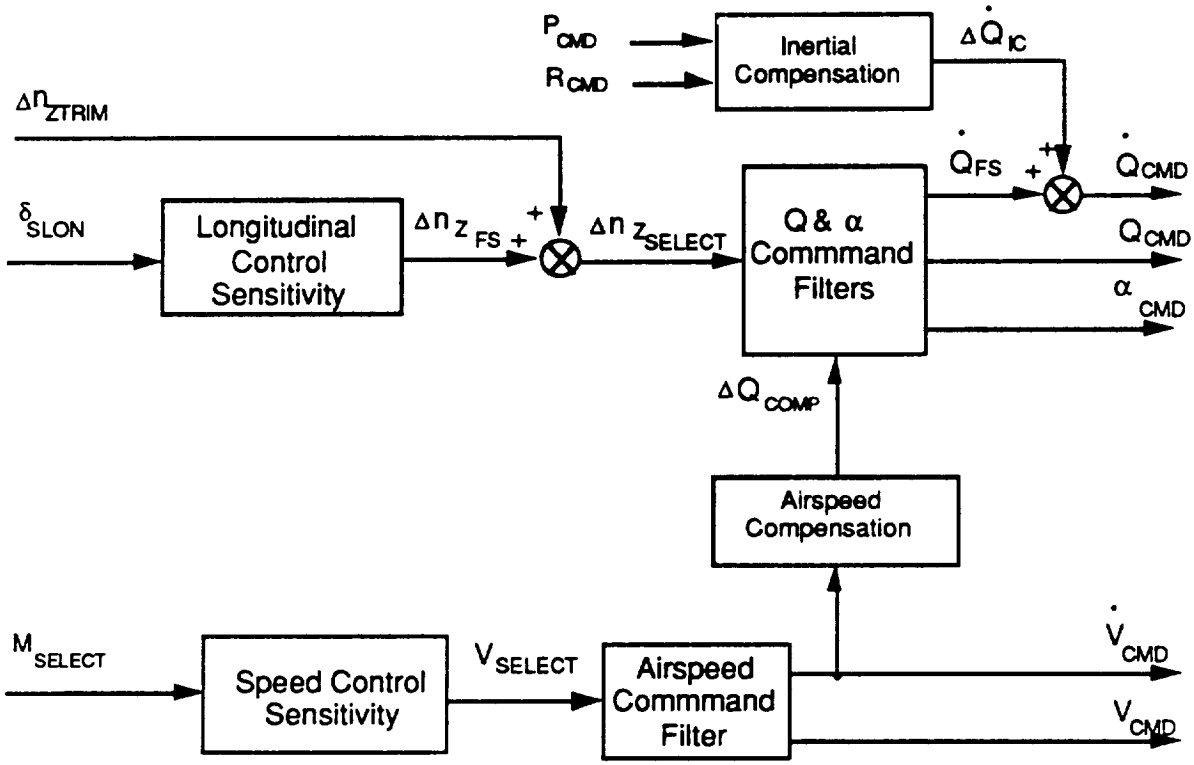

Figure 4-2 Longitudinal MCG

Pitch Rate and Angle-of-Attack Commands

Longitudinal control sensitivity is defined in terms of (F_S/g) (the stick force per g) MIL-F-8785 specifies that the F_S/g must be in the following range for Level 1 flying qualities based on a limit load factor of $n_{z\ LIMIT}$ = 4 g's

$$7.0 \leq \frac{F_s}{g} \leq 15.6 \text{ lbs/g}$$

F_S/g is computed from the following expression with the above limitations

$$\frac{F_s}{g} = \frac{\Delta F_s}{\Delta n_z} = \frac{\left(\Delta Q/\Delta n_z\right)_{ss}}{\left(\Delta Q/\Delta F_s\right)_{ss}}$$

$$= \frac{2929}{V_{RW}} \qquad for \quad \left(\frac{\Delta Q}{\Delta F}\right)_{ss} = 0.63\, deg/sec/lb$$

For the nine flight conditions considered, F_S/g is always set by the minimum requirement of F_S/g = 7 lbs/g.

Selected short period dynamics are tailored to provide acceptable load factor and pitch rate responses. The following expressions define both responses:

$$\frac{\Delta n_{Z_{CMD}}}{\Delta n_{Z_{SS}}} = \frac{\omega_{sp}^2}{s^2 + 2\zeta_{sp}\omega_{sp}\, s + \omega_{sp}^2}$$

$$\frac{\Delta Q_{CMD}}{\Delta Q_{ss}} = \frac{\omega_{sp}^2 \tau_{\theta 2}\left(s + \frac{1}{\tau_{\theta 2}}\right)}{s^2 + 2\zeta_{sp}\omega_{sp}\, s + \omega_{sp}^2}$$

Thus, the short period dynamics are characterized by the selected short period frequency (ω_{sp}), short period damping (ζ_{sp}) and the pitch rate zero ($1/\tau_{\theta 2}$). Without direct lift control, $1/\tau_{\theta 2}$ is a function of only the aircraft's lift-curve slope ($C_{L\alpha}$) and its flight condition. Thus, its value is flight condition dependent and cannot be altered. Short period damping must be greater than ζ_{sp} > .035 to satisfy Level 1 requirements from MIL-F-5785C. A value of ζ = 0.8944 is selected for the MCG design to provide a response that is essentially deadbeat.

When direct lift control is not available, the speed of the load factor response and the ratio of the maximum pitch rate overshoot relative to the steady state pitch rate (Q_{MAX}/Q_{SS}) are both a function of the short period frequency. Increasing ω_{SP} quickens the load factor response and increases the magnitude of pitch rate overshoot. Thus, selection of ω_{SP} involves a compromise between loader factor and pitch rate response requirements. MIL-F-8785C provides a rational for selecting desired values for ω_{SP} as a function of n_{z_α} (the change in load factor per a change in angle-of-attack) and a parameter called CAP. CAP is the control anticipation parameter, and it is defined as the ratio of the initial pitch acceleration to the steady state load factor ($\dot{\Delta Q}_{t=0} / \Delta n_{Z_{SS}}$).

The relationship between ω_{sp}, CAP and Q_{MAX}/Q_{SS} is illustrated in Figure 4.-3. The Level 1 flying quality requirements for both Category A and B Flight Phases are noted in Figure 4-3. Figure 4-4 illustrates the impact of CAP on the load factor and pitch rate responses for a step stick force command. The overdriven pitch rate response is for Category A Flight Phases (CAP = 0.28). The slower set of responses is for the Category B Flight Phase where CAP = 0.085. The Flight Category B value of CAP was selected for the OWRA longitudinal MCG design task because it minimizes the pitch rate overshoot.

The following expressions model the desired short period parameters for the longitudinal MCG.

- $\tau_{\theta_2} = \dfrac{W\, V_{RW}}{g\, \bar{q}\, S_W C_{L_\alpha}}$

  W : aircraft weight ~ lbs
  V_{RW} : airspeed ~ fps
  g : gravity constant (32.2 fps^2)
  $\bar{q}$: dynamic pressure ~ psf
  S_W : reference wing area ~ ft^2
  C_{L_α} : aircraft lift curve slope ~ 1/rad

- $n_{Z_\alpha} = \dfrac{\bar{q}\, S_w}{W} C_{L_\alpha}$

- $\omega_{sp} = \sqrt{CAP \cdot n_{Z_\alpha}}$ rad/sec

Values for these three parameters for each of the nine flight conditions are summarized in Table 4-1.

Table 4-1

Summary of Longitudinal MCG Design Parameters

Flight Cond No	Altitude (ft)	Mach No	Wing Skew (deg)	n_{z_α} (g's/rad)	ω_{SP} (rad/sec)	t_{θ_2} (sec)
1	20,000	0.8	45	20.33	1.31	1.27
2	20,000	0.8	55	18.84	1.27	1.37
3	20,000	0.8	65	12.56	1.03	2.07
4	29,000	0.8	55	12.83	1.04	1.95
5	29,000	1.2	55	31.86	1.65	1.19
6	29,000	1.4	55	38.73	1.81	1.14
7	34,000	0.9	65	10.31	0.94	2.74
8	34,000	1.2.	65	17.62	1.22	2.03
9	34,000	1.6	65	26.33	1.50	1.87

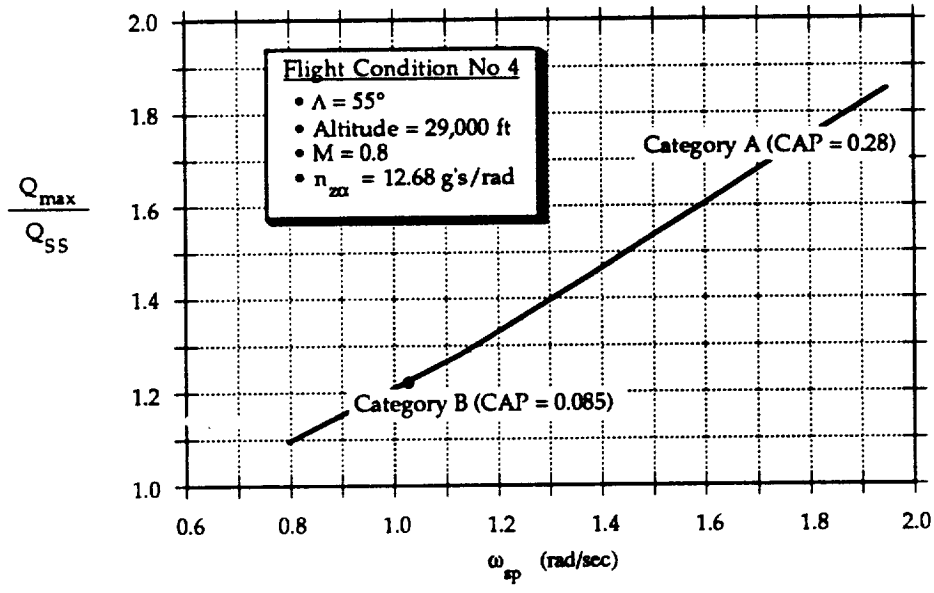

Figure 4-3a Trade-off Between Short Period Frequency and Pitch Rate Overshoot

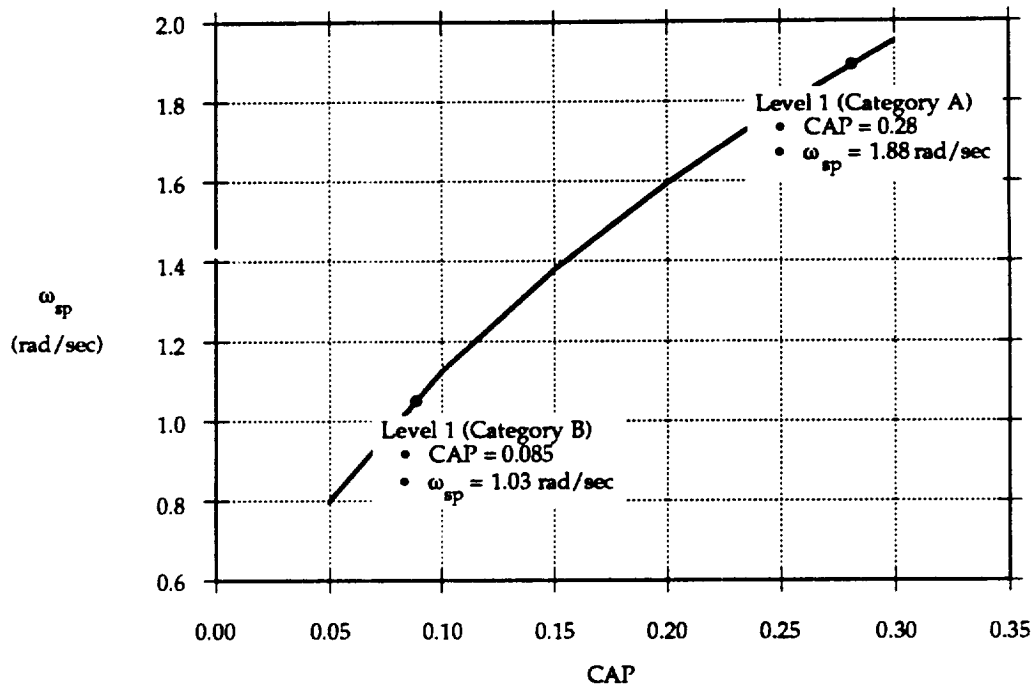

Figure 4-3b Impact of CAP on Short Period Frequency (Flight Condition #4)

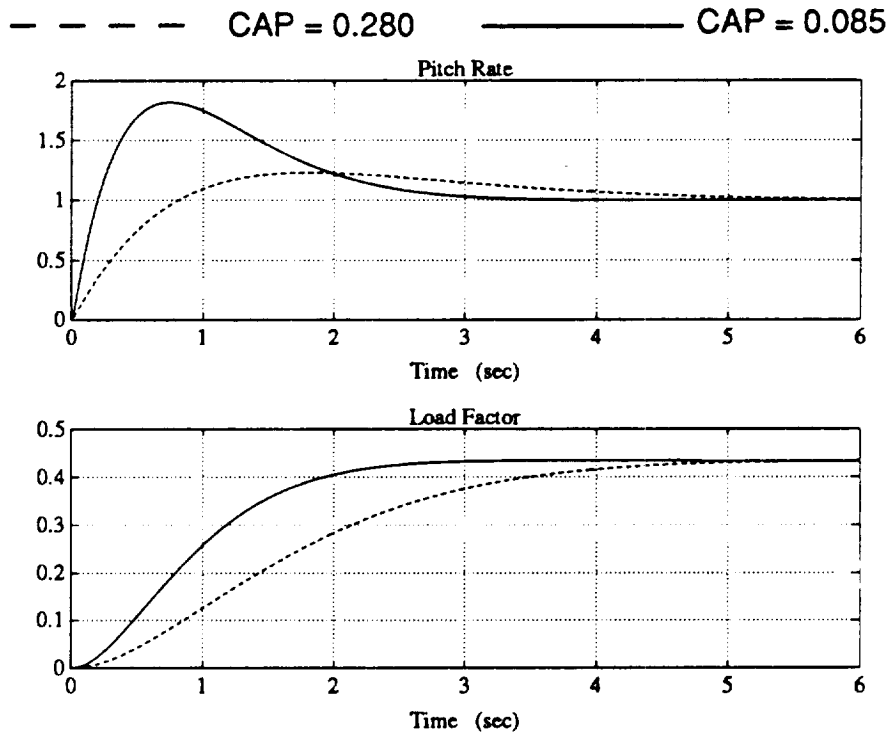

Figure 4-4 Effect of CAP on MCG Response (Flt Cond #4)

Airspeed Command

The speed control sensitivity function for the longitudinal MCG provides a simple transformation between Mach number and airspeed and limiting based on the aircraft's performance capabilities. The Mach number to true airspeed transformation is

$$V_{SELECT} = 1117.6 \sqrt{\theta_{amb}}\, M_{SELECT}$$

The commanded speed response is designed to have a five second rise time, and it is defined by the following transfer function.

$$\frac{V_{CMD}}{V_{SEL}} = \frac{\omega_v^2 \tau_v \left(s + \frac{1}{\tau_v}\right)}{s^2 + 2\zeta_v \omega_v s + \omega_v^2}$$

where,

$$\tau_V = 3.20 \text{ sec} \quad ; \quad \omega_V = 3.50 \text{ rad/sec} \quad \text{and} \quad \zeta_V = 0.8944$$

The coupling between $\Delta\dot{V}$ and Q_{cmd} is included to cause a change in commanded angle of attack for a change in airspeed. This compensation produces a decrease in angle of attack for an increase in airspeed. This angle-of-attack command can be generated by varying attitude while holding flight path angle constant (i.e., $\cos\phi * \Delta\alpha = \Delta\theta - \Delta\gamma$). Since $\Delta\theta = \int Q$, the compensation loop from velocity into attitude is identical to $\Delta\dot{V} \rightarrow \Delta Q$. The gain between $\Delta\theta$ and ΔV (also, ΔQ and $\Delta\dot{V}$) is developed from first principles:

$$W = 1/2\, \rho V^2 S_W\, C_L$$

where the lift coefficient is defined by

$$C_L = C_{L_0} + C_{L_\alpha}\, \alpha$$

By substituting the lift coefficient expression into the equation relating weight and lift coefficient

$$W = 1/2\, \rho V^2 S\, (C_{L_0} + C_{L_\alpha}\, \alpha)$$

and taking the derivative of above equation with respect to V

$$0 = \rho V S_W C_{L_0} + 1/2 \rho V^2 S_W C_{L_\alpha} \partial\alpha/\partial V$$

the following expression results

$$\frac{\Delta\alpha}{\Delta V} = \frac{-2 C_{L_0}}{V C_{L_\alpha}}$$

Since $\Delta\theta = \Delta\alpha$ for $\Delta\gamma = 0$,

$$\frac{\Delta\theta}{\Delta V} = \frac{\Delta Q}{\dot{\Delta V}} = \frac{-2 C_{L_0}}{V C_{L_\alpha}}$$

4.2.2 Lateral-Directional MCG Design

The lateral directional Maneuver Command Generation is designed to provide decoupled control of roll attitude and sideslip. Lateral stick commands roll rate with roll attitude being held whenever the stick is in detent (i.e., rate command/attitude hold). Decoupling sideslip and the roll rate/attitude responses provides good turn coordination for roll commands and a wings level sideslip response for pedal inputs. The latter feature is useful for managing crosswinds close to the runway. The sideslip from rudder pedal command filter provides good Dutch roll damping and a predictable sideslip response. With the wings held level for pedal inputs, small heading changes can be made rapidly with pedal commands (i.e., $\Delta\psi = \Delta\beta$ for $\phi = 0$). Figure 4-5 presents the block diagram of the lateral-directional MCG.

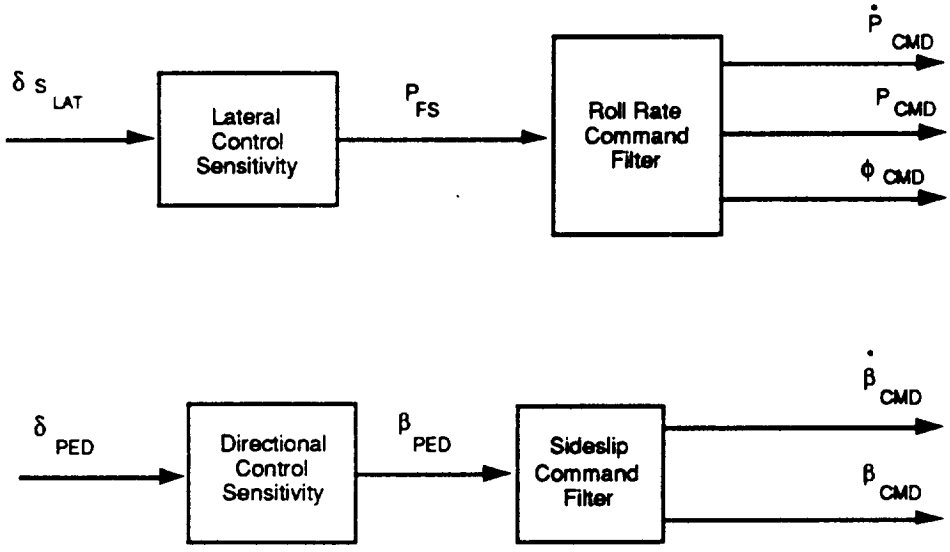

Figure 4-5 Lateral-Directional MCG.

Roll Rate Command

Lateral control sensitivity is defined in terms of the ratio of maximum steady state roll rate to the maximum lateral stick displacement (i.e., $\Delta P_{SS}/\Delta\delta_{SLAT}$). Lateral control sensitivity is selected to provide a steady state roll rate of 200 °/sec for a 4 in. stick deflection:

$$\frac{\Delta P_{SS}}{\Delta\delta_{SLAT}} = \frac{200 \text{ deg/sec}}{4 \text{ in}} = 50 \text{ deg/sec/in}$$

A second order filter with a first order numerator is used to model the desired roll response.

$$\frac{P_{CMD}}{P_{SS}} = \frac{\omega_p^2 \tau_p (s + 1/\tau_p)}{s^2 + 2\zeta_p \omega_p s + \omega_p^2}$$

where,

$$\tau_P = 0.625\ t_{P\,90} \quad ; \quad \omega_P = \frac{1.789}{t_{P\,90}} \quad \text{and} \quad \zeta_P = 0.8944$$

The parameters of this filter are selected to produce a first-order like response. The selected value for the response rise time is t_{P90} = 1 sec. As shown in Figure 4-6, this rise time produces a response that is similar to a first-order response which has a time constraint of T_R = 0.38 sec. This is well below the one second limit as specified within MIL–F–8785C for Level 1 flying qualities.

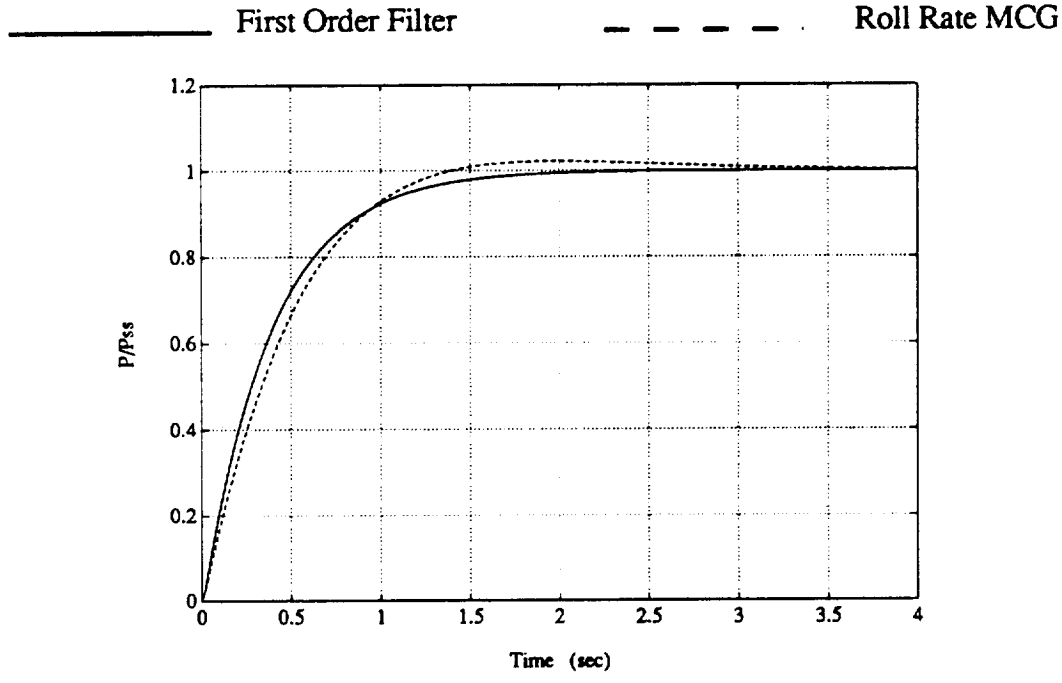

Figure 4-6 Comparison of First Order Filter and Roll Rate MCG Filter Responses

Sideslip Command

Directional control sensitivity is defined as the ratio between maximum sideslip and maximum pedal force (i.e., $\Delta\beta/\Delta F_{PED}$). Directional control sensitivity is selected to provide $\Delta\beta$ = 3 ° for a pedal force of 120 lbs.

$$\frac{\Delta\beta}{\Delta F_{PED}} = \frac{3\ \text{deg}}{120\ \text{lbs}} = 0.025\ \text{deg/lb}$$

The structures of the sideslip command filter is given by:

$$\frac{\beta_{CMD}}{\beta_{SS}} = \frac{\omega_\beta^2 \tau_\beta (s + 1/\tau_\beta)}{s^2 + 2\zeta_\beta \omega_\beta s + \omega_\beta^2}$$

For this filter, its parameters are set by equating ω_β to the aircraft's value of Dutch roll frequency. The damping ratio and the numerator time constant are defined as follows:

$$\zeta_\beta = 0.8944 \quad ; \quad \omega_\beta = \omega_{DR} \quad \text{and} \quad \tau_\beta = \frac{1}{\zeta_\beta \omega_\beta}$$

The following approximation is used to define Dutch roll frequency:

$$\omega_\beta = \omega_{DR} = \sqrt{N_\beta} = 0.2765 \sqrt{\bar{q}\, c_{n_\beta}}$$

For the nine flight conditions studied ω_{DR} has the following range of values: $2.46 < \omega_{DR} < 4.58$ rad/sec. With $\zeta_\beta = 0.8994$, all Dutch roll requirements for Level 1 flying qualities ($\zeta_{DR} > .49$; $\zeta_{DR}\ \omega_{DR} > .35$; $\omega_{DR} > 1.0$) are all surpassed by the selected design.

4.3 GENERALIZED ACTUATORS

When the flight control system regulator is designed, generalized controls are used to represent the control power that can be produced by the aerodynamic control surfaces and the propulsion system. The flight control structure as presented in Figure 3-2 can be redrawn as shown in Figure 4-7 when generalized controls are used. The generalized controls description includes two elements: actuator dynamics and control power.

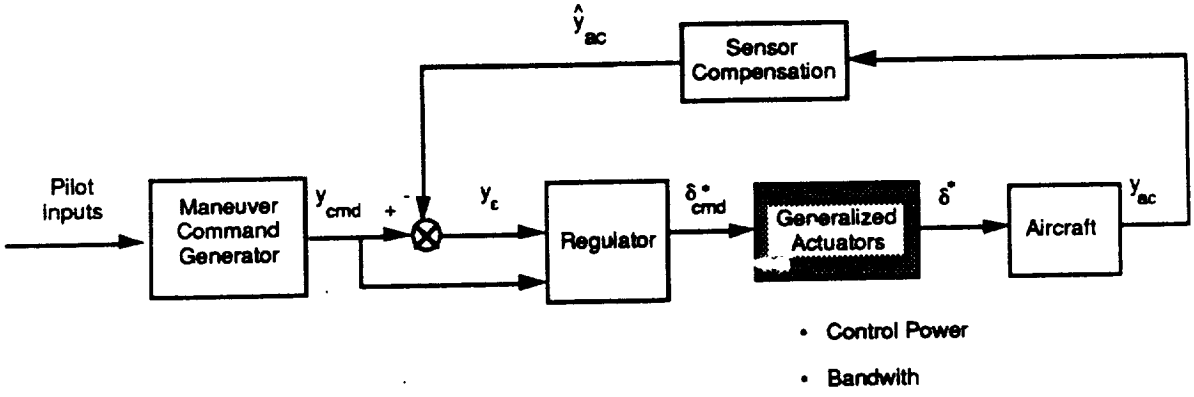

Figure 4-7 Flight Control Structure with Generalized Controls

For the OWRA flight control system design, the generalized actuator dynamics are modeled by the following transfer function:

$$\frac{\delta^*}{\delta^*_{CMD}} = \frac{\omega_\delta^2 \tau_\delta \left(s + \frac{1}{\tau_\delta}\right)}{s^2 + 2\zeta_\delta \omega_\delta s + \omega_\delta^2}$$

where,

$$\tau_\delta = 0.625\ t_{\delta\,90} \quad ; \quad \omega_\delta = \frac{1.789}{t_{\delta\,90}} \quad \text{and} \quad \zeta_\delta = 0.8944$$

where,

$t_{\delta\,90}$ is the desired actuator rise time

The need to represent the generalized actuator dynamics by a second order transfer function stems from the methodology which is used to determine the regulator control law gains. The regulator control law synthesis is based on solving a Linear Quadratic Regulator problem that includes actuator deflection rates as elements of the performance function and a transformation that maps state feedback gains to a corresponding set of output feedback gains. The structure of this second order transfer function is based on a desire to match the first order properties of the actual control surface actuators. The selected values for the damping ratio (ζ_δ) and the relative geometry of the zero with respect to the complex poles (i.e., $1 / \tau_\delta = \zeta_\delta \omega_\delta$) provide a deadbeat response. The speed of the response is set by the value which is selected for the desired rise time ($t_{90\delta}$). Based on the time constants for the OWRA ailerons, elevator and rudder control surface actuators plus an estimate for the engine's response, the following values were used to represent the generalized actuator's dynamics:

Axis	t_{90_δ} (sec)	Selection Criteria
Axial	1.500	Engine Dynamics
Vertical	0.130	Aileron Actuator Dynamics
Roll	0.130	Aileron Actuator Dynamics
Pitch	0.170	Horizontal Tail Actuator Dynamics
Yaw	0.065	Rudder Actuator Dynamics

Each of the five generalized controls (i.e., axial, vertical, pitch, roll and yaw acceleration) has an associated control power level. The control distribution matrix (B^*_{AC}) is defined as a diagonal matrix where the diagonal elements represent the maximum control power normalized by 100%; thus, the generalized controls (e.g., δ^*_W) have the units of % maximum control. Because the OWRA does not have the capability to generate direct side force, the generalized control distribution matrix (B^*_{AC}) includes an off-diagonal term to account for the side force due to the directional control surface. The maximum control does not represent an actual control limit, but a reasonable level of the available control power that can be achieved in a decoupled manner.

Based on an assessment of the control power available for the nine flight conditions, the generalized control distribution matrix is defined as follows for all nine flight conditions:

$$B^*_{AC} = \begin{bmatrix} 0.0805 & 0 & 0 & 0 & 0 & 0 \\ 0 & 0 & 0 & 0 & 0 & -0.05 \\ 0 & 0 & 0.0580 & 0 & 0 & 0 \\ 0 & 0 & 0 & 0.0698 & 0 & 0 \\ 0 & 0 & 0 & 0 & 0.0180 & 0 \\ 0 & 0 & 0 & 0 & 0 & .0061 \end{bmatrix}$$

4.4 MULTIVARIABLE REGULATOR DESIGN

Linear Quadratic Regulator (LQR) synthesis techniques were used to design the multivariable control laws for the OWRA integrated flight control system. The reasons for choosing LQ were as follows:

- The method is well suited for designing multivariable control laws for aircraft such as the OWRA which have coupled dynamics.

- The control law is optimal in the sense that it minimizes the control effort required to keep the mean-square deviation of the tracking errors as small as possible.

- Cross-coupling of control on states is automatically included so that controls will not be fighting each other.

- Once the performance index and weighting matrices have been chosen, the procedure is highly automatic. The design procedure which was used for this program had been developed previously by SCT for the DMICS program [14, 16].

As illustrated in Figure 4-1 the regulator design procedure includes several steps. First a system state model is assembled. Next, the control law are developed for each of the nine flight conditions. Finally, gain scheduled control laws are developed from the nine individual solutions. Features of each step are described below.

4.4.1 System Model Definition

This section describes the state model formulation which is required for synthesizing explicit model-following control laws. For the OWRA design process the complete 6-DOF system model comprises 35 states, 10 controls and 51 output quantities. The state model includes formulations of the open-loop airframe, the MCG, the generalized actuators, and integral error states. Incorporation of the actuator states (deflection and rates) and the integral error states provides the means for producing desired frequency shaping. Generally, weighting the actuator states is used to attenuate the control energy (gain) at high frequencies. The integral error states are used to increase the control gain at low frequency, and thus, improve steady-state model-following accuracy.

Figure 4-8 illustrates the general form of design state model. The tracking errors (y_ε), which represent the difference between the MCG command and the aircraft's response, are included as a subset of the design model output vector. The control vector for the design model includes actuator commands and pilot commands (i.e., MCG model inputs).

State Equations

$$\begin{bmatrix} \dot{x}_{ac} \\ \dot{x}_{\delta} \\ \dot{x}_{MCG} \\ \dot{x}_{\int\varepsilon} \end{bmatrix} = \begin{bmatrix} A_{ac} & B^{*}_{ac} & 0 & 0 \\ 0 & A_{\delta} & 0 & 0 \\ 0 & 0 & A_{MCG} & 0 \\ -C_{ac_{\int\varepsilon}} & -D^{*}_{ac_{\int\varepsilon}} & C_{MCG_{\int\varepsilon}} & 0 \end{bmatrix} \begin{bmatrix} x_{ac} \\ x_{\delta} \\ x_{MCG} \\ x_{\int\varepsilon} \end{bmatrix} + \begin{bmatrix} 0 & 0 \\ B_{\delta} & 0 \\ 0 & B_{MCG} \\ 0 & D_{MCG_{\int\varepsilon}} \end{bmatrix} \begin{bmatrix} u^{*}_{\delta_c} \\ u_{pilot} \end{bmatrix}$$

Output Equations

$$\begin{bmatrix} y_{ac} \\ y_{\delta} \\ y_{MCG} \\ y_{\varepsilon} \\ y_{\int\varepsilon} \end{bmatrix} = \begin{bmatrix} C_{ac} & D^{*}_{ac} & 0 & 0 \\ 0 & C_{\delta} & 0 & 0 \\ 0 & 0 & C_{MCG} & 0 \\ -C_{ac_{\varepsilon}} & -D^{*}_{ac_{\varepsilon}} & C_{MCG_{\varepsilon}} & 0 \\ 0 & 0 & 0 & I \end{bmatrix} \begin{bmatrix} x_{ac} \\ x_{\delta} \\ x_{MCG} \\ x_{\int\varepsilon} \end{bmatrix} + \begin{bmatrix} 0 & 0 \\ D_{\delta} & 0 \\ 0 & D_{MCG} \\ 0 & D_{MCG_{\varepsilon}} \\ 0 & 0 \end{bmatrix} \begin{bmatrix} u^{*}_{\delta_c} \\ u_{pilot} \end{bmatrix}$$

Figure 4-8. System Model for Flight Control System Design

The formulation for each of the component state models shown in Figure 4-8 is described below with the exception of the MCG model. MCG modeling has already been described in the previous section.

Aircraft State Model

Linear state models of the aircraft were obtained from the NASA Dryden developed nonlinear simulation of the OWRW by using a linear model extraction (LME) technique. In the LME process, the nonlinear simulation independent variables (inputs and states) are perturbed relative to an operating point (trim solution). The effects of these perturbations on the dependent variables (state-derivatives and outputs) is used to compute the stability derivatives. This method for extracting linear state models captures the aerodynamics and inertial coupling effects of the oblique wing configuration. The resulting six DOF state model contains the following states, controls and outputs:

$$x_{ac} = [u,v,w,\ p,q,r,\ \phi,\theta,\psi,\ ]^T$$

$$u_{ac} = [\delta_{E_L},\delta_{E_R},\delta_{A_L},\delta_{A_R},\delta_R]^T$$

$$y_{ac} = [V_T,\ \alpha,\ \beta,\ p,\ q,\ r,\ \phi,\ \theta,\ n_y,\ n_z,\ \gamma,\ \dot{\beta},\ M,\ h]^T$$

The control vector produced by the LME procedure is for physical controls. The system state model, which is used for the regulator design, replaces the physical controls with the generalized controls as discussed in Section 4.3.

Generalized Actuators State Model

The generalized actuators are modeled by the transfer function representation presented in section 4.3. The following state model structure is used for each of the generalized controls. The output vector includes the generalized actuator output and their deflection rate.

$$A_\delta = \begin{bmatrix} -2\zeta_\delta \omega_\delta & 1 \\ \omega_\delta^2 & 0 \end{bmatrix} \qquad B_\delta = \begin{bmatrix} \tau_\delta \omega_\delta^2 \\ \omega_\delta^2 \end{bmatrix}$$

$$C_\delta = \begin{bmatrix} 1 & 0 \\ -2\zeta_\delta \omega_\delta & 1 \end{bmatrix} \qquad D_\delta = \begin{bmatrix} 0 \\ \tau_\delta \omega_\delta^2 \end{bmatrix}$$

4.4.2 Regulator Synthesis

The regulator gain synthesis process includes several steps. The first step involves solving for the state feedback gain matrix using a steady-state solution of the Riccati equation minimize a quadratic performance index. The next step involves transforming the state feedback control law to an output feedback control law where the outputs are aircraft sensor measurements. The final step involves simplifying the control law by removing less important gains. This last step is important since the control law mechanization is based on in-line code (i.e., matrix operations are not used).

The basis of the LQ method is that a control system is designed which is optimal relative to a specified performance index. The most common choice for this performance index is the quadratic form given by

$$J = \int_0^\infty \left[x^T Q_x x + x^T N_x u + u^T N_x^T x + u^T R_x u \right] dt$$

Ctrl-C is used to generate the steady-state quadratic optimal regulator gains for this performance index. Minimization of this performance index results in a constant linear control law: i.e.,

$$u = -K_x x$$

In order to simplify the designer's task in selecting a suitable structure and parameter values for the weighting matrices Q_X, N_X and R_X, the performance index is redefined in terms of system outputs instead of system states: i.e.,

$$J = \int_0^\infty \left[y^T Q y + y^T N u + u^T N^T y + u^T R u \right] dt$$

By doing this and also using a design model structure like the one just described, the designer can directly relate Q to those quantities that are of interest (i.e., tracking error, control actuator rate and control authority). The following transformations are used to relate the output weighting matrices (Q, R) to those required for the LQ solution:

$$Q_x = C^T Q C$$

$$R_x = R + D^T N + N^T D + D^T Q D$$

$$N_x = C^T Q D + C^T N$$

The matrices *C* and *D* are from the system state model described in the previous section. The resulting control law is still a state feedback solution: i.e.,

$$u = - K_x x$$

As a part of the regulator synthesis process, the state control law is converted to an output control law by a transformation that maintains the eigenvalues of the closed loop system. This step is useful in that the engineering interpretation of the resulting LQ gain synthesis process is often enhanced by having an output gain solution. This transformation can be made whenever the output vector of the system model which is used for the LQ synthesis provides observability for all of the system's states and has at least as many output elements as there are states. The following equation defines the transformation between the state and output control laws.

$$K_y = \left[I - K_x \left(C^T W C \right)^{-1} C^T W D \right]^{-1} K_x \left(C^T W C \right)^{-1} C^T W$$

Again, the matrices *C* and *D* are from the system state model described in the previous section. The matrix *W* is a diagonal matrix, and it is used to select those elements of the output vector which are used for the transformation. The diagonal elements are either unity of some very small number (e.g., 10^{-6}). None of the diagonal elements can be zero because this would cause a singular solution. There must be at least as many unity elements as there are states. These requirements are satisfied for the OWRA control law synthesis task.

For the original LQ design work, the full six degree-of-freedom (6-DOF) model was used to determine the regulator gains for a combined longitudinal and lateral-directional control law. Because of the size of the system model (e.g., 35 states, 10 controls and 51 output quantities), the required computer solution time was too long for interactive design. When the resulting control laws were evaluated, it was observed that they were decoupled. The longitudinal control laws (i.e., the gains for ($\delta_{\dot{J}}$, $\delta_{\dot{W}}$ & $\delta_{\dot{Q}}$) included only longitudinal MCG commanded variables and longitudinal response variables). Similarly, the lateral-directional control laws (i.e., the gains for ($\delta_{\dot{P}}$ & $\delta_{\dot{R}}$) included only lateral-directional MCG commanded variables and lateral-directional response variables. Based on this observation, the closed loop eigenvalues were computed for two cases to see if it was possible to perform the OWRA control law synthesis with conventional longitudinal and lateral-directional problem formulations. The eigenvalues were computed by starting with a 6-DOF open loop model and then closing the loop first with the 6-DOF LQ design and secondly with a control law that was an amalgamation of separate longitudinal and lateral-directional LQ designs. The results of this comparison, illustrated in Figure 4-9, show that the closed loop stability is essentially the same for both design approaches. Because of this, separate longitudinal and lateral-directional control laws were designed for each of the nine flight conditions.

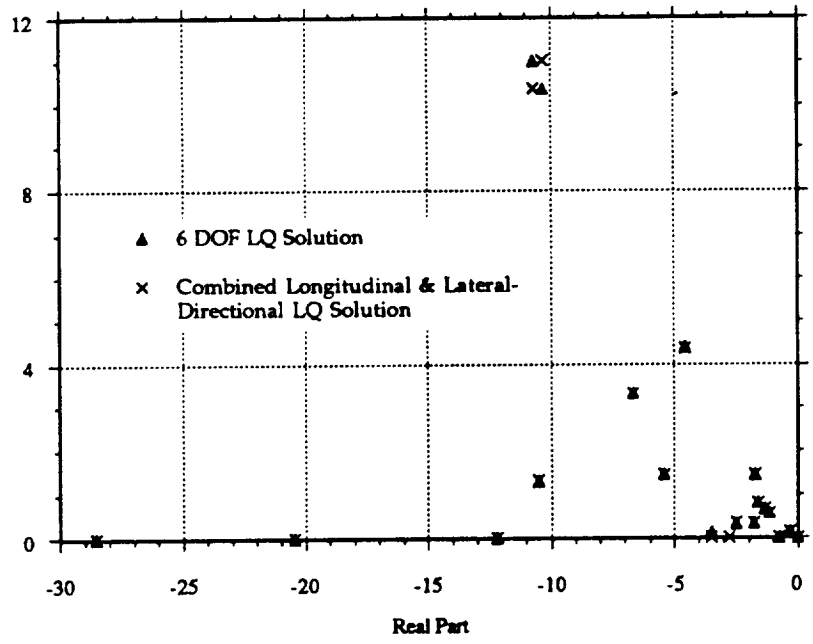

Figure 4-9 Comparison of Closed Loop Eigenvalues for 6-DOF and Separate Longitudinal and Lateral-Directional LQ Solutions

The regulator synthesis process is based on selecting values for the output weighting and control usage performance indices Q and R. The process is basically iterative in nature. The goal is to vary the diagonal terms of Q and R until good model-following and modal decoupling are achieved without using excessive control. These assessments can be based on simulating aircraft responses to pilot inputs. The tracking accuracy is evaluated by comparing aircraft and MCG

commanded responses. In addition, closed-loop eigenvalues also need to be evaluated in order to assess system stability.

For the tracking problem, as characterized by the system model presented in Figure 4-8, proportional and integral tracking errors, control surface displacement, and control surface rate are weighted. All other diagonal terms (i.e., MCG elements for y_{ac} and y_{mcg}) are set to zero. Initial selection of the nonzero Q_{ii} terms can be based on something like Bryson's rule (i.e., $(Q_{ii} = 1/y^2_{ii_{max}})$. Experience has shown that the control weighting indices (R_{ii}) associated with the generalized actuator commands can be set initially to unity. The weighting terms for the generalized actuators can be reduced to improve tracking performance. The other terms in the control vector (i.e., MCG and gust inputs) must be assigned very large values. By doing this, these inputs are effectively eliminated from the control law. As a test, the R_{ii} terms associated with the MCG inputs need to be large enough such that the closed-loop and open-loop eigenvalues of the MCG state model are the same.

Selection of diagonal elements of Q & R is an iterative process. The first design goal is to select values for Q_{ii} and R_{ii} that yield good model-following performance and disturbance rejection. This is best done through the evaluation of transients for both pilot and gust inputs. For example, the weighting parameters for Q_ε, θ_ε, $\int\theta_e$, and $\delta_q^{\bullet}$ can be adjusted to achieve good pitch rate tracking performance. After good tracking performance, disturbance rejection, and response decoupling are achieved, control surface rate can be penalized to reduce the high frequency control activity. Frequency responses of the generalized controls are a good means for assessing high frequency control activity. Selected values for the weighting matrices for both the longitudinal and lateral-directional control laws are presented in Figures 4-9 and 4-10, respectively.

Figures 4-9 and 4-10 also provide specifications for the W_{ii}'s which are part of the state to output control law transformation. For the longitudinal control law, the combination of actuator deflections and rates, commanded variables and tracking errors exceeds the number of states. A subset of these variables were selected for the transformation based on an analysis of the resulting output gain matrices. For example,when some of the commanded variables were included in the transformation, the gain relating $\dot{Q}_c$ to $\delta_{\dot{Q}}$ had the wrong sign. This type of analysis led to the elimination of n_{zc} and Q_c from the longitudinal weighting matrix.

Output Weighting: Q				Control Weighting: R	
i	y_i	Q_{ii}	W_{ii}	u_i	R_{ii}
1	V	0	10^{-5}	$\delta_{U_c}^{\bullet}$	0.001
2	α	0	10^{-5}	$\delta_{\dot{W}_c}^{\bullet}$	1.0
3	Q	0	10^{-5}	$\delta_{Q_c}^{\bullet}$	.01
4	θ	0	10^{-5}	δ_{SLON}	10^{5}
5	n_z	0	10^{-5}	V_{SEL}	10^{5}
6	$\delta_U^{\bullet}$	R(1,1)	1		
7	$\delta_{\dot{W}}^{\bullet}$	R(2,2)	1		
8	$\delta_Q^{\bullet}$	R(3,3)	1		
9	$d(\delta_U^{\bullet})/dt$	0	1		
10	$d(\delta_{\dot{W}}^{\bullet})/dt$	0	1		
11	$d(\delta_Q^{\bullet})/dt$	.001	1		
12	n_{zc}	0	10^{-5}		
13	$\dot{Q}_c$	0	1		
14	Q_c	0	10^{-5}		
15	θ_c	0	1		
16	α_c	0	1		
17	$\dot{V}_c$	0	1		
18	V_c	0	1		
19	Q_ε	50	1		
20	α_ε	500	1		
21	θ_ε	500	1		
22	V_ε	1	1		
23	$\int\alpha_\varepsilon$	0	1		
24	$\int\theta_\varepsilon$	5000	1		
25	$\int V_\varepsilon$	4	1		

Figure 4.9 Longitudinal Control Law Performance Index Specification

Output Weighting: Q				Control Weighting: R	
i	y_i	Q_{ii}	W_{ii}	u_i	R_{ii}
1	β	0	10^{-5}	$\delta_{V_c}^{\bullet}$	1.0
2	P	0	10^{-5}	$\delta_{P_c}^{\bullet}$	.10
3	R	0	10^{-5}	$\delta_{R_c}^{\bullet}$	.20
4	ϕ	0	10^{-5}	F_{PED}	10^{5}
5	n_y	0	10^{-5}	δ_{SLAT}	10^{5}
6	$\dot{\beta}$	R(1,1)	10^{-5}		
7	$\delta_V^{\bullet}$	R(1,1)	1		
8	$\delta_P^{\bullet}$	R(2,2)	1		
9	$\delta_R^{\bullet}$	R(3,3)	1		
10	$d(\delta_V^{\bullet})/dt$	0	1		
11	$d(\delta_P^{\bullet})/dt$	.001	1		
12	$d(\delta_R^{\bullet})/dt$	.001	1		
13	$\dot{\beta}_c$	0	1		
14	β_c	0	1		
15	$\dot{P}_c$	0	1		
16	P_c	0	1		
17	ϕ_c	0	1		
18	P_ε	4.0	1		
19	ϕ_ε	400	1		
20	$\dot{\beta}_\varepsilon$	100	1		
21	β_ε	4000	1		
22	$\int\beta_\varepsilon$	20000	1		
23	$\int\phi_\varepsilon$	4000	1		

Figure 4-10 Lateral-Directional Control Law Performance Index Specification

4.4.3 Control Law Simplification and Gain Scheduling

The objective for this step is to develop control law definitions that provide a continuous variation in gains with flight condition and aircraft configuration parameters. A second objective is to reduce the complexity of each control law by eliminating those gain elements which can be removed without causing a significant change in either the closed loop eigenvalues or the aircraft's model-following performance. This simplification step is important since a reduction in the number of gain elements directly reduces the amount of time which is required to process the control law with in-line code. A second reason for eliminating some of the gain terms, specifically some of the feedforward gains, is to improve the transient response to pilot commands when a common regulator gain solution (i.e., gain scheduling) is used for a broad range of operating points.

Structural considerations were used to eliminate a number of gains from the control laws. First, the actuator frequency command shaping, which results from the feedback of generalized actuator position and its rate, was decoupled for each generalized actuator. For example, the pitch axis control law ($\delta\dot{Q}_c$) contains only $\delta\dot{Q}$ and $d(\delta\dot{Q})/dt$ for actuator frequency compensation. Second, each feedforward acceleration command from the MCG was connected to only a single controller (e.g., $\dot{Q}_c \rightarrow \delta\dot{Q}_c$). Finally, integral error control was isolated to a single axis of control (e.g., $\int \phi_\varepsilon \rightarrow \delta\dot{P}_c$).

Because all gains for the vertical axis controller were found to be small, the vertical axis control law was eliminated from the control system. The largest gains would at the most produce $\delta\dot{W}$ commands of only one or two percent. This result is not too surprising because the longitudinal MCG was designed to generate commands for a conventional aircraft response (i.e., the load factor and pitch rate responses did not presume the availability of direct lift control).

Because all of the longitudinal gains were essentially independent of the design flight condition, average values were determined for each gain. Because the gains for both the roll and yaw axis control laws varied with flight condition, regression techniques were used used to establish appropriate scheduling schemes. Figures 4-11 and 4-12 present the longitudinal and lateral-directional control laws that resulted from the gain scheduling and simplification analysis.

Once the control law has been simplified as defined in Figures 4-11 and 4-12, it is necessary to check both the closed-loop eigenvalues for stability and transient response performance at each of the design poirts. The evaluation of the control system with the gain scheduled control laws is presented in Section 5.

Axial Axis Control Law

$$\dot{\delta_{U_C}} = K_{U_1} * \theta_C + K_{U_2} * \dot{V}_C + K_{U_3} * V_C + K_{U_4} * V_\varepsilon + K_{U_5} * \int V_\varepsilon$$

where,

$K_{U_1} = 7.00$	(%/deg)
$K_{U_2} = 10.76$	(%/fps^2)
$K_{U_3} = -0.20$	(%/fps)
$K_{U_4} = 26.59$	(%/fps)
$K_{U_5} = 23.25$	(%/fps-sec)

Pitch Axis Control Law

$$\dot{\delta_{Q_C}} = K_{Q_1} * \dot{Q}_C + K_{Q_2} * \alpha_C + K_{Q_3} * Q_\varepsilon + K_{Q_4} * \alpha_\varepsilon + K_{Q_5} * \theta_\varepsilon + K_{Q_6} * \int \theta_\varepsilon$$

where,

$K_{Q_1} = 0.0226$	(%/deg/sec^2)
$K_{Q_2} = 14.23$	(%/deg)
$K_{Q_3} = 12.17$	(%/deg/sec)
$K_{Q_4} = -13.12$	(%/deg/sec)
$K_{Q_5} = 59.55$	(%/deg)
$K_{Q_6} = 85.04$	(%/deg-sec)

Figure 4-11 Longitudinal Control Laws

Roll Axis Control Law

$$\dot{\delta_{P_C}} = K_{P_1} * \dot{P_c} + K_{P_2} * P_c + K_{P_3} * P_\varepsilon + K_{P_4} * \phi_\varepsilon + K_{P_5} * \dot{\beta_\varepsilon} + K_{P_6} * \beta_\varepsilon + K_{P_7} * \int \phi_\varepsilon$$

$$K_{P_1} = 0.20 + .065*\cos\Lambda + .027*q_{r_1} - .018*q_{r_3}$$
$$K_{P_2} = -55.0 + 1.77*\cos\Lambda + .40*q_{r_1} - .24*q_{r_3}$$
$$K_{P_3} = 2.59 + 1.11*\sin\Lambda + .17*q_{r_1} - .38*q_{r_1}*\cos\Lambda$$
$$K_{P_4} = 33.87 - 9.36*\sin\Lambda + 1.95*q_{r_1} - 1.02*q_{r_3}$$
$$K_{P_5} = 0.17 - 1.99*q_{r_1}$$
$$K_{P_6} = -5.51 - 112.5*q_{r_1} + 16.3*q_{r_3} + 130.3*q_{r_1}*\cos\Lambda$$
$$K_{P_7} = -67.4 + 18.7*\sin\Lambda - 3.89*q_{r_1} + 1.97*q_{r_3}$$

Yaw Axis Control Law

$$\dot{\delta_{R_C}} = K_{R_1} * \dot{\beta_c} + K_{R_2} * \beta_c + K_{R_3} * P_\varepsilon + K_{R_4} * \phi_\varepsilon + K_{R_5} * \dot{\beta_\varepsilon} + K_{R_6} * \beta_\varepsilon + K_{R_7} * \int \beta_\varepsilon$$

$$K_{R_1} = 2.57 - 8.50*q_{r_1} + 5.58*q_{r_2}$$
$$K_{R_2} = 14.58 - 45.39*q_{r_1} + 24.59*q_{r_2} - 14.71*\cos\Lambda$$
$$K_{R_3} = 4.35 - 5.02*\cos\Lambda - 0.79*q_{r_1} + 0.48*q_{r_3}$$
$$K_{R_4} = 18.91 - 19.43*\cos\Lambda$$
$$K_{R_5} = -23.46 + 5.95*q_{r_1} - 3.17*q_{r_2}$$
$$K_{R_6} = -90.54 + 39.89*q_{r_1} - 21.82*q_{r_2}$$
$$K_{R_7} = -160.00$$

where,

$$q_{r_1} = \left(\frac{\bar{q}_c}{435.59} - 1.0\right); \quad q_{r_2} = q_{r_1} * |q_{r_1}|; \quad q_{r_3} = q_{r_1}^2$$

Figure 4-12 Lateral-Directional Control Laws

4.5 CONTROL SELECTOR DESIGN

The primary function of the control selector is to transform the generalized control commands, which are generated by the flight control system regulator, to commands for the aircraft's control surface actuators and the propulsion control system. The design requirement for this transformation is to match the loop gain of the integrated flight/propulsion control system with a closed loop system based on generalized controls. With reference to Figure 4-13, the MIMO transfer function from $\delta_c^* \rightarrow \Delta \dot{x}_{CONT}$ must be matched. Both control power and actuator dynamics must be considered in matching the transfer functions between the generalized control mechanization (top part of Figure 4-13 and the IFPC mechanization (lower part of Figure 4-13). The process for transforming generalized controls (δ_c^*) to physical controls (δ_c) is based on a transformation matrix: i.e.,

$$\delta_c = T_{CS}\, \delta_c^*$$

The control transformation matrix (T_{CS}) is based on solving a pseudo inverse on-line. The following expression defines the expression for computing T_{CS}:

$$T_{CS} = N_{MAX} \left(B_{AC}\, N_{MAX}\right)^{\#} B_{AC}^*$$

$\left(B_{AC}\, N_{MAX}\right)^{\#}$ is the pseudo inverse of the control distribution matrix for the physical controls B_{AC}. B_{AC}^* is the control distribution matrix for the generalized controls, and N_{MAX} is a normalization matrix[1] for the pseudo inverse computation.

Each element of B_{AC} is computed from models that define the effectiveness of the aerodynamic control surfaces and that due to net thrust. These computations are computed on line and they account for the aircraft's current flight condition and operating point. B_{AC}:

---

[1] *The scaling matrix (N_{MAX}) is normally inverted for solving the pseudo inverse of a matrix. When it is inverted, the pseudo inverse solution also requires an inverse of the scaling matrix. For real time considerations, the requirement for solving a double inverse is eliminated by using the above expression for the pseudo inverse and the definition for the weighting matrix as defined below.*

$$B_{AC} = \begin{bmatrix} X_{T_N} & X_{\delta_{H_{SYM}}} & 0 & X_{\delta_{A_{SYM}}} & 0 & 0 \\ 0 & 0 & L_{\delta_{H_{ASY}}} & 0 & L_{\delta_{A_{ASY}}} & L_{\delta_R} \\ 0 & M_{\delta_{H_{SYM}}} & 0 & M_{\delta_{A_{SYM}}} & 0 & 0 \\ 0 & 0 & N_{\delta_{H_{ASY}}} & 0 & N_{\delta_{A_{ASY}}} & N_{\delta_R} \end{bmatrix}$$

Aerodynamic terms are modeled by equations that define the dimensional stability parameters as a function of the reference geometry, mass and inertia properties, the dynamic pressure and a nondimensional stability derivative: i.e.,

$$X_{\delta_0} = \frac{\bar{q}\ S_W}{m} C_{X_{\delta 0}}$$

$$M_{\delta_0} = \frac{\bar{q}\ \bar{C}_W\ S_W}{I_Y} C_{m_{\delta 0}}$$

$$L_{\delta_0} = \frac{\bar{q}\ b_W\ S_W}{I_X} C_{l_{\delta 0}}$$

$$N_{\delta_0} = \frac{\bar{q}\ b_W\ S_W}{I_Z} C_{n_{\delta 0}}$$

Aircraft mass and inertias are computed on line as a function of wing skew position (see Figure 2-3) and aircraft fuel weight. The nondimensional stability derivatives (e.g., $C_{m_{\delta H_{SYM}}}$: the change in pitching moment coefficient due to symmetric horizontal tail deflection) are based on the OWRA's aerodynamic data base. Table lookup or curve fitted expressions could be used to implement the stability derivatives. The single stability parameter for net thrust (X_{T_N}) is modeled as follows:

$$X_{T_N} = \frac{T_{TRIM}}{m}$$

The normalization matrix N_{MAX} is used to establish relative weighting between the various aerodynamic controls and propulsion system force/moment producers. N_{MAX} is a diagonal matrix with each element along the diagonal being the maximum allowed control deflection or change in thrust magnitude at any point during the flight.

V. DESIGN EVALUATION

5.1 OVERVIEW

An evaluation of the explicit model-following control system designed for the Oblique Wing Research Aircraft is presented in this section of the report. The primary objective of this evaluation centered on demonstrating the model-following performance of the gain scheduled control system. Because the MCG was designed to embody Level 1 flying quality properties and its structure assumes decoupled control of the longitudinal and lateral-directional degrees of freedom, the model-following performance is indicative of how well the design goals (see Section 4.2.1) have been achieved.

Evaluation results are presented in three subsections. The first presents an analysis of the closed loop stability of the OWRA with the gain scheduled control system. Next, frequency responses of the MCG commanded variables and corresponding aircraft responses are compared. Finally, transient responses for pilot stick, pedal and speed commands are presented for all nine flight conditions.

5.2 SYSTEM STABILITY ANALYSIS

The purpose of the stability analysis was to assess how much the closed loop stability was affected by the selected gain schedule formulation of the control law. This assessment is based on plotting the eigenvalues of the gain scheduled control laws and those from the individual designs for each of the nine flight conditions (see Figures 5-1 through 5-9). As shown, the closed loop eigenvalues are altered by the gain scheduling, but the overall system stability is retained.

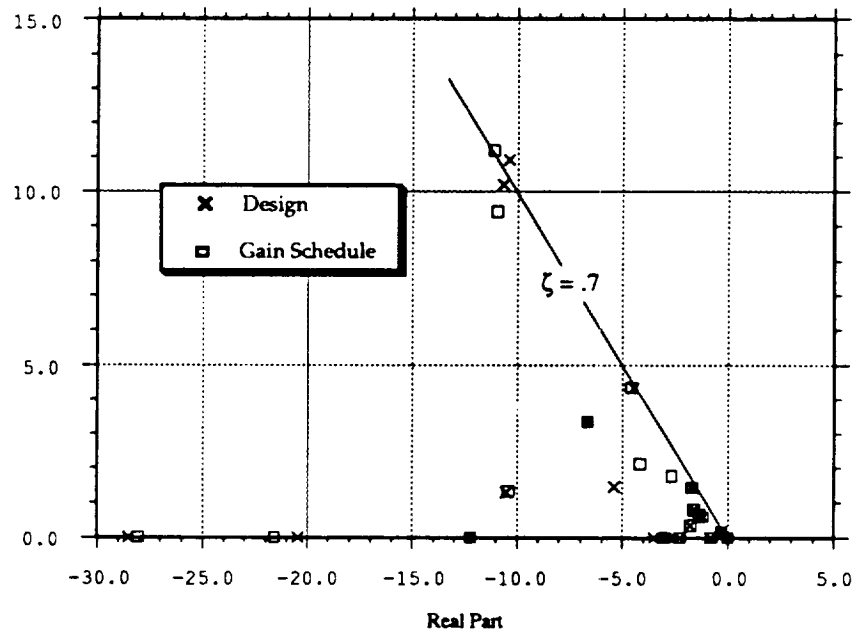

Figure 5-1 Effect of Gain Scheduling on Closed Loop Stability: Case 1

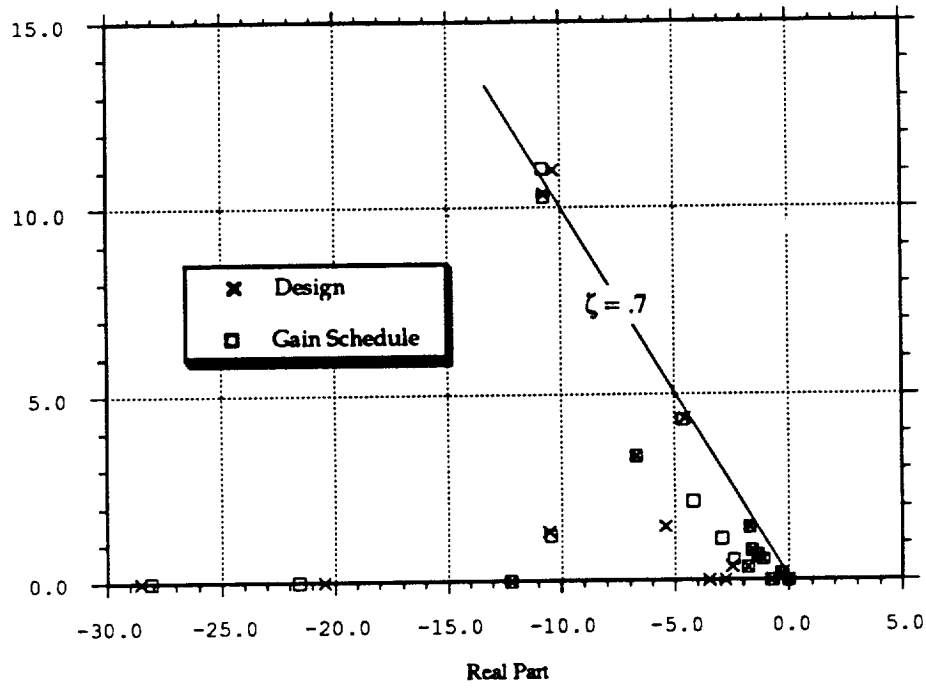

Figure 5-2 Effect of Gain Scheduling on Closed Loop Stability: Case 2

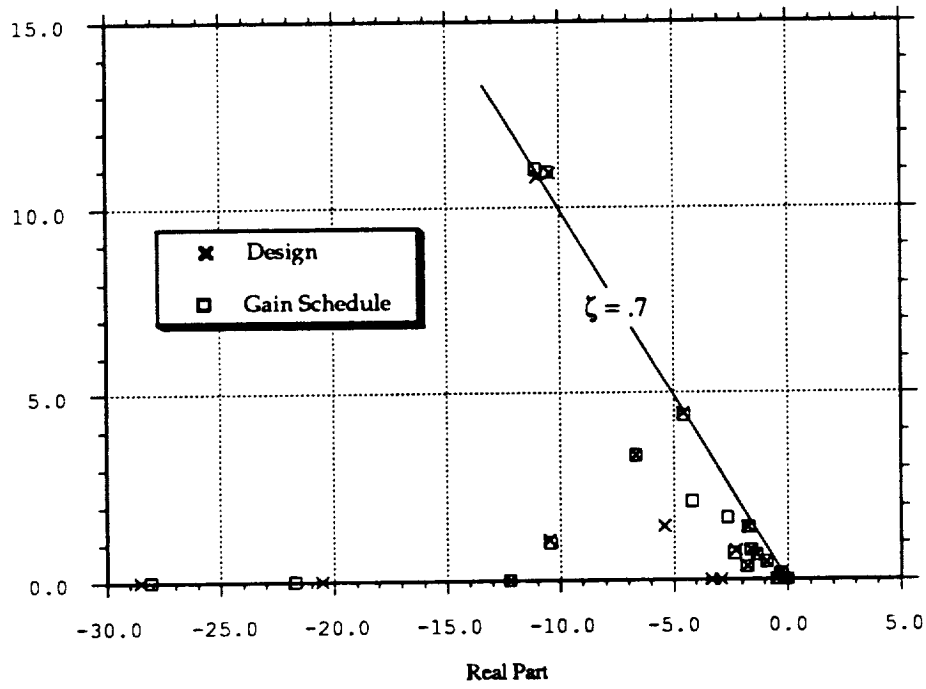

Figure 5-3 Effect of Gain Scheduling on Closed Loop Stability: Case 3

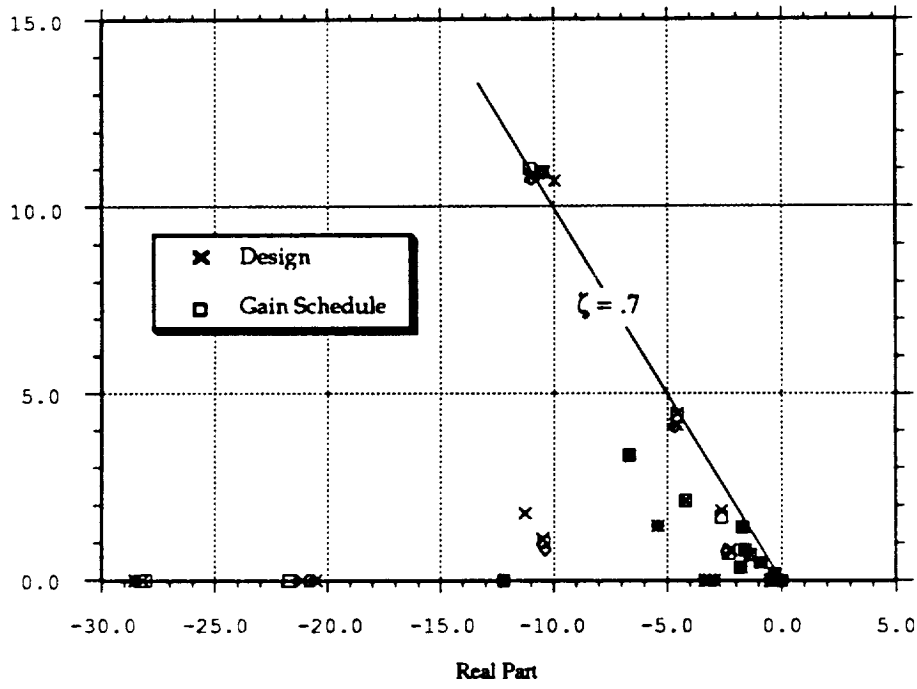

Figure 5-4 Effect of Gain Scheduling on Closed Loop Stability: Case 4

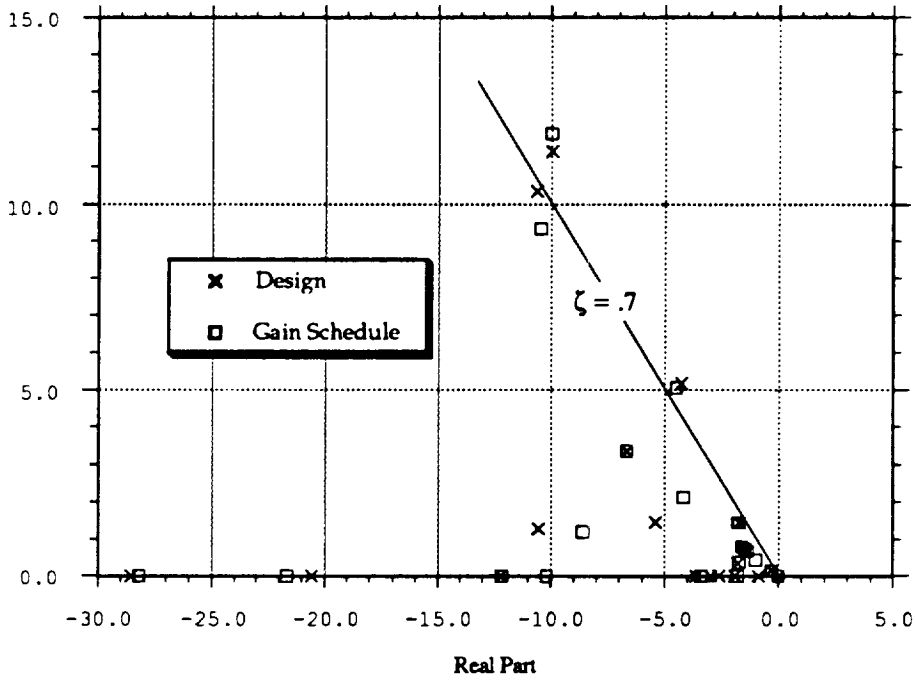

Figure 5-5 Effect of Gain Scheduling on Closed Loop Stability: Case 5

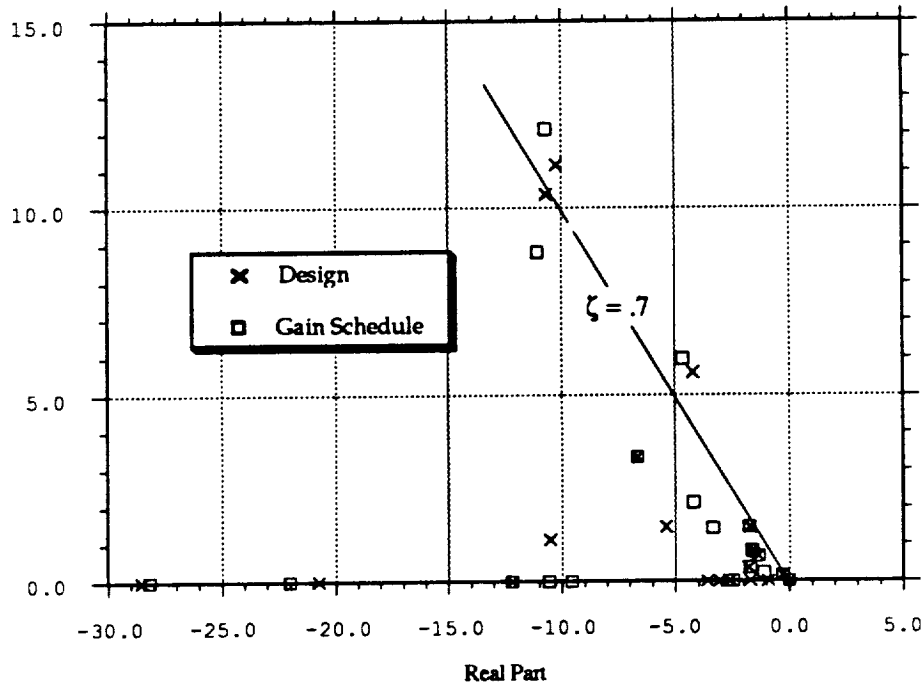

Figure 5-6 Effect of Gain Scheduling on Closed Loop Stability: Case 6

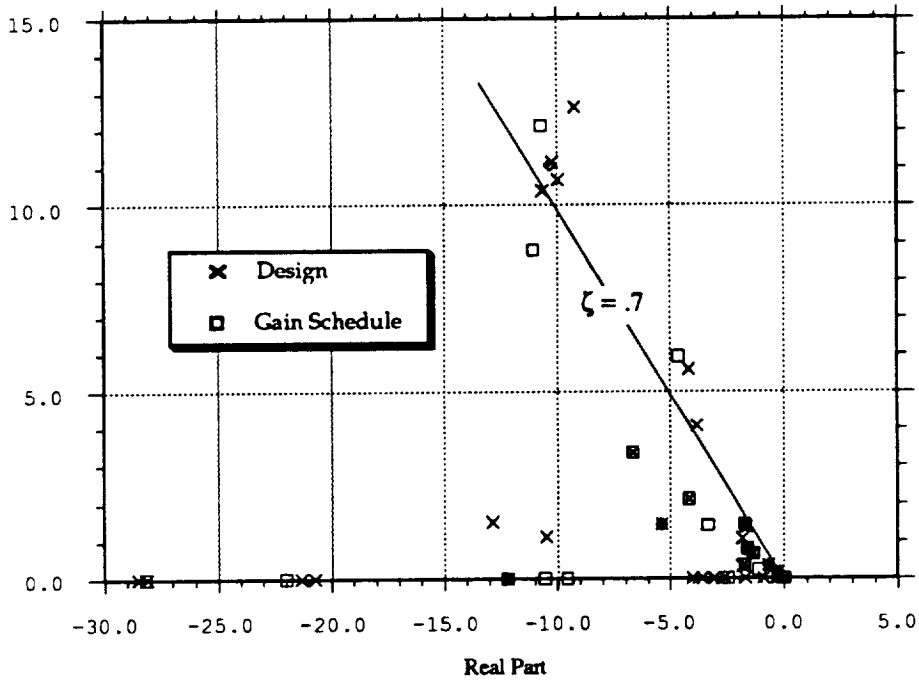

Figure 5-7 Effect of Gain Scheduling on Closed Loop Stability: Case 7

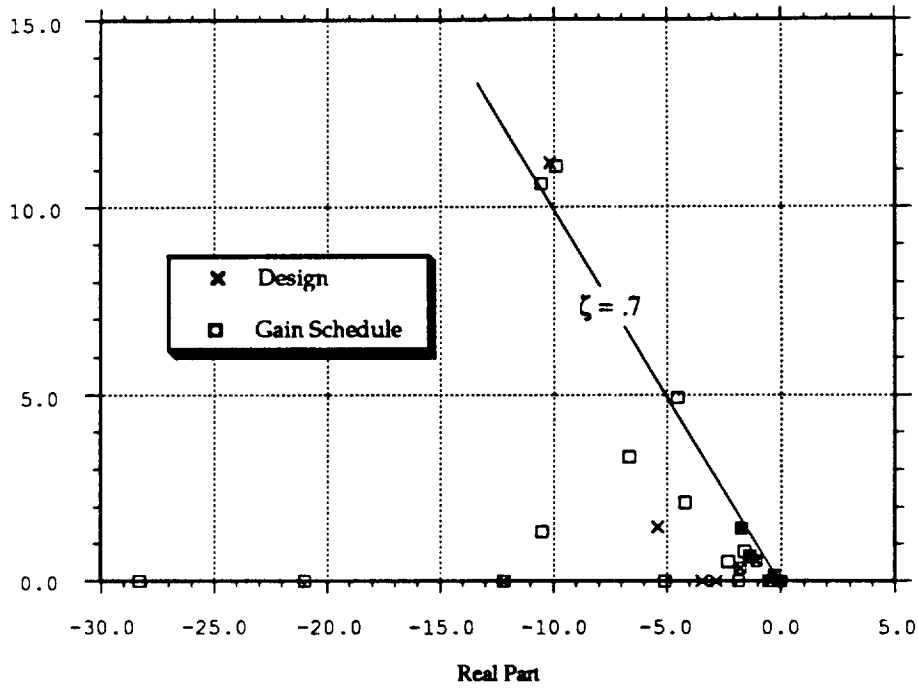

Figure 5-8 Effect of Gain Scheduling on Closed Loop Stability: Case 8

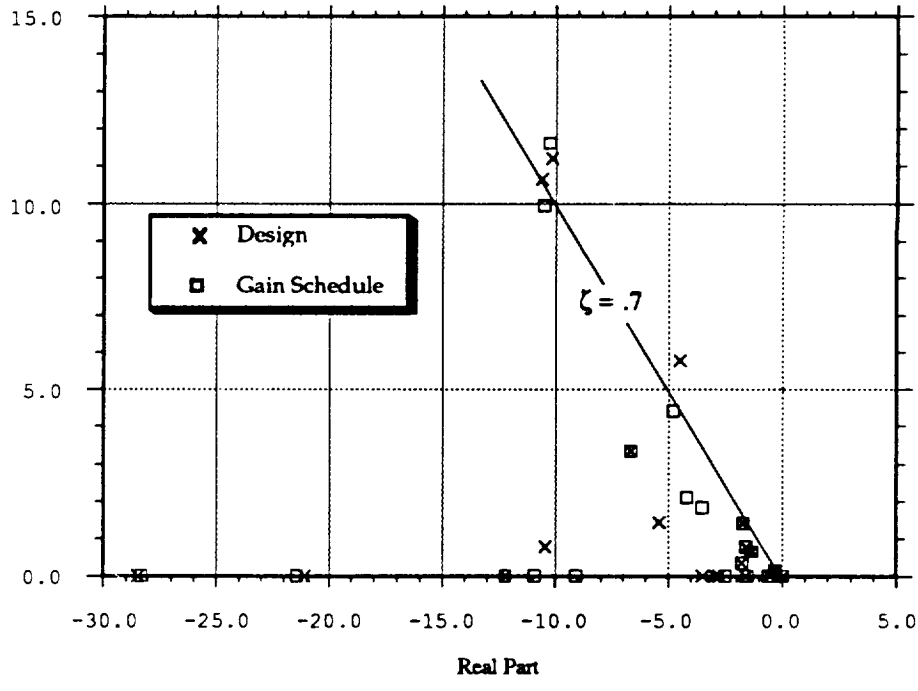

Figure 5-9 Effect of Gain Scheduling on Closed Loop Stability: Case 9

5.3 FREQUENCY RESPONSES

Figures 5-10 through 5-13 present frequency responses that compare the MCG commands with the aircraft's response for pitch rate, airspeed, roll rate and sideslip, respectively. These frequency responses were generated for the gain scheduled control system for design flight condition #2 (Λ =55°; M = 0.8; h = 20,000 ft). As shown by these frequency responses, the steady state tracking is perfect. This is to be expected as a result of including integral error control as a part of the control strategy. Tracking accuracy is very good with the response of the aircraft being nearly identical to that of the MCG up to the frequency at which the roll-off in the response exceeds -20 db. The difference in the phase responses at high frequencies is due to the fact that the aircraft's response includes additional dynamics (i.e., the generalized actuators).

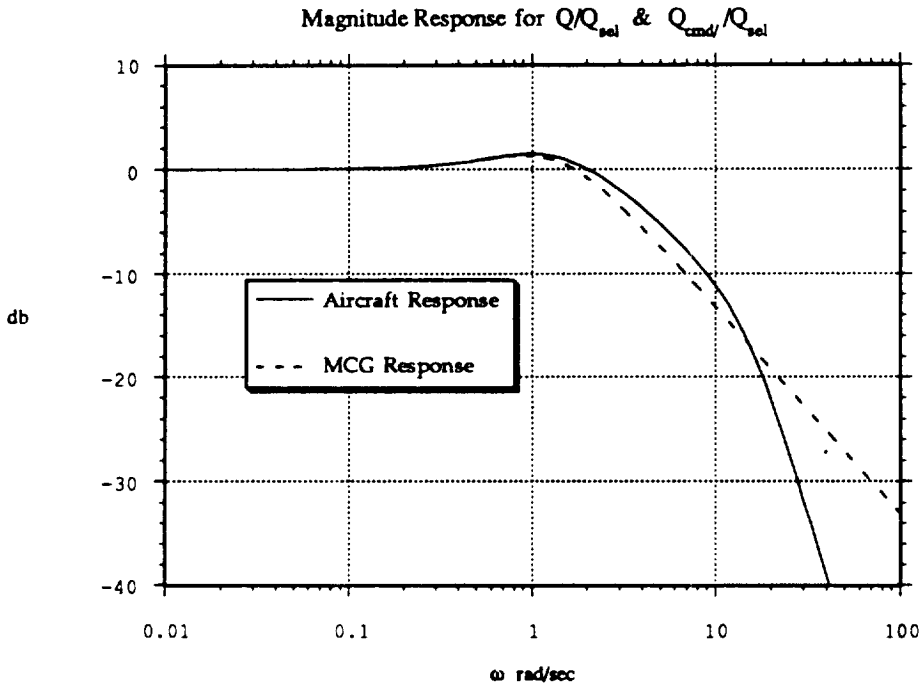

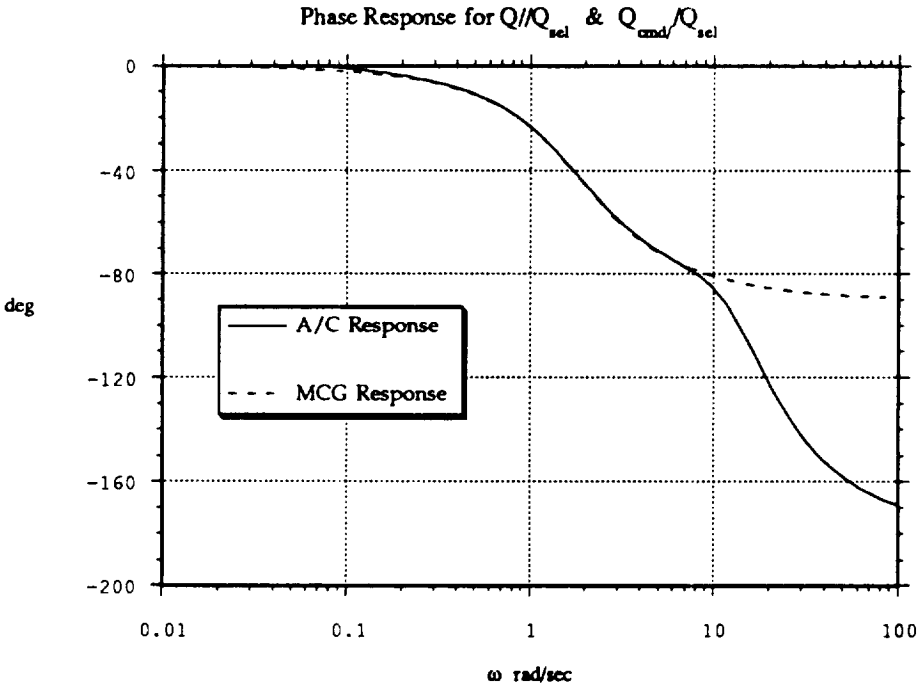

Figure 5-10 Pitch Rate Model-Following Performance

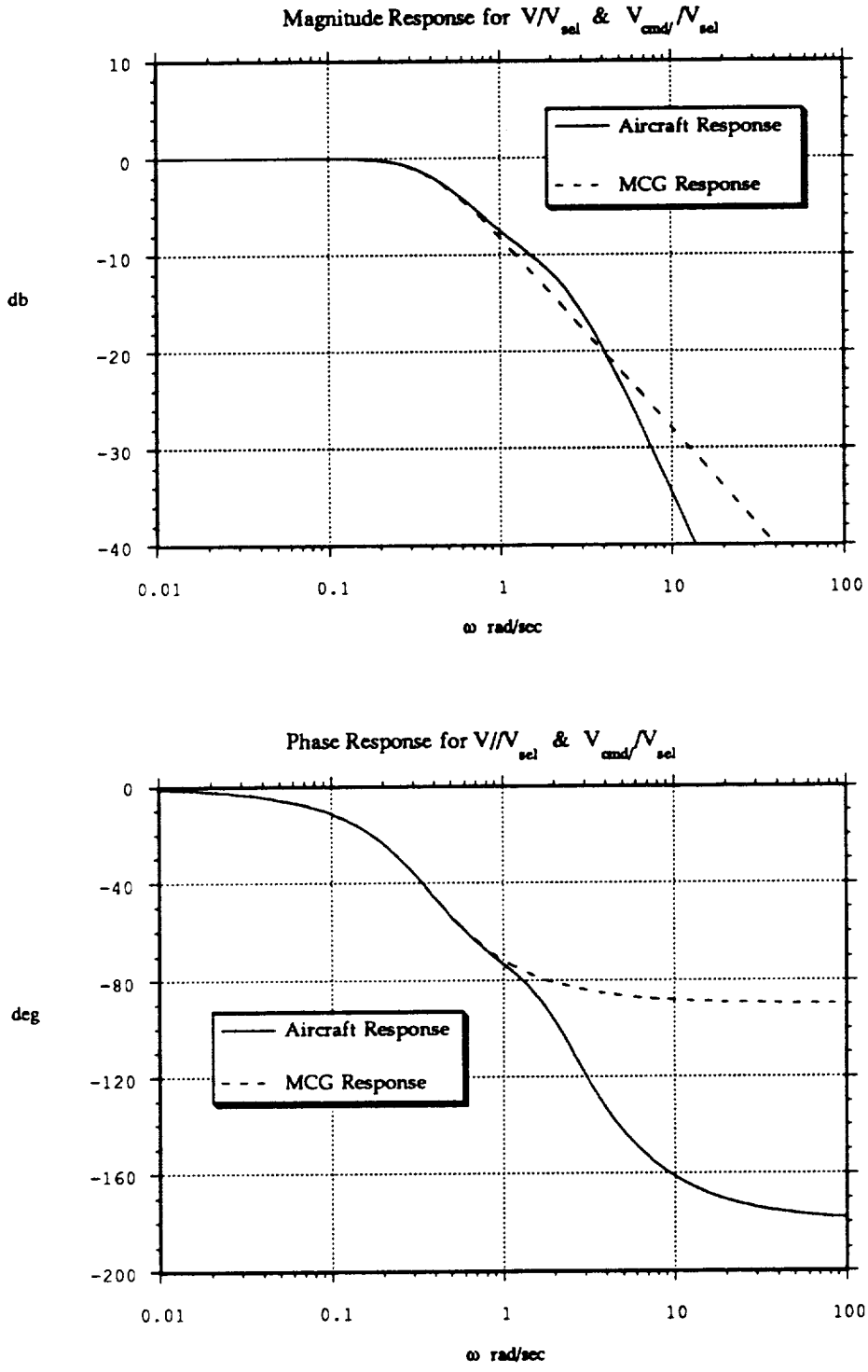

Figure 5-11 Airspeed Model-Following Performance

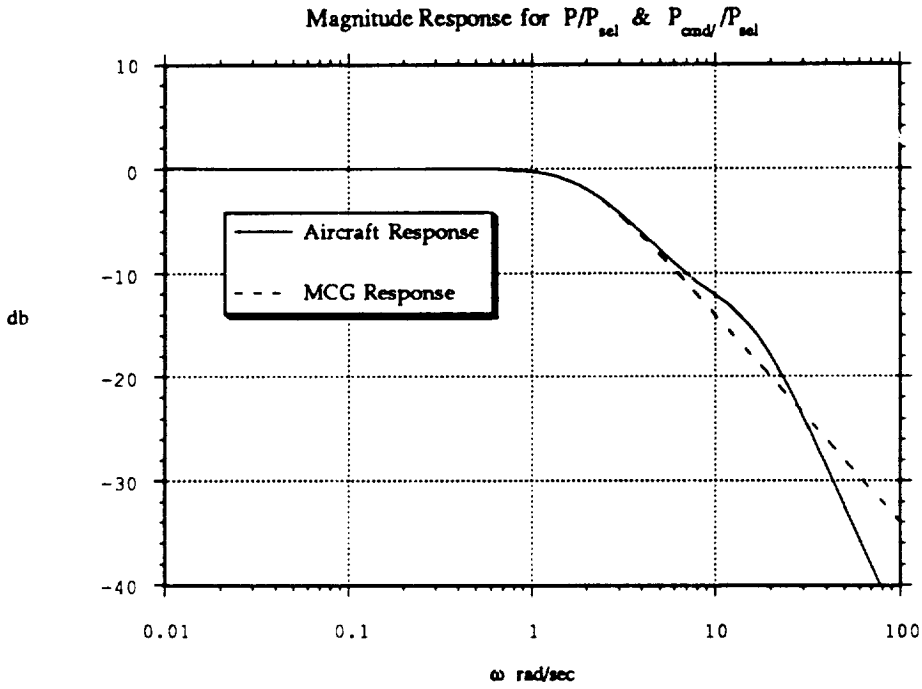

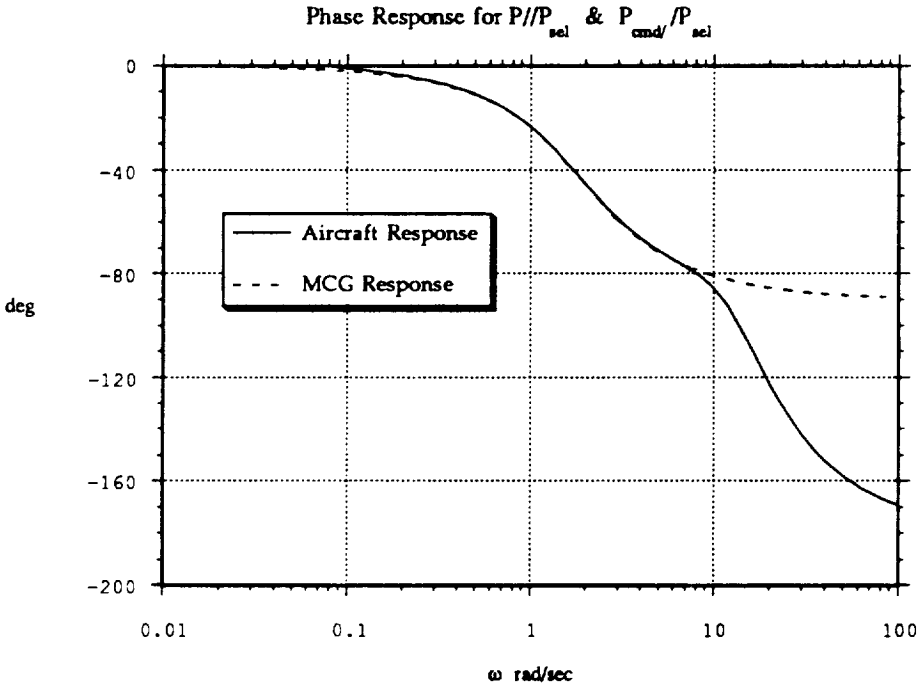

Figure 5-12 Roll Rate Model-Following Performance

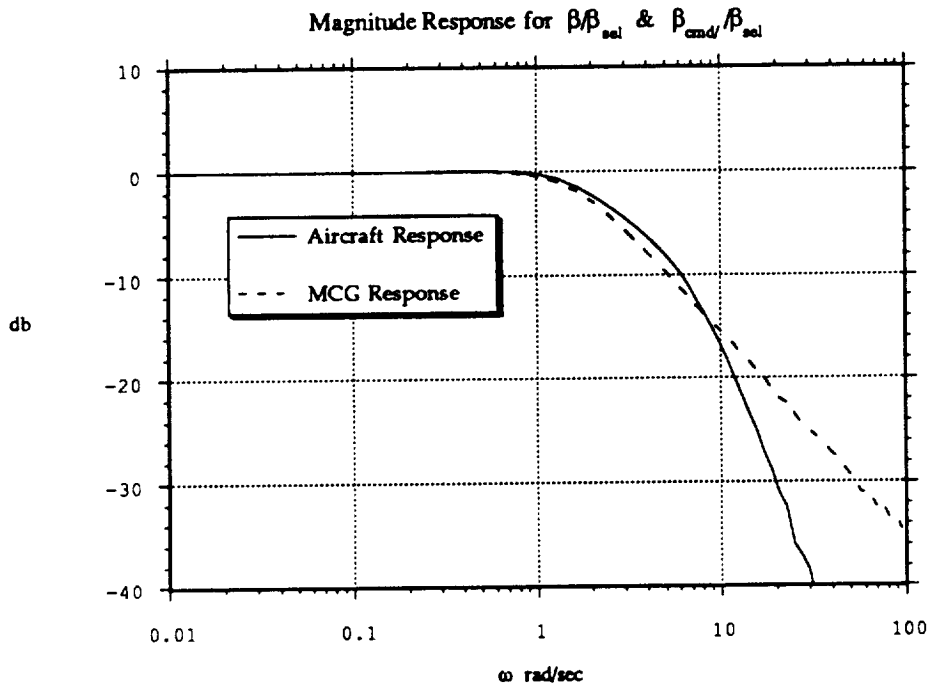

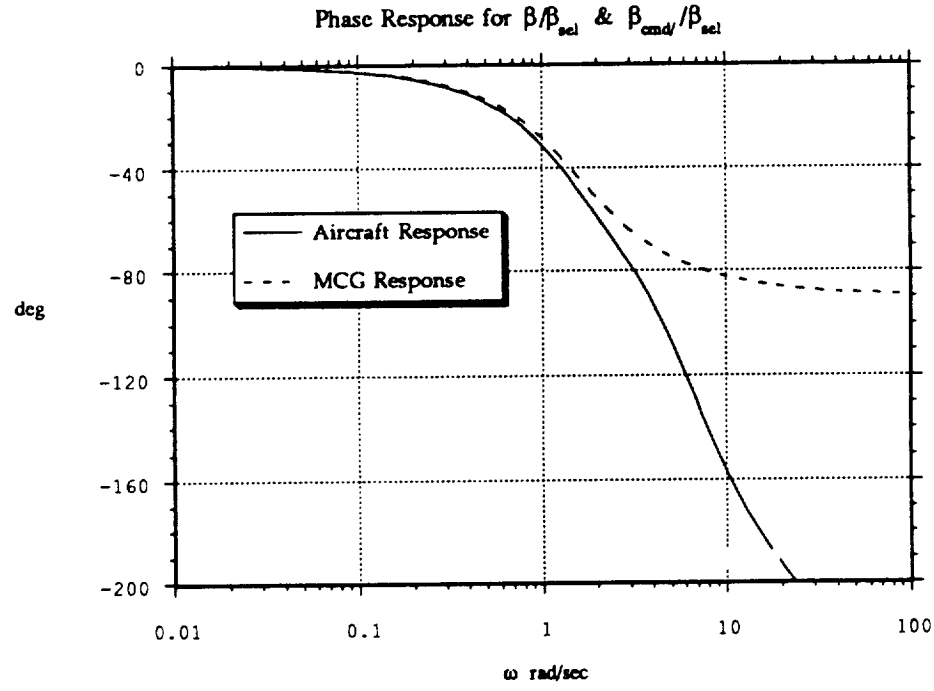

Figure 5-13 Sideslip Model-Following Performance

5.4 TRANSIENT RESPONSES

Transient responses have been generated for longitudinal stick deflection (δ_{slon}), airspeed commands (ΔV), lateral stick deflection (δ_{slat}), and pedal force commands (ΔF_{ped}) for each of the nine flight conditions (see Table 1-1). The properties of the standard set of command variables are defined in Figure 5-14. The aircraft's longitudinal, lateral-directional and control surface responses are presented to document the transient performance of the gain scheduled flight control system. Responses for the following set of variables are presented in Figures 5-15 through 5-50.

Plot Variable	Variable Description	Units
Q	pitch rate	deg/sec
α	angle-of-attack	deg
V	airspeed	fps
θ	pitch attitude	deg
P	roll rate	deg/sec
R	yaw rate	deg/sec
β	sideslip	deg
ϕ	bank angle	deg
$\delta_U^{\bullet}$	generalized axial acceleration control	%
$\delta_Q^{\bullet}$	generalized pitch acceleration control	%
$\delta_P^{\bullet}$	generalized roll acceleration control	%
$\delta_R^{\bullet}$	generalized yaw acceleration control	%

The responses for each of the nine flight conditions are generally similar. This is a reflection of the explicit model-following design philosophy and the design features of the Maneuver Command Generator. The model-following capability of the proportional/integral error control regulator contributes to the overall uniformity of these responses. Basically, the aircraft's response mirrors the MCG commands when the regulator provides good tracking performance. Thus, the differences in the responses from one flight condition to the next reflect mostly changes in the MCG's commands. As it was discussed in Section 4, the properties of the roll and airspeed command generators are identical for all nine flight conditions. The properties for the pitch rate MCG and the desired frequency for the directional MCG are flight condition dependent. However, the variation from one flight condition to the next is well behaved.

The transient performance for each of the four inputs is summarized as follows:

Longitudinal Stick Commands

- The pitch rate response reflects the desired short period dynamics and the rate command/ attitude hold design feature.
- Airspeed is held constant throughout the pitch maneuver.
- Lateral-directional responses are essentially suppressed completely.
- Generalized control responses are well behaved; the large change in $\delta_U^{\bullet}$ reflects the axial control required to retrim the aircraft after an approximate 8° change in pitch attitude and flight path angle.

Airspeed Commands

- The airspeed response is rapid and well damped.
- The changes in α and θ with airspeed are due to the retrimming logic in the longitudinal MCG (i.e., the $\Delta\dot{V} \rightarrow \Delta Q$ path). Because the changes in α and θ are nearly identical, the desired result of keeping flight path constant is achieved.
- Lateral-directional responses are essentially suppressed completely.
- Generalized control responses are well behaved; the large initial value for $\delta_U^{\bullet}$ reflects the level of control required to accelerate the OWRA from a trimmed flight condition.

Lateral Stick Commands

- The roll rate command/attitude hold design feature is achieved.
- Turn coordination is excellent.
- Longitudinal responses are essentially suppressed completely.
- Generalized control responses are well behaved and small.

Pedal Commands

- The sideslip response is rapid and well damped.
- The desired roll response is completely decoupled.
- Longitudinal responses are essentially suppressed completely.
- Generalized control responses are well behaved; the large value for $\delta_R^{\bullet}$ reflects the level of available directional control power for the OWRA.

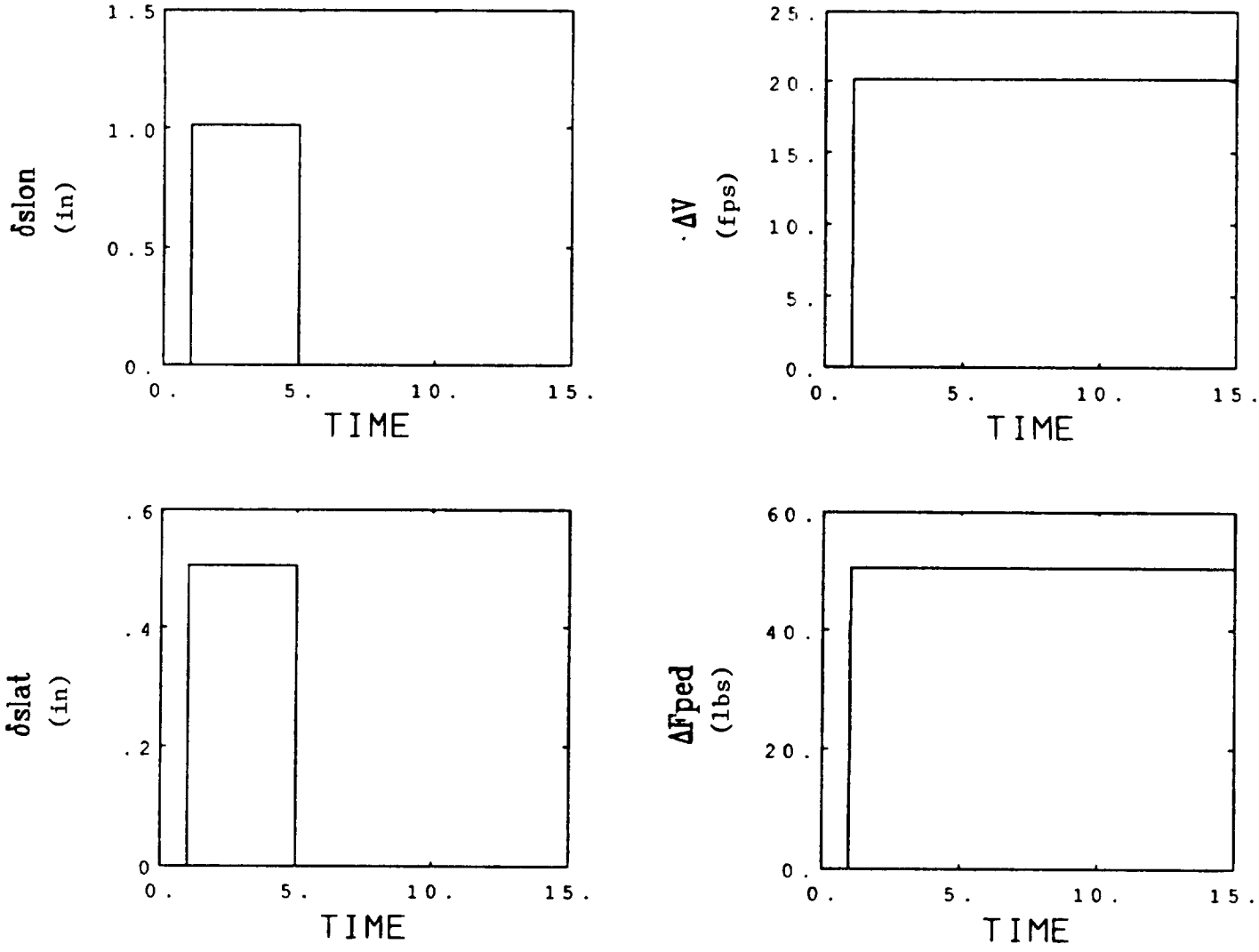

Figure 5-14 Pilot Controller Commands for Transient Performance Analysis

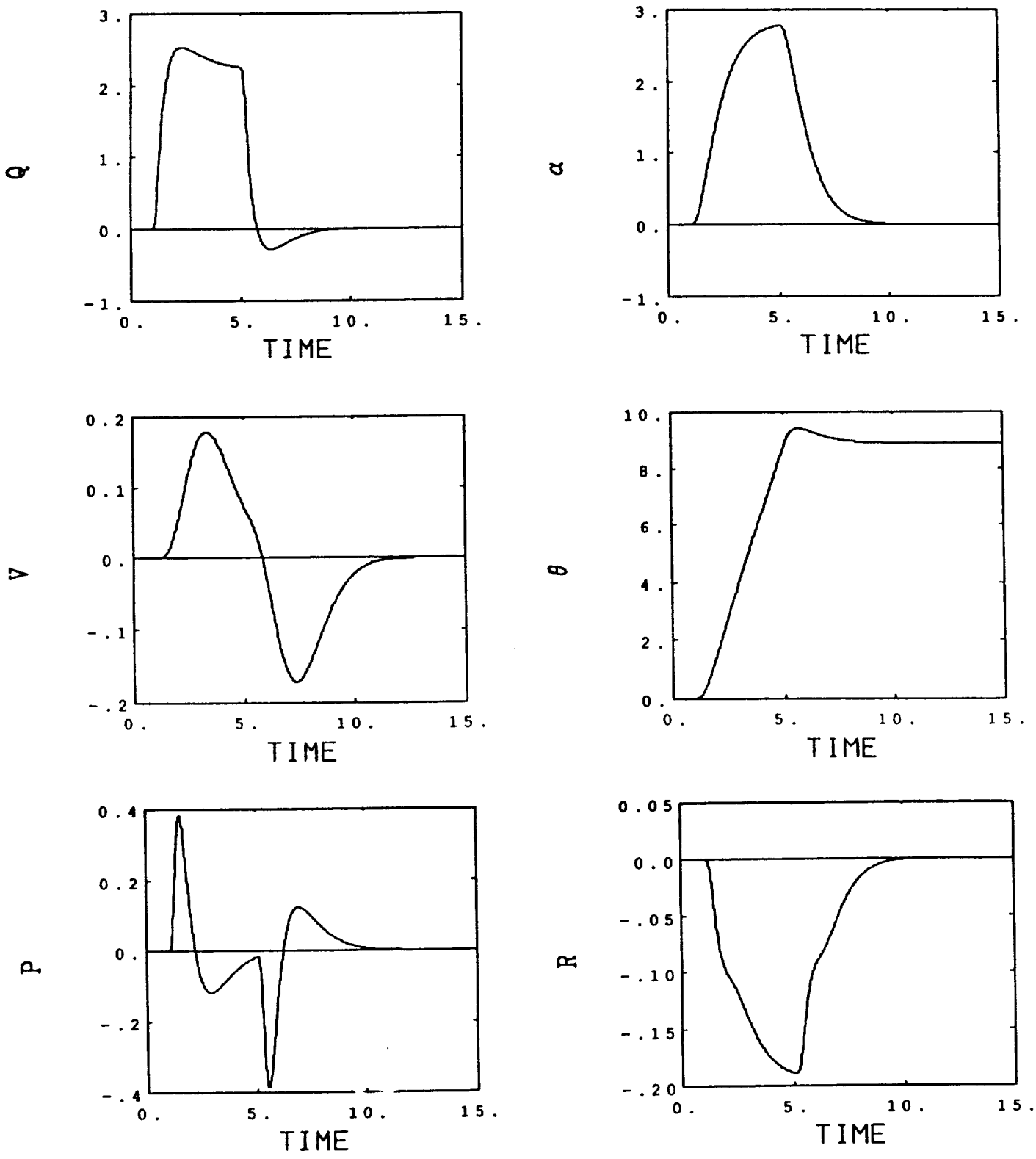

Figure 5-15a Longitudinal Stick Command: Case 1

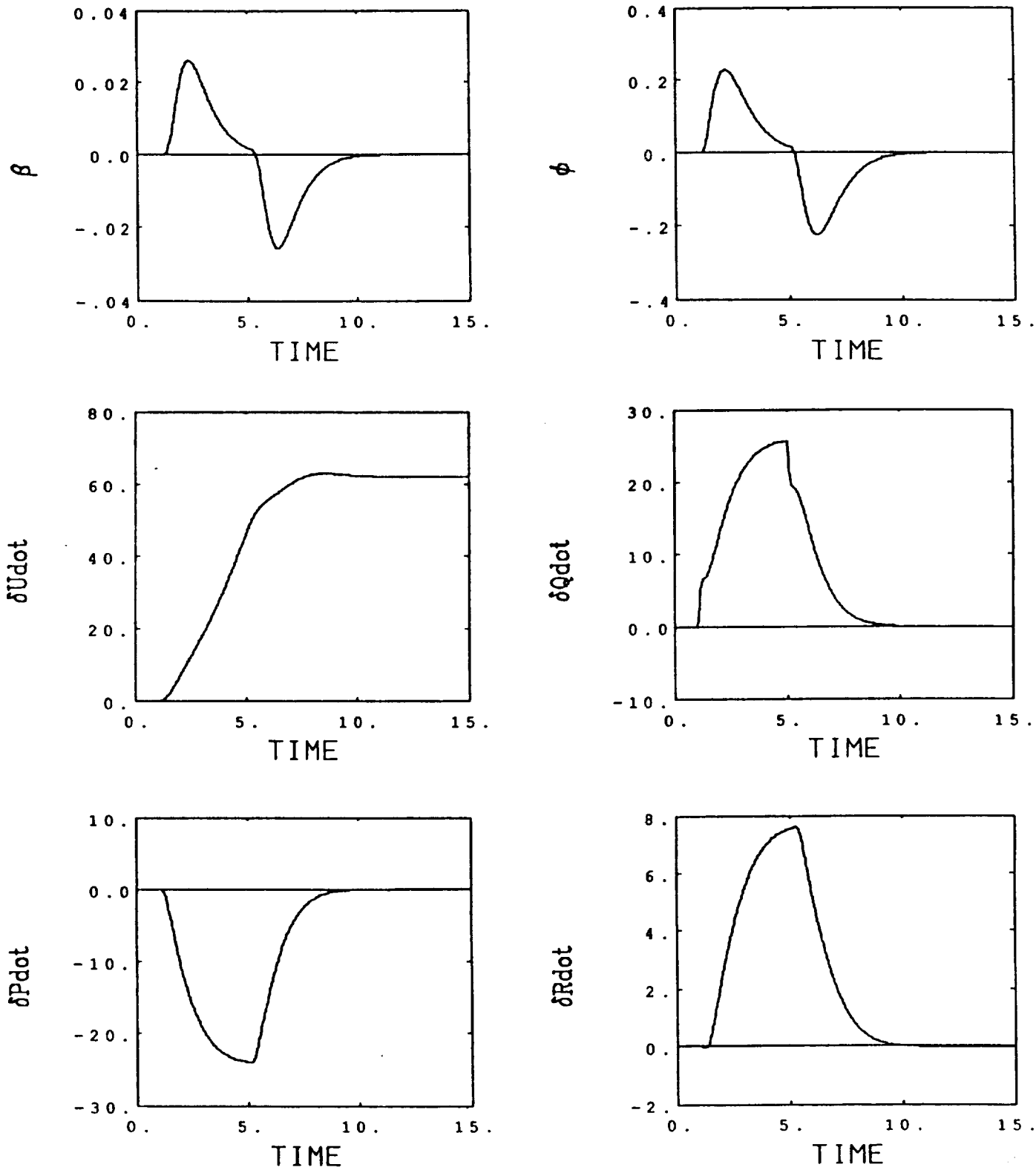

Figure 5-15b Longitudinal Stick Command: Case 1

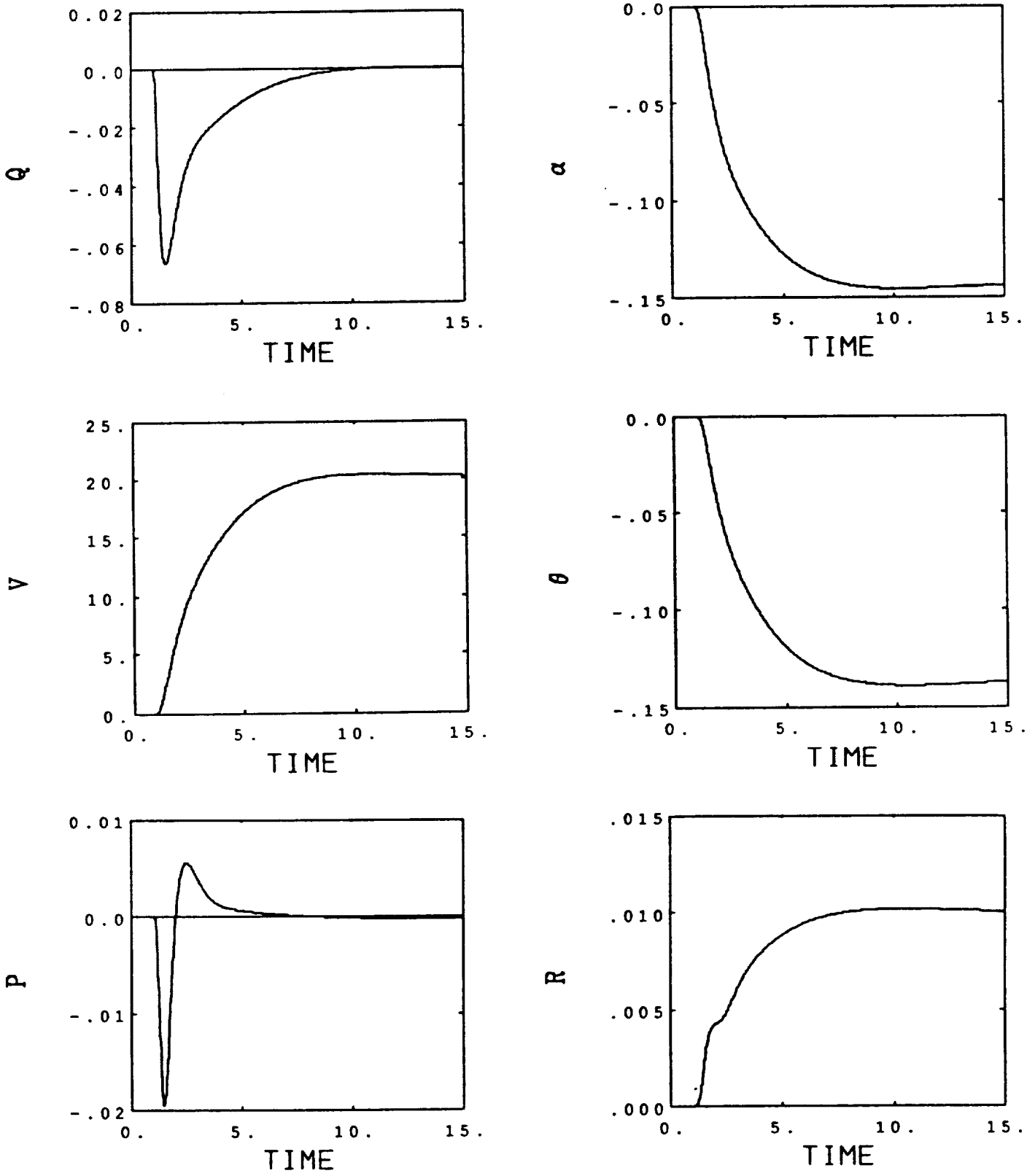

Figure 5-16a Airspeed Command: Case 1

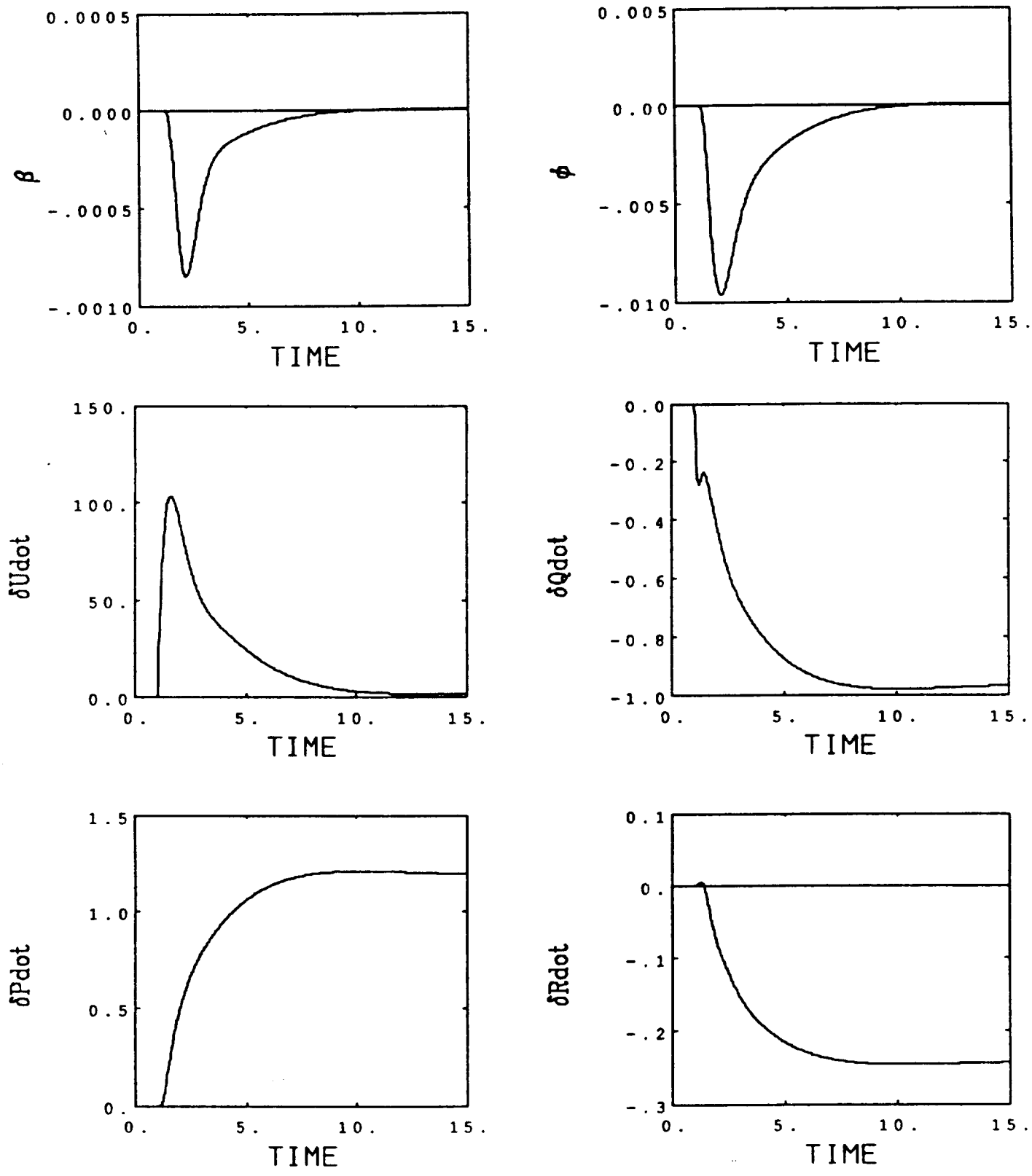

Figure 5-16b Airspeed Command: Case 1

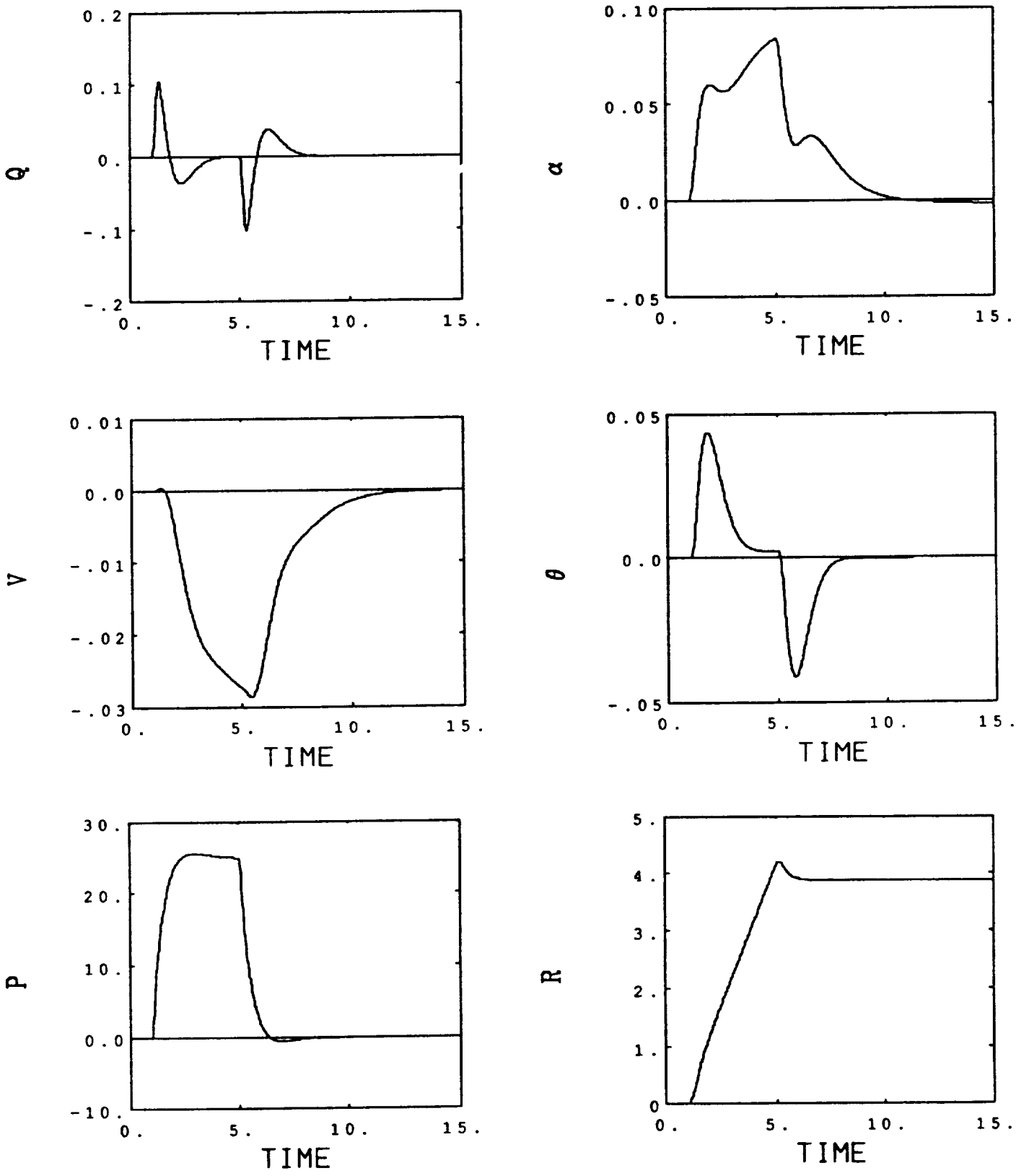

Figure 5-17a Lateral Stick Command: Case 1

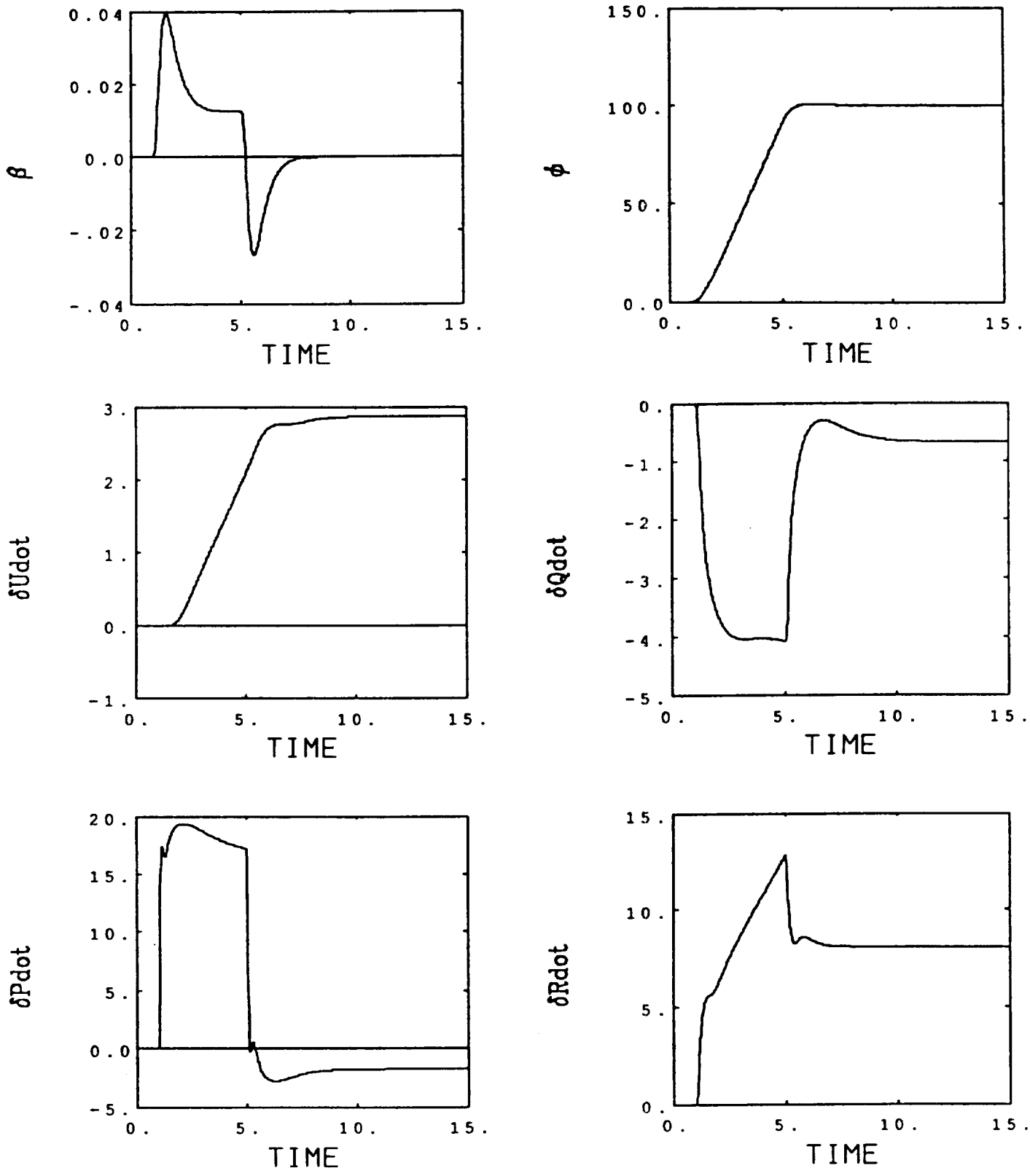

Figure 5-17b Lateral Stick Command: Case 1

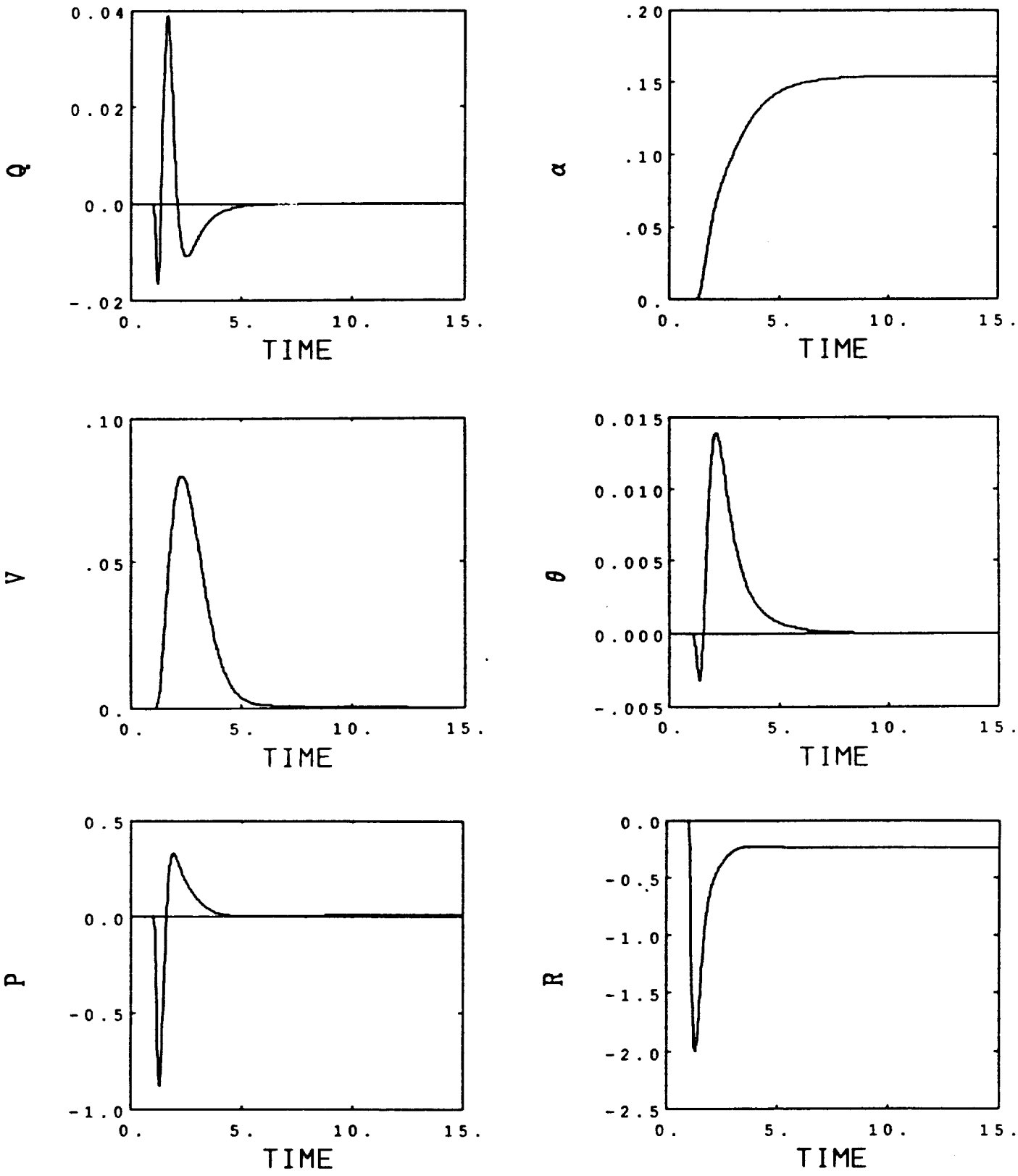

Figure 5-18a Pedal Command: Case 1

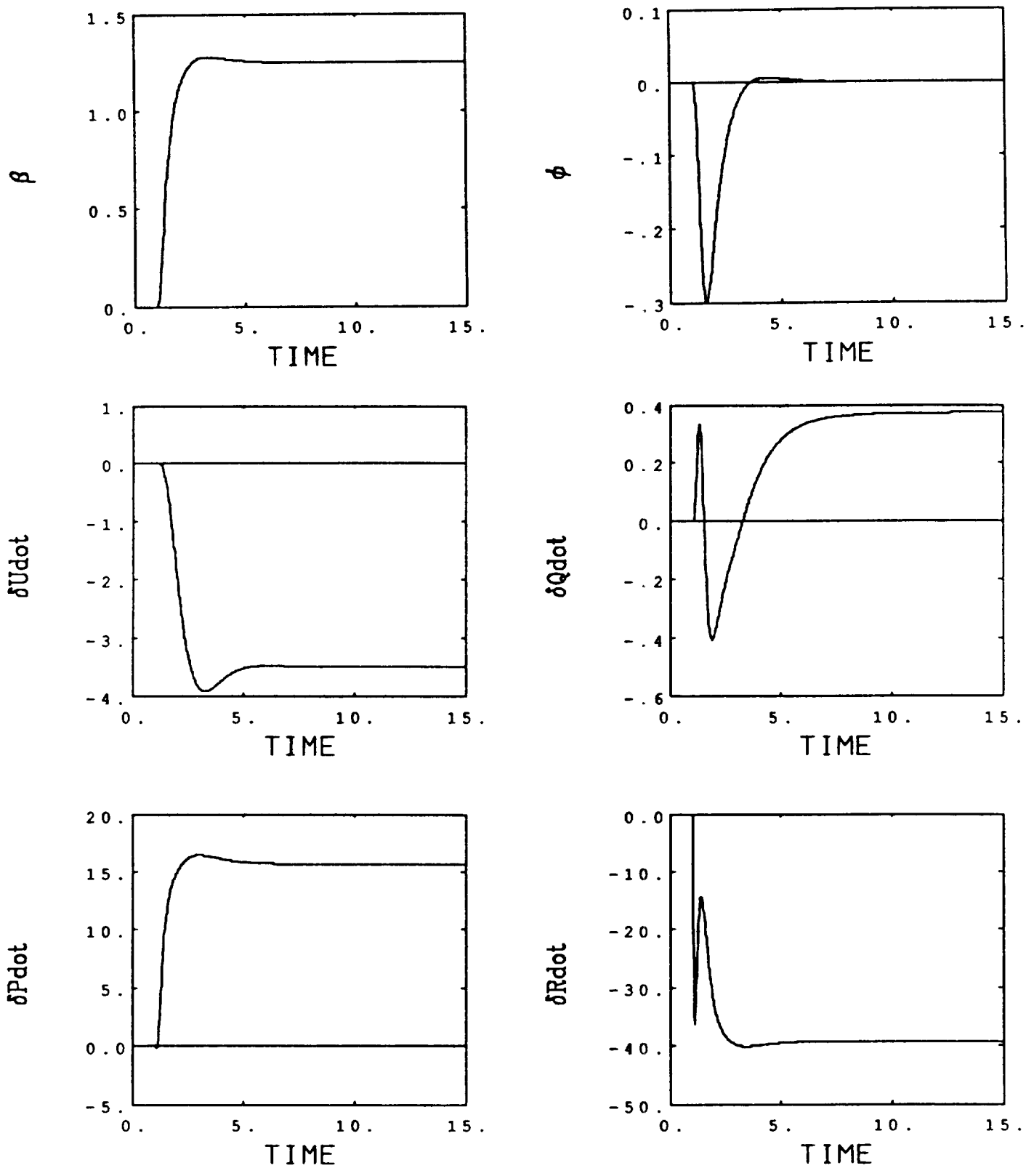

Figure 5-18b Pedal Command: Case 1

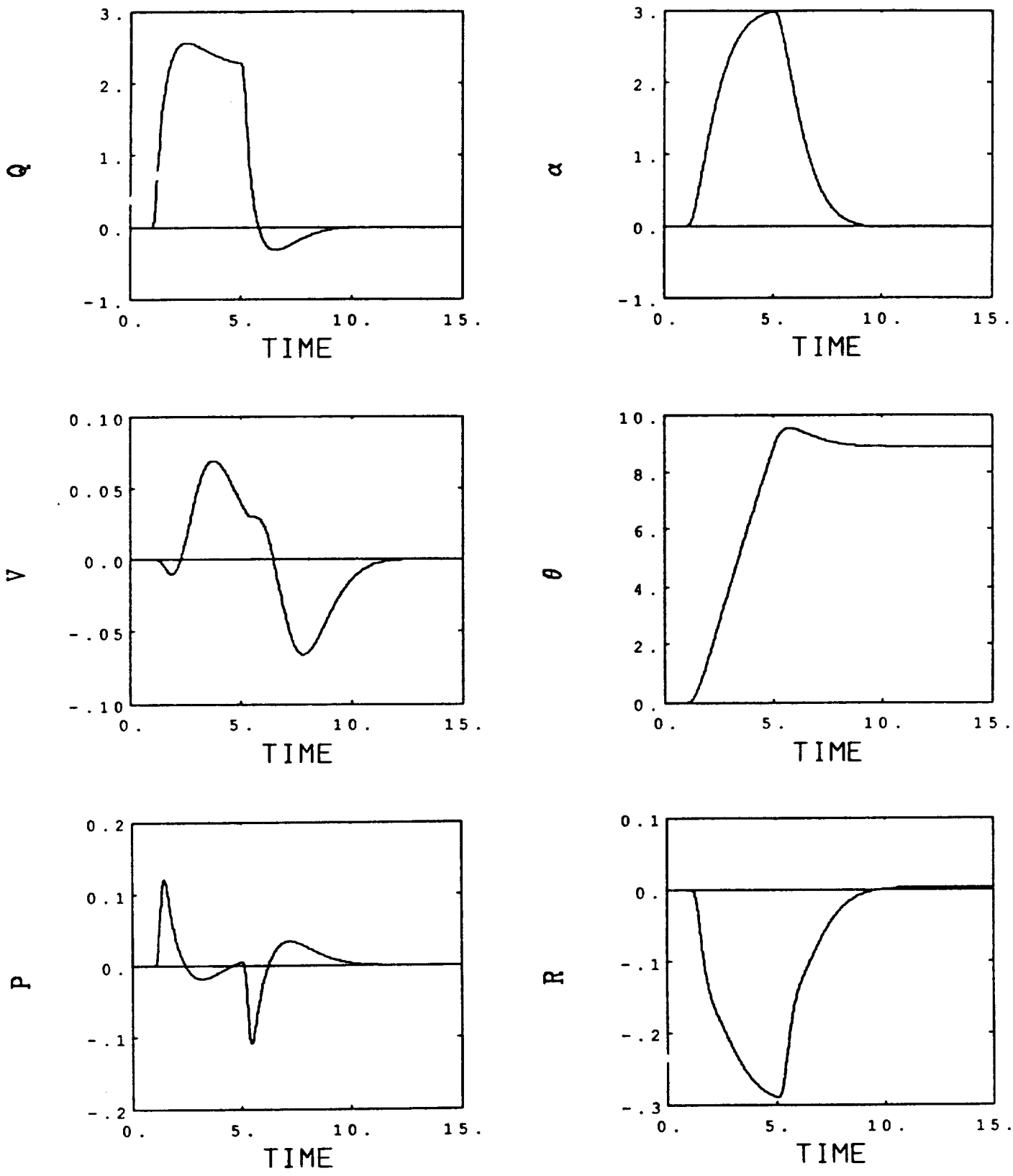

Figure 5-19a Longitudinal Stick Command: Case 2

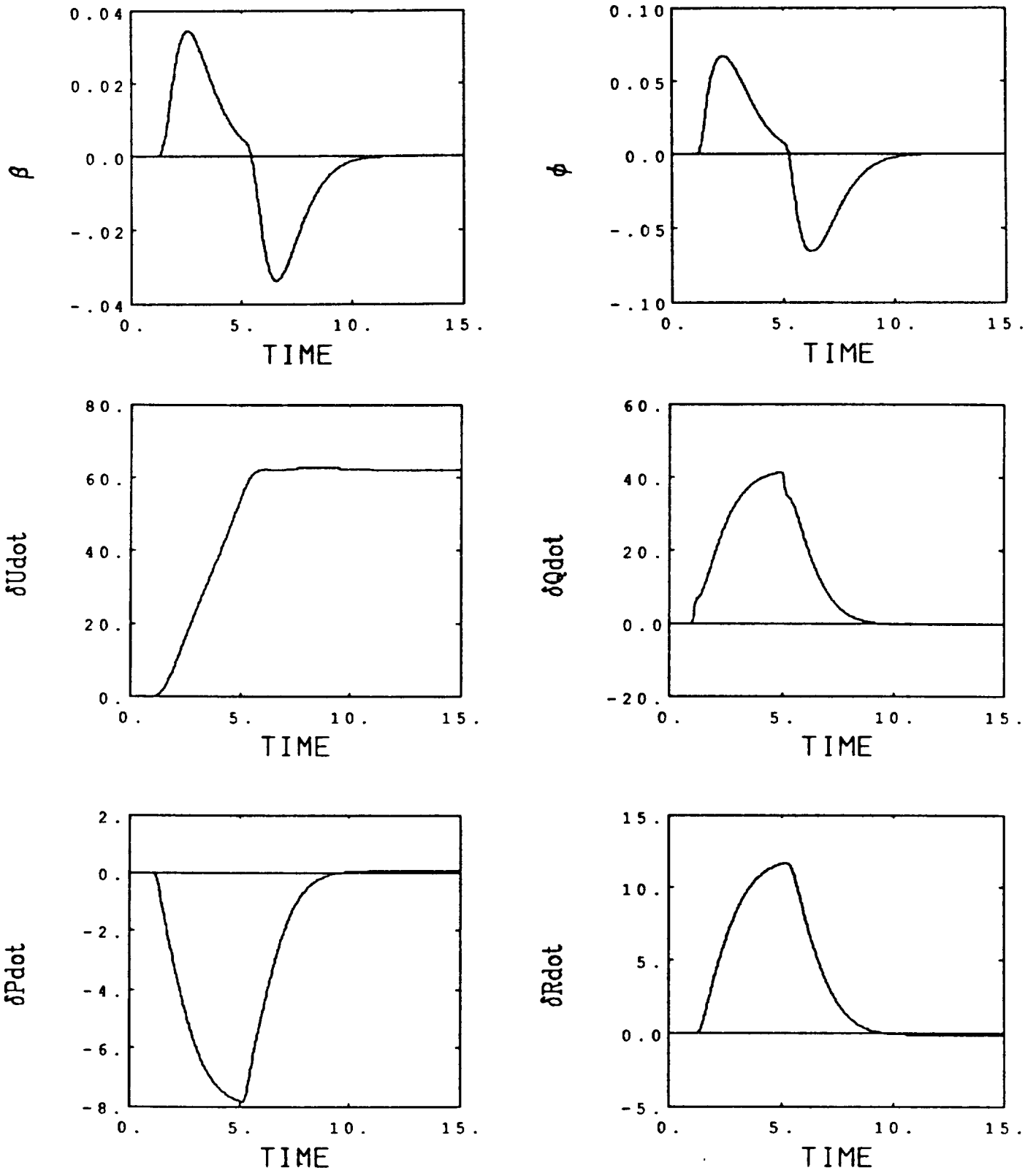

Figure 5-19b Longitudinal Stick Command: Case 2

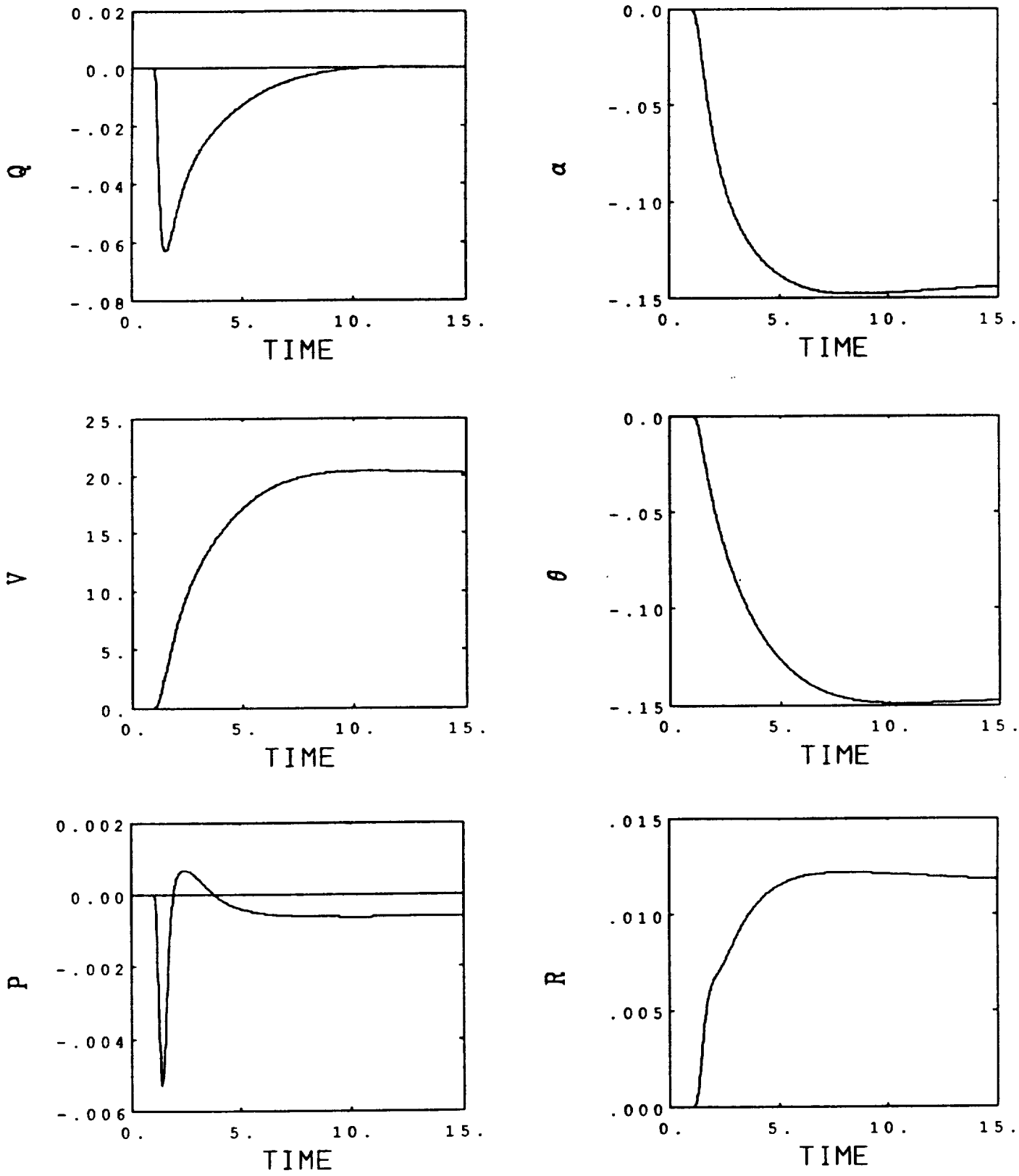

Figure 5-20a Airspeed Command: Case 2

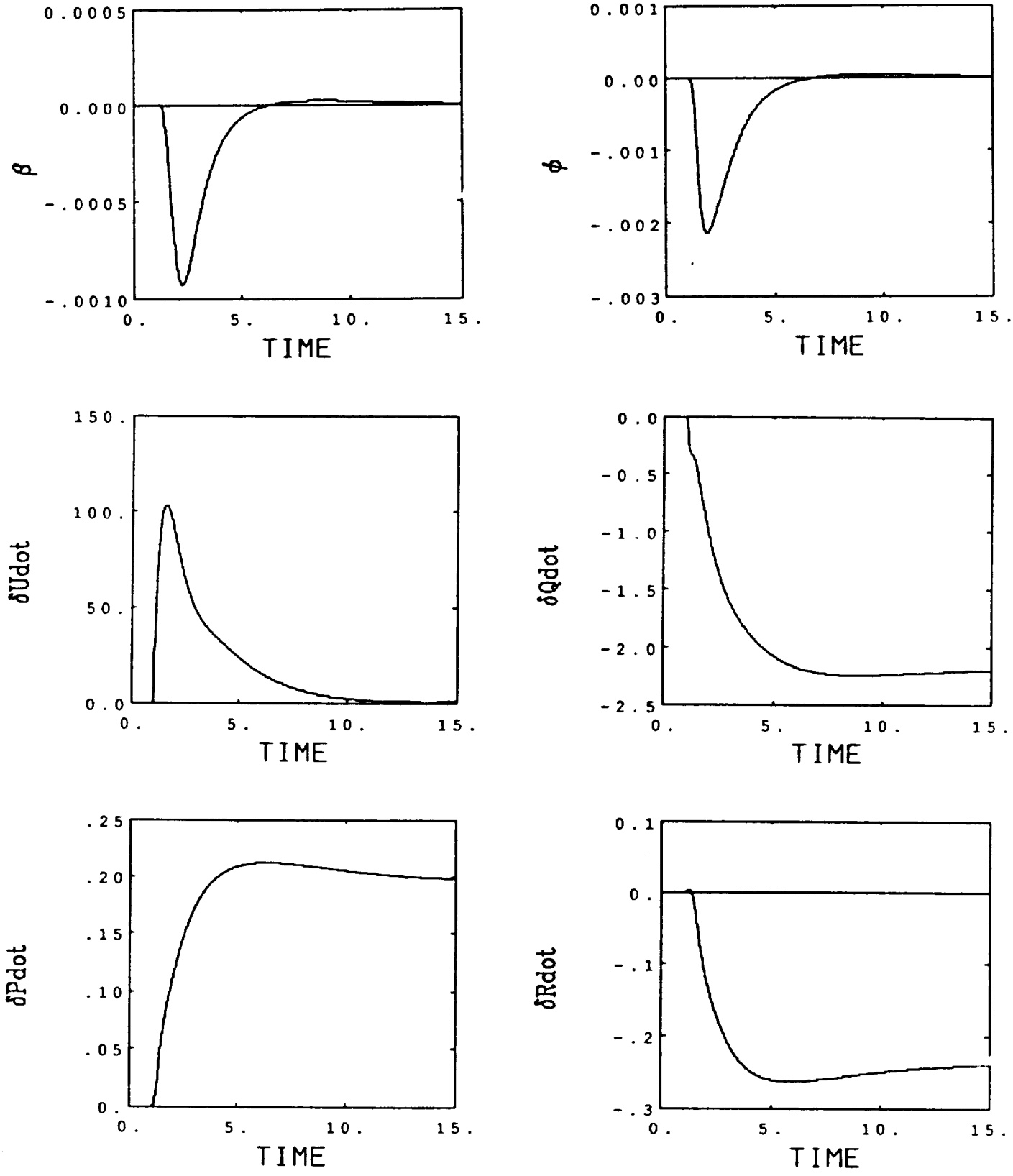

Figure 5-20b Airspeed Command: Case 2

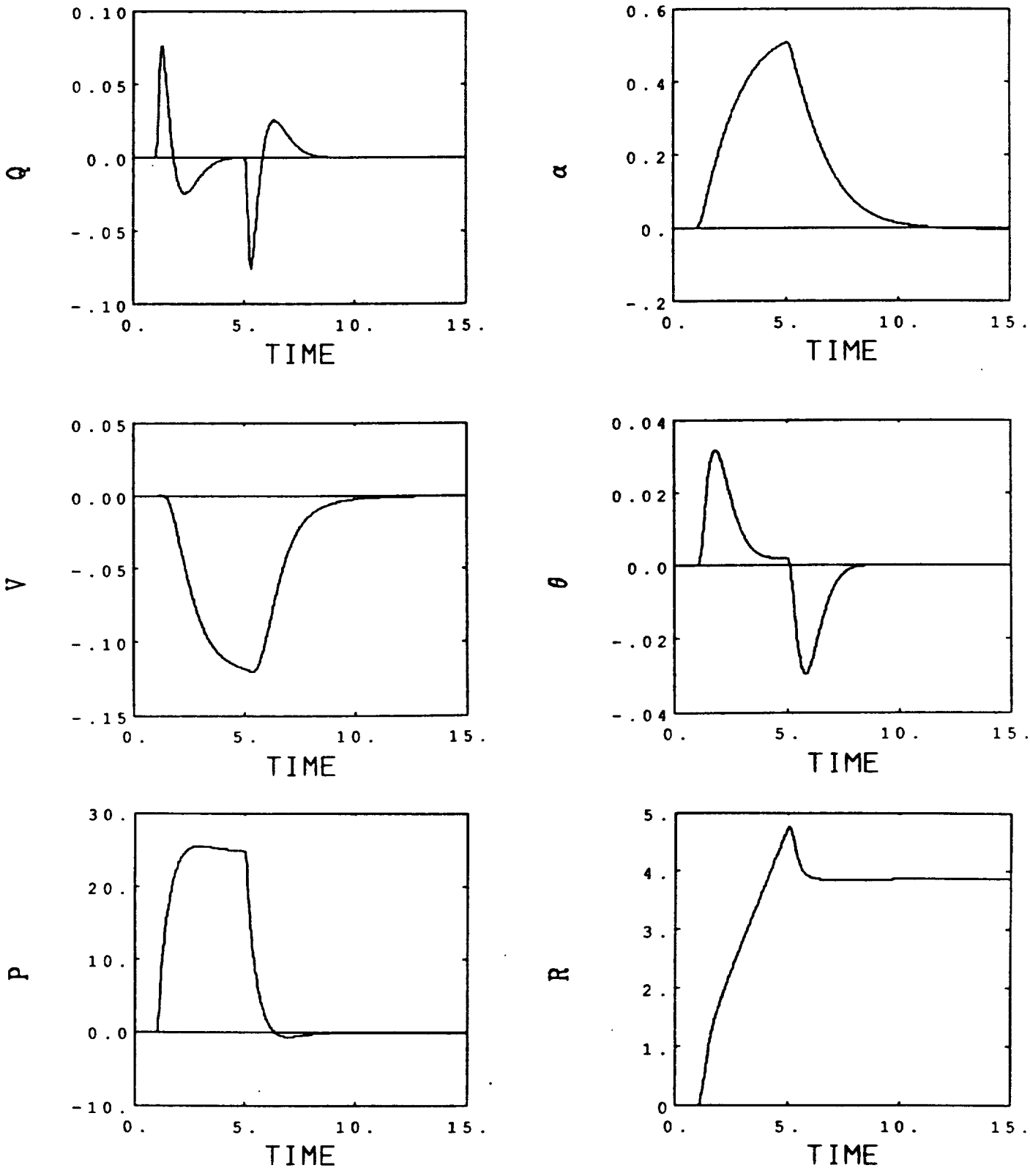

Figure 5-21a Lateral Stick Command: Case 2

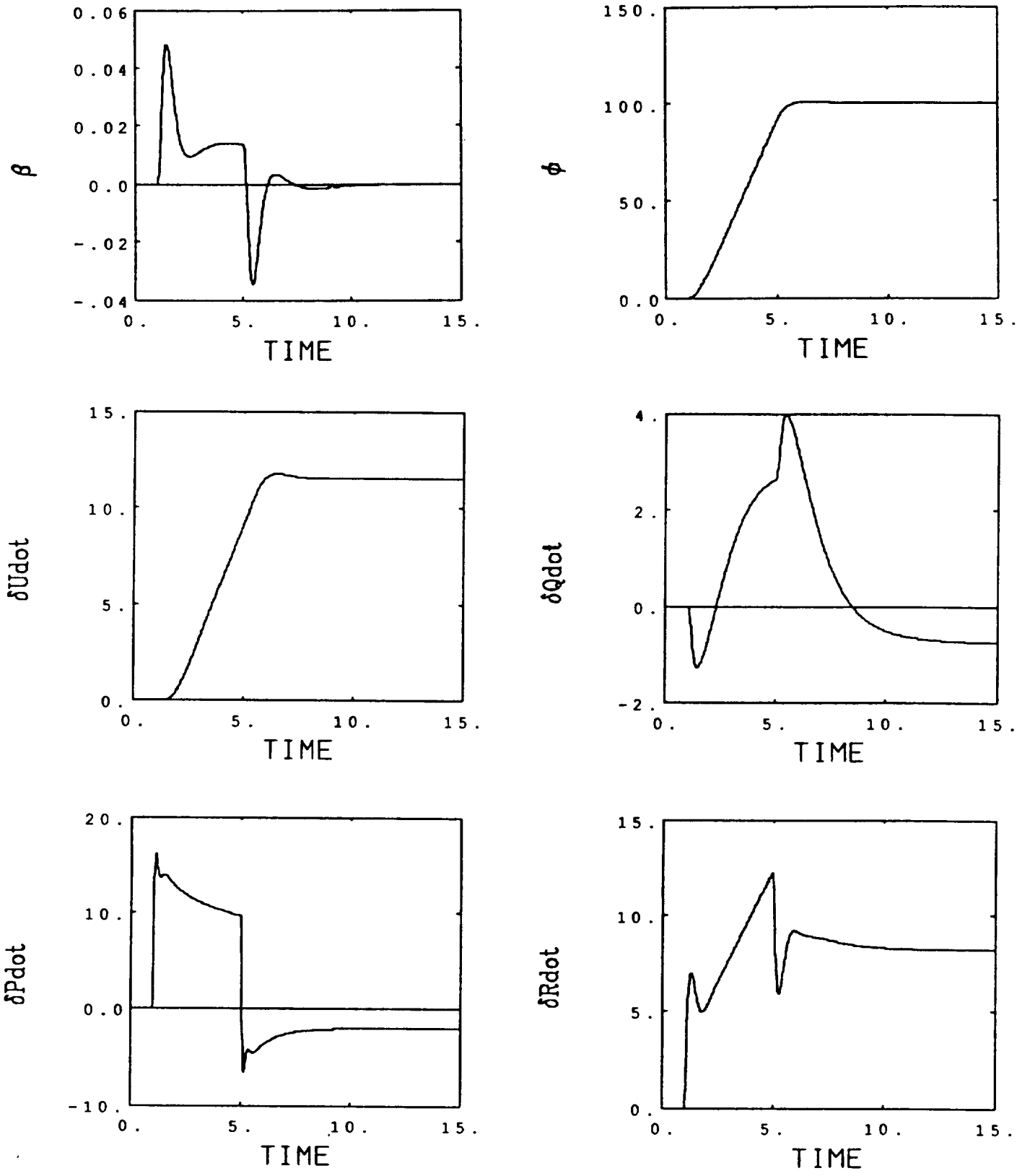

Figure 5-21b Lateral Stick Command: Case 2

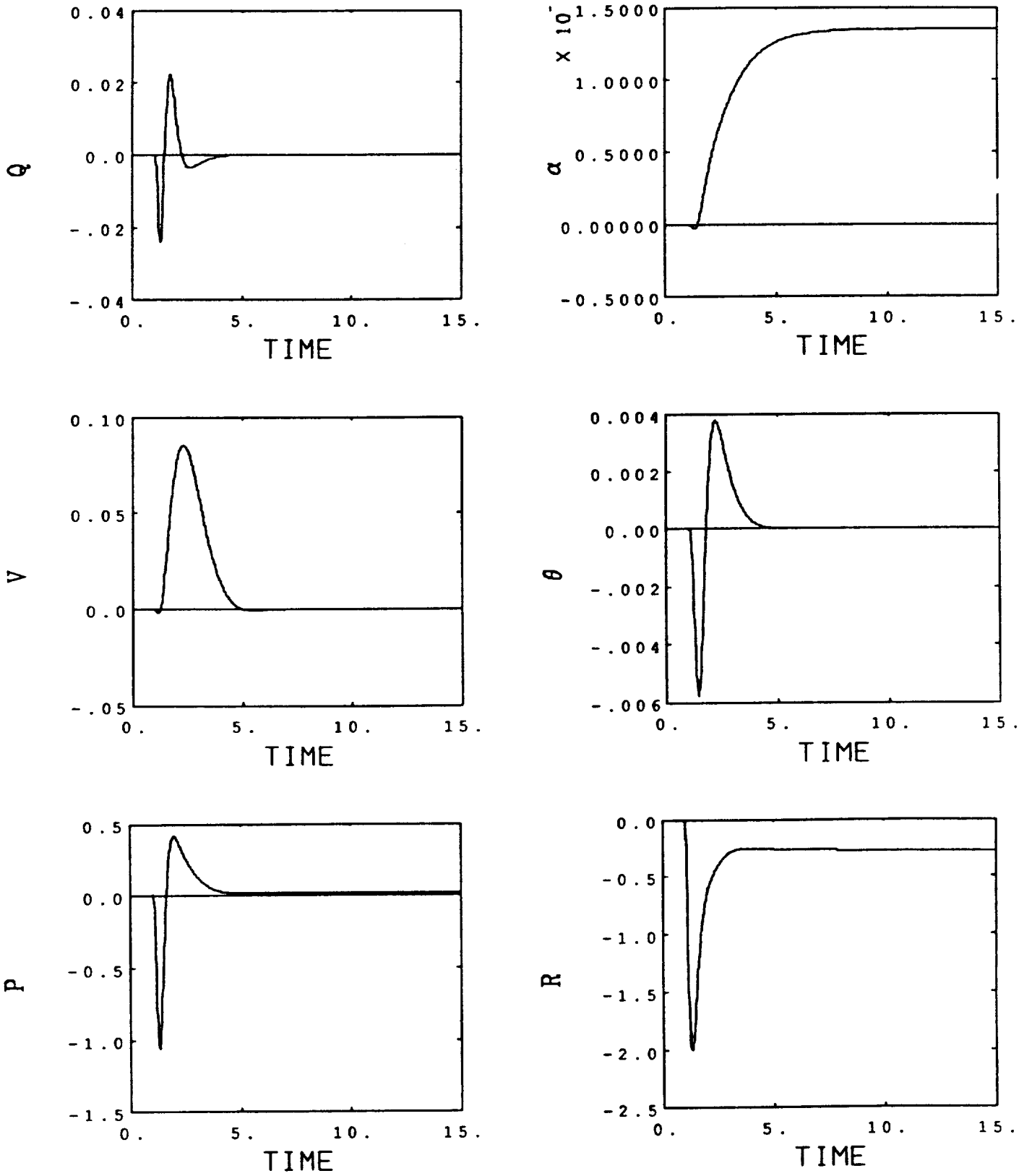

Figure 5-22a Pedal Command: Case 2

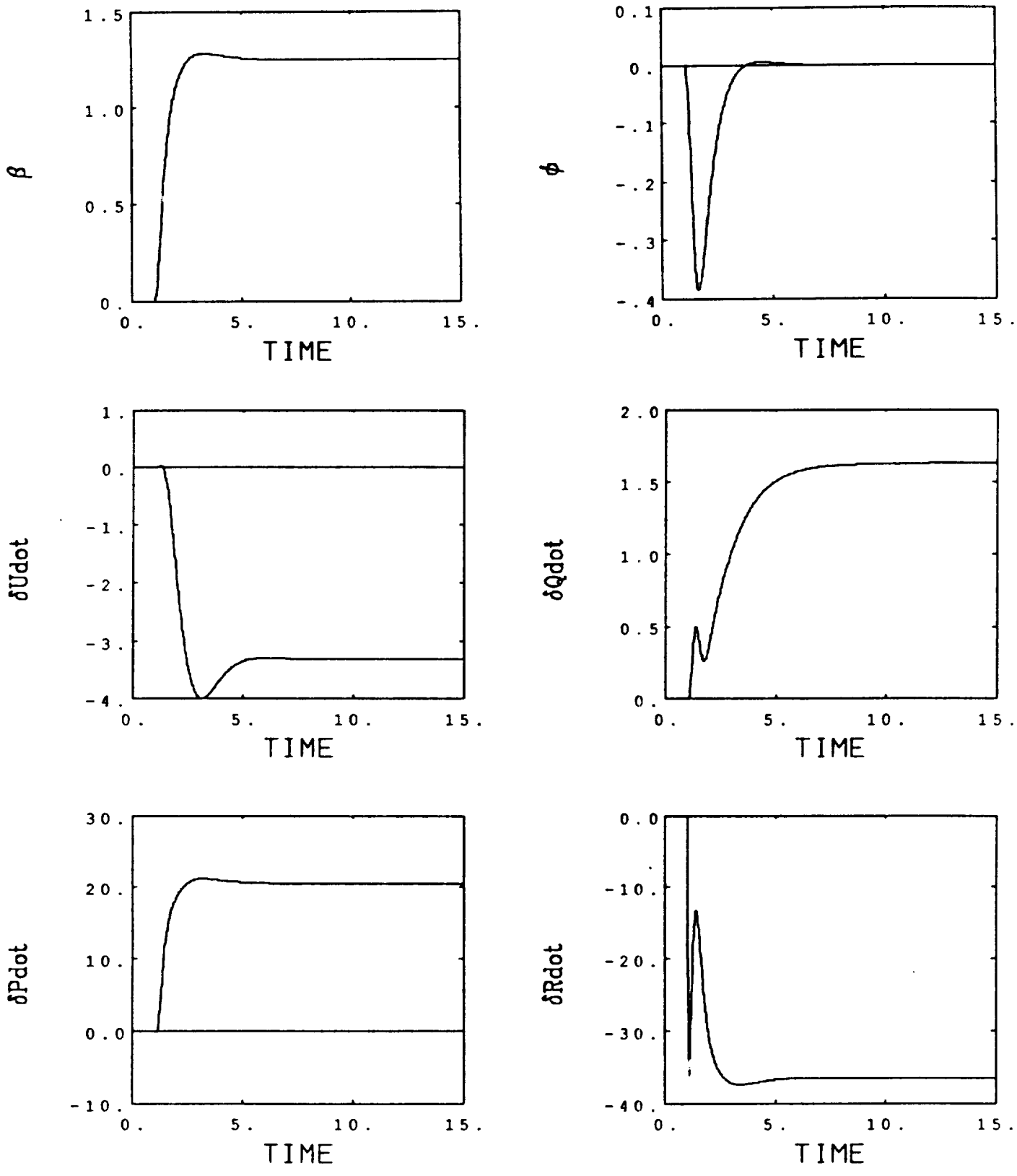

Figure 5-22b Pedal Command: Case 2

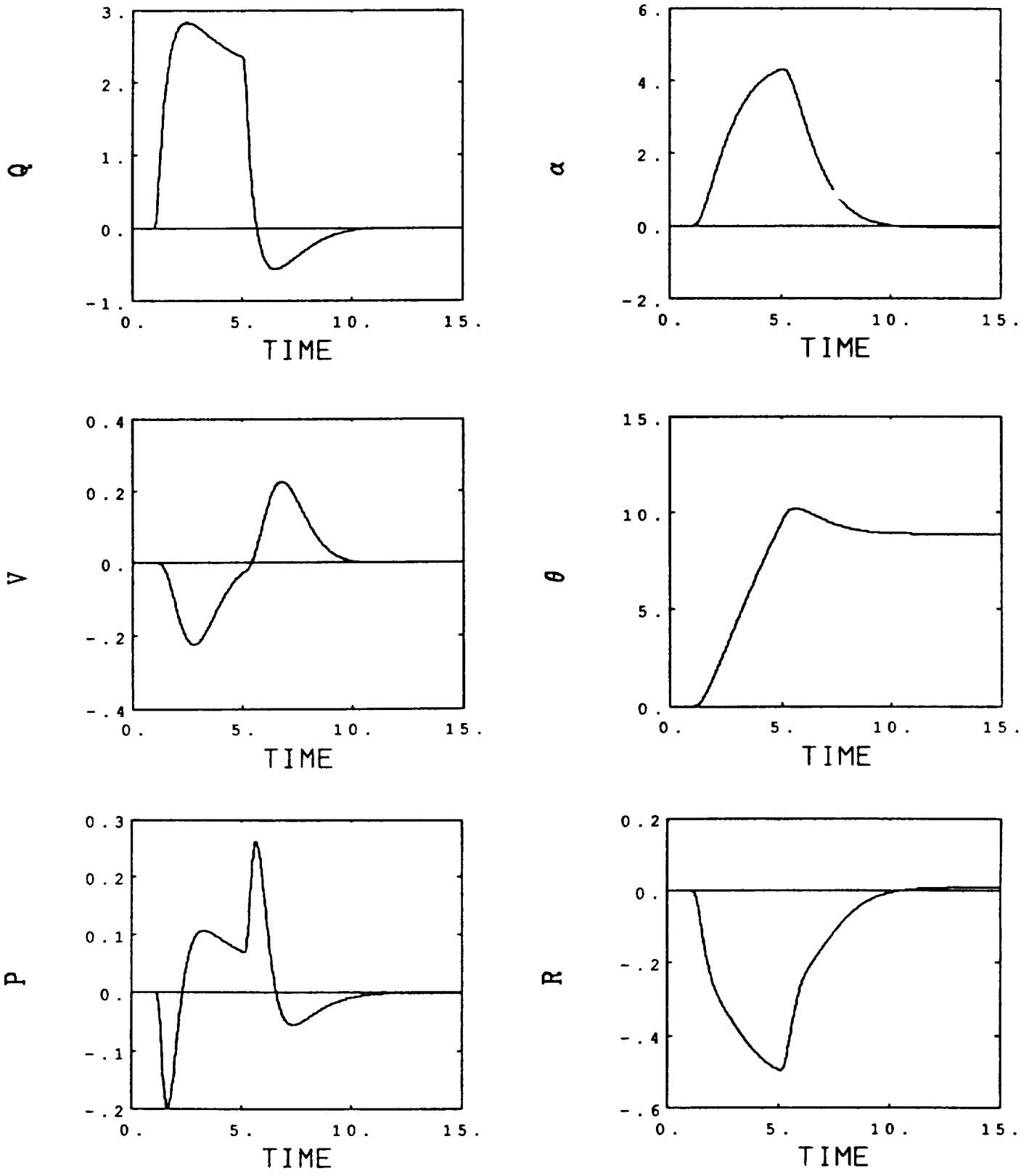

Figure 5-23a Longitudinal Stick Command: Case 3

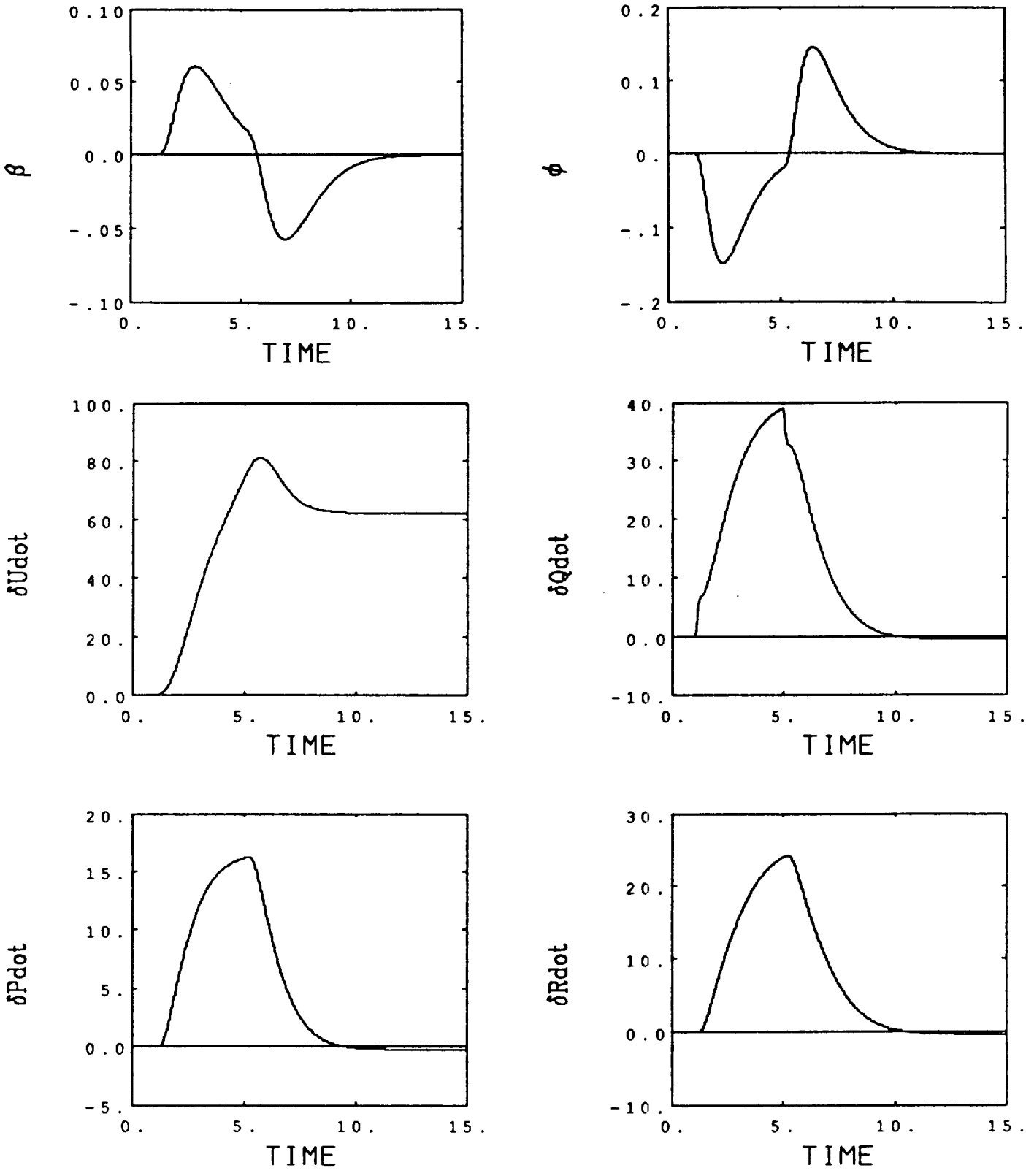

Figure 5-23b Longitudinal Stick Command: Case 3

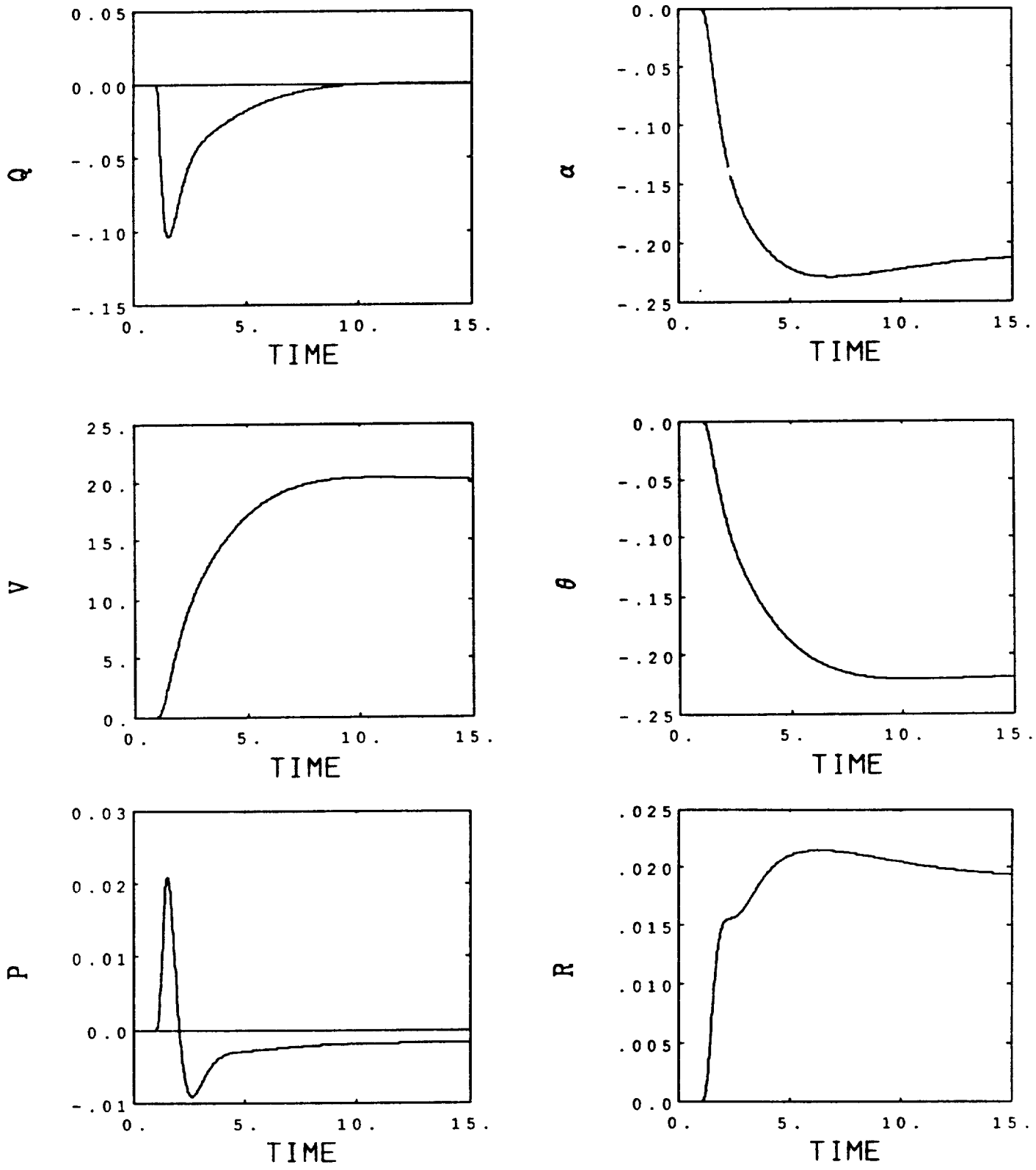

Figure 5-24a Airspeed Command: Case 3

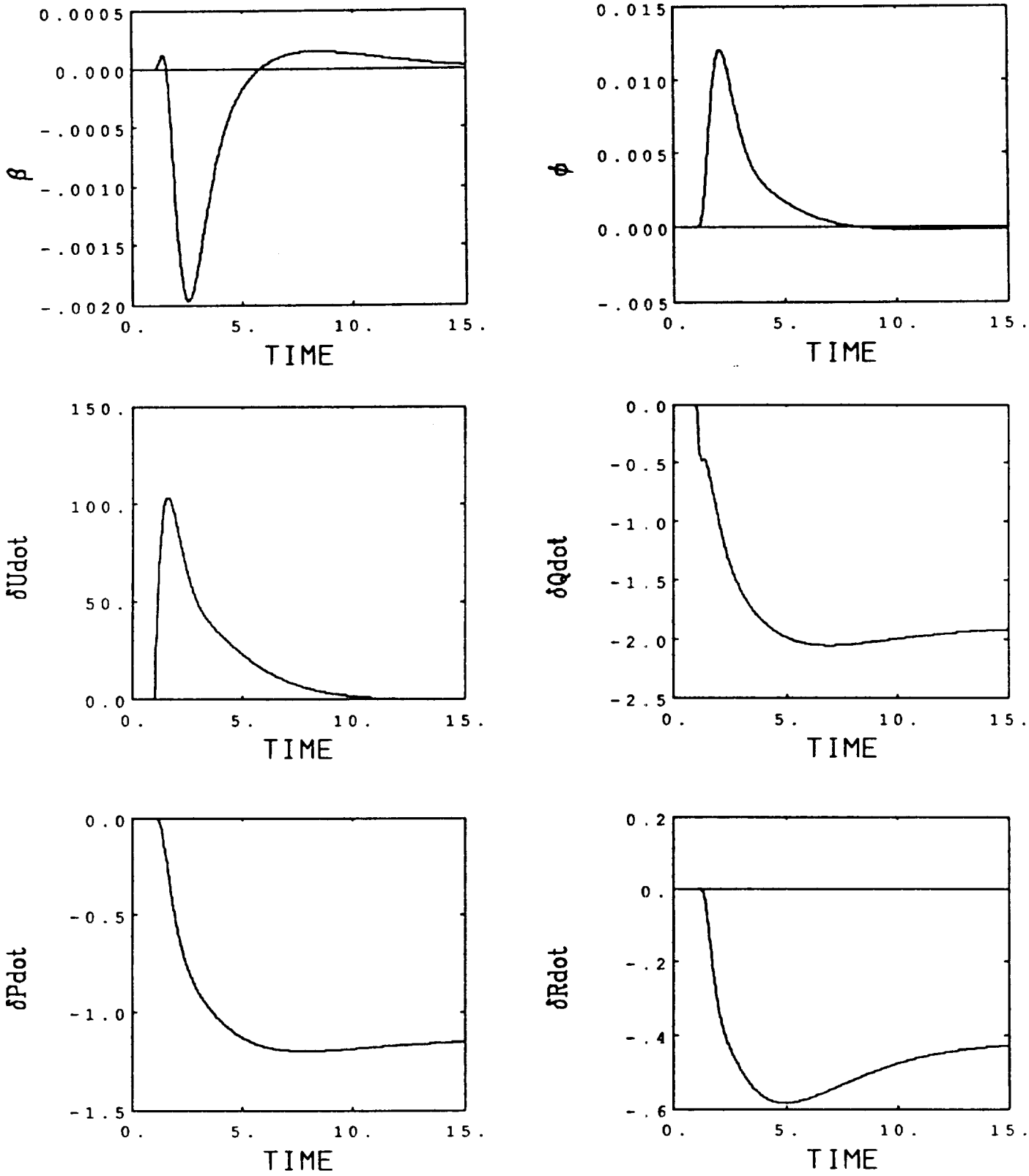

Figure 5-24b Airspeed Command: Case 3

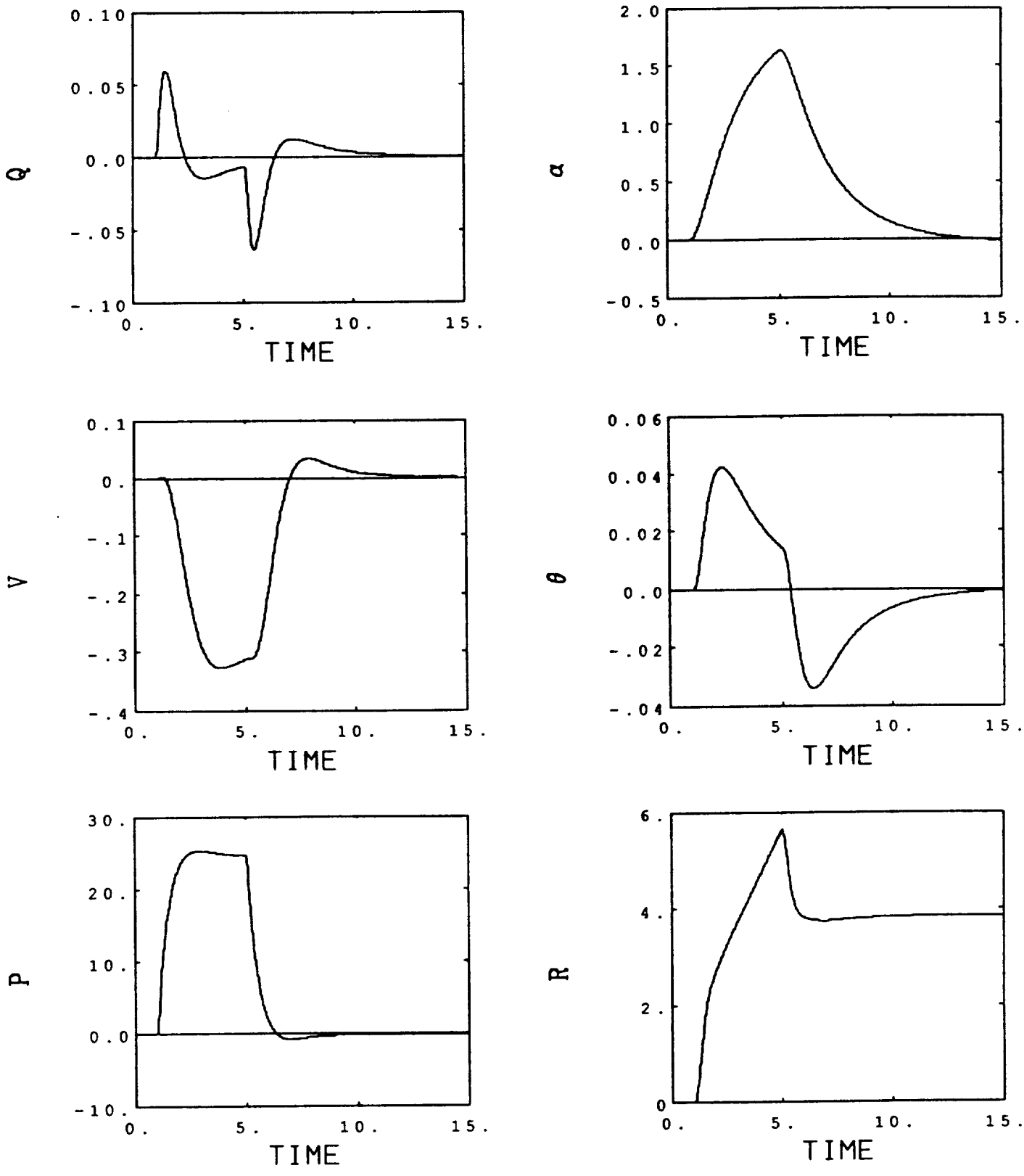

Figure 5-25a Lateral Stick Command: Case 3

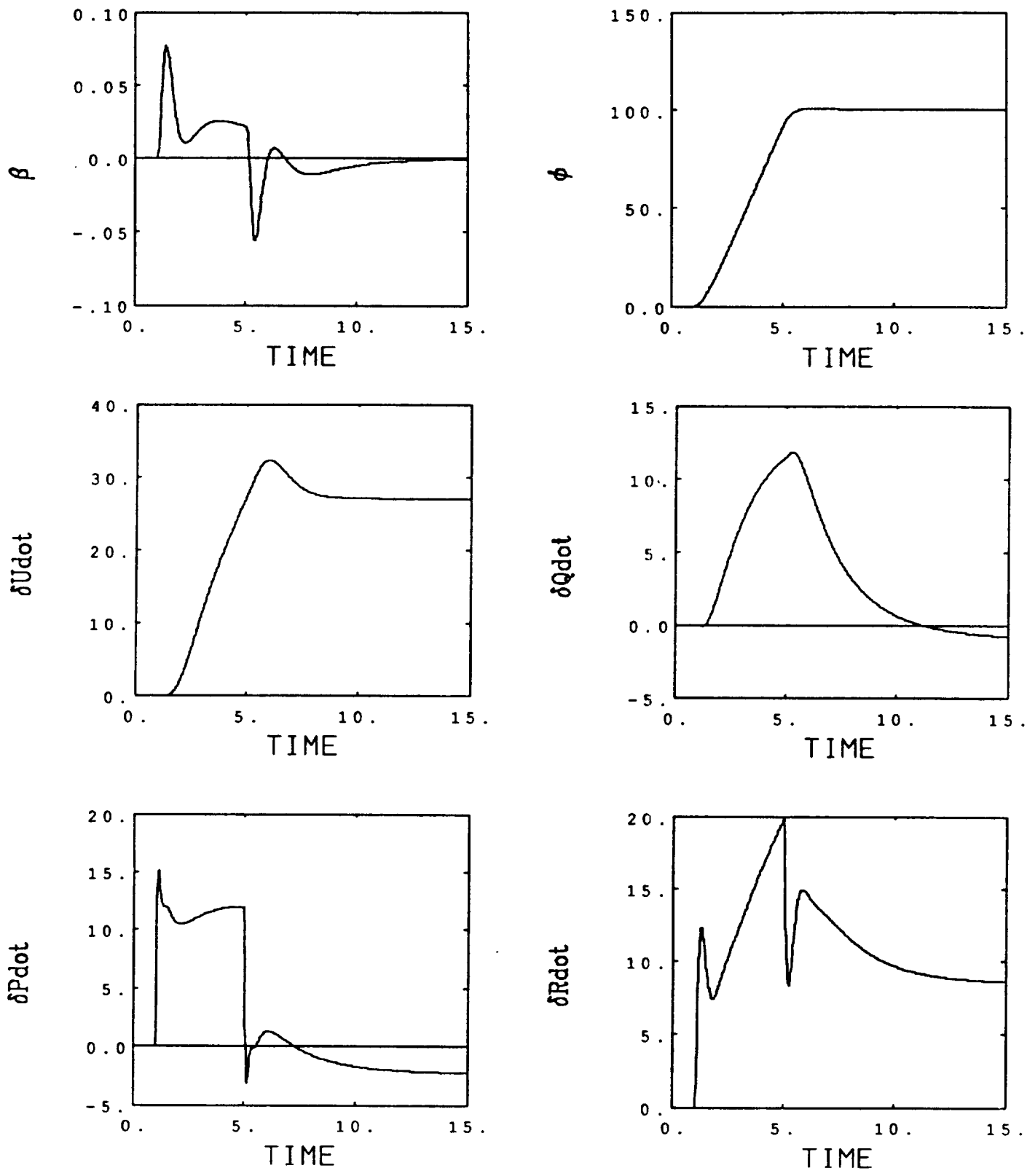

Figure 5-25b Lateral Stick Command: Case 3

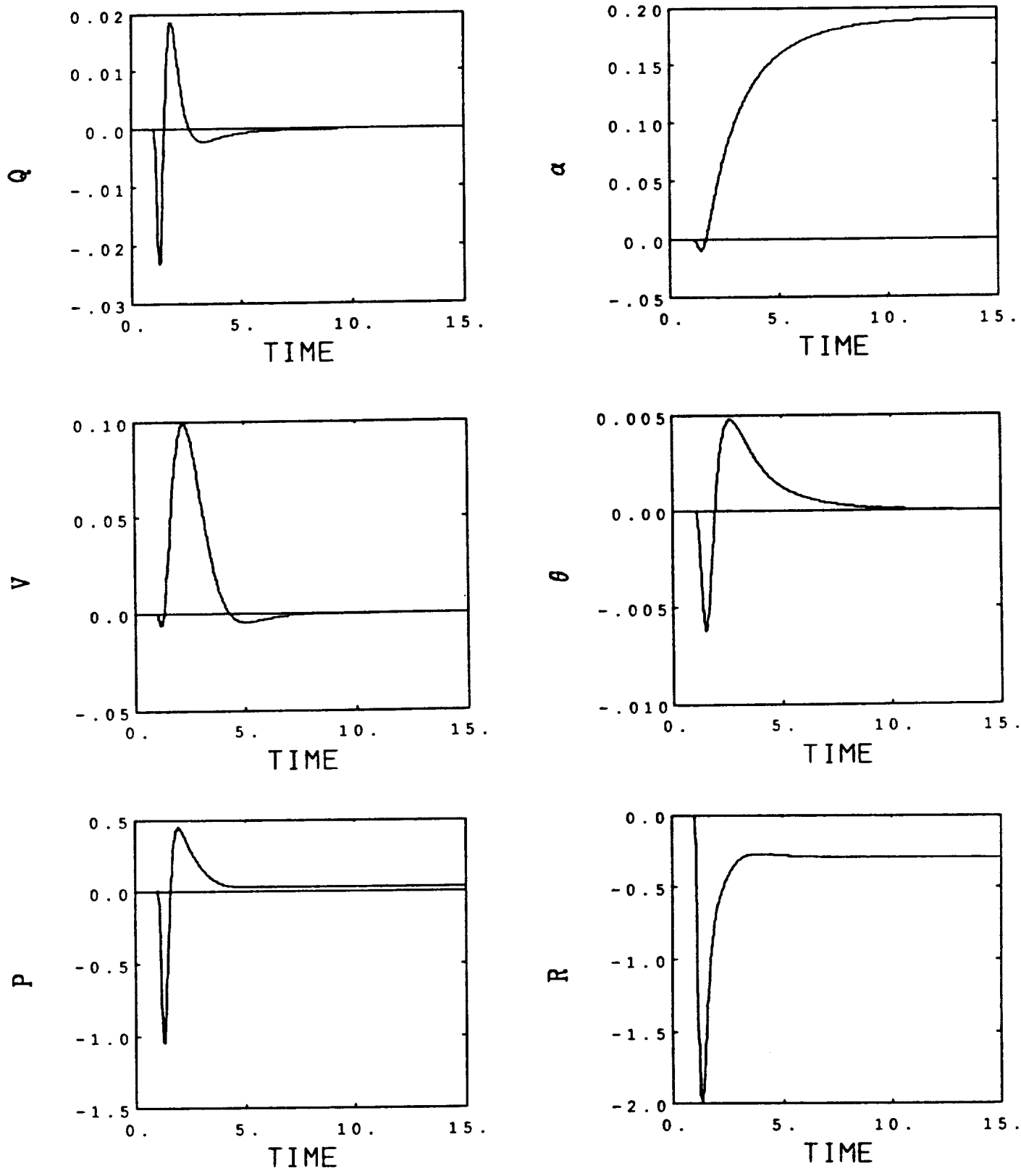

Figure 5-26a Pedal Command: Case 3

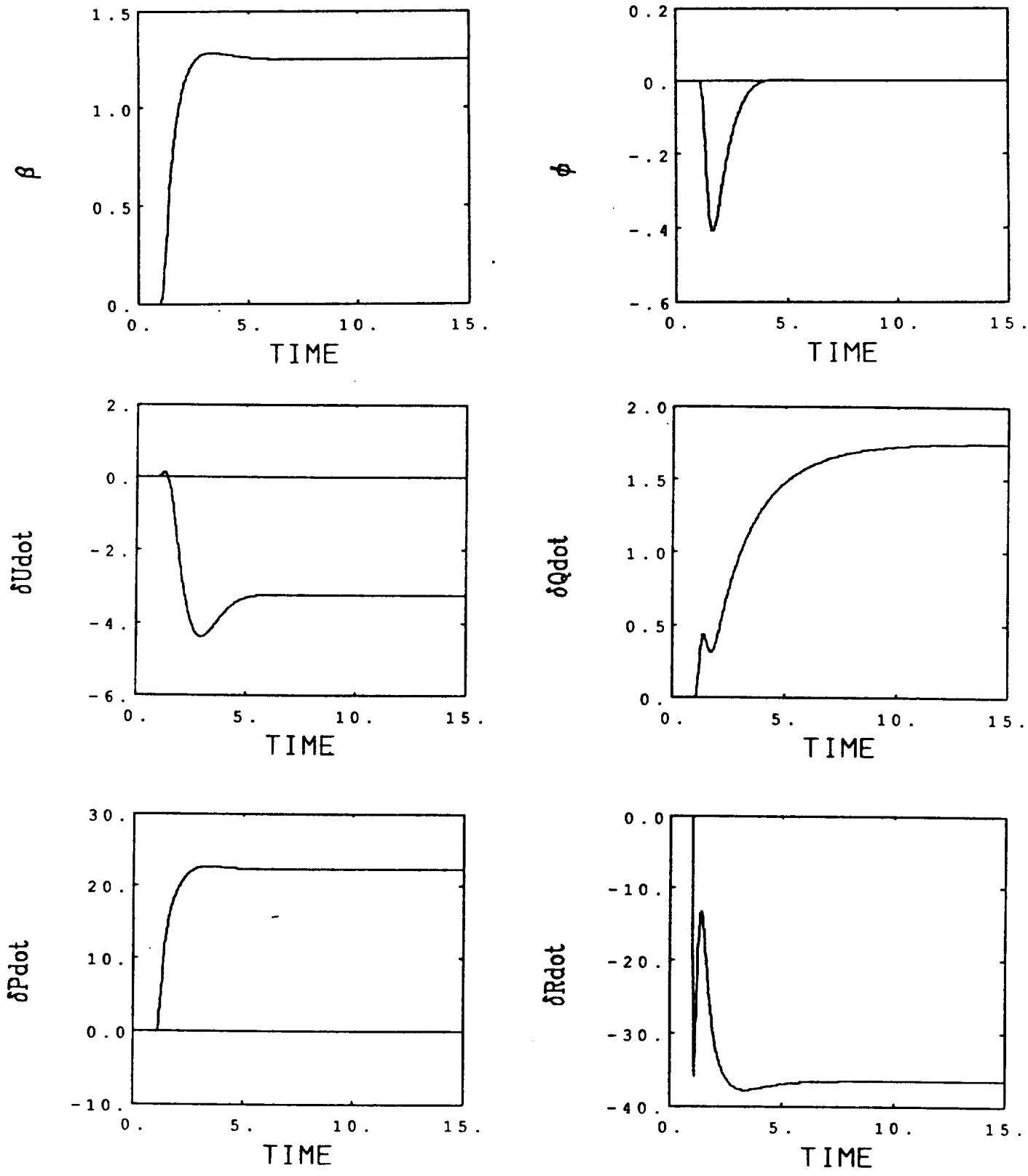

Figure 5-26b Pedal Command: Case 3

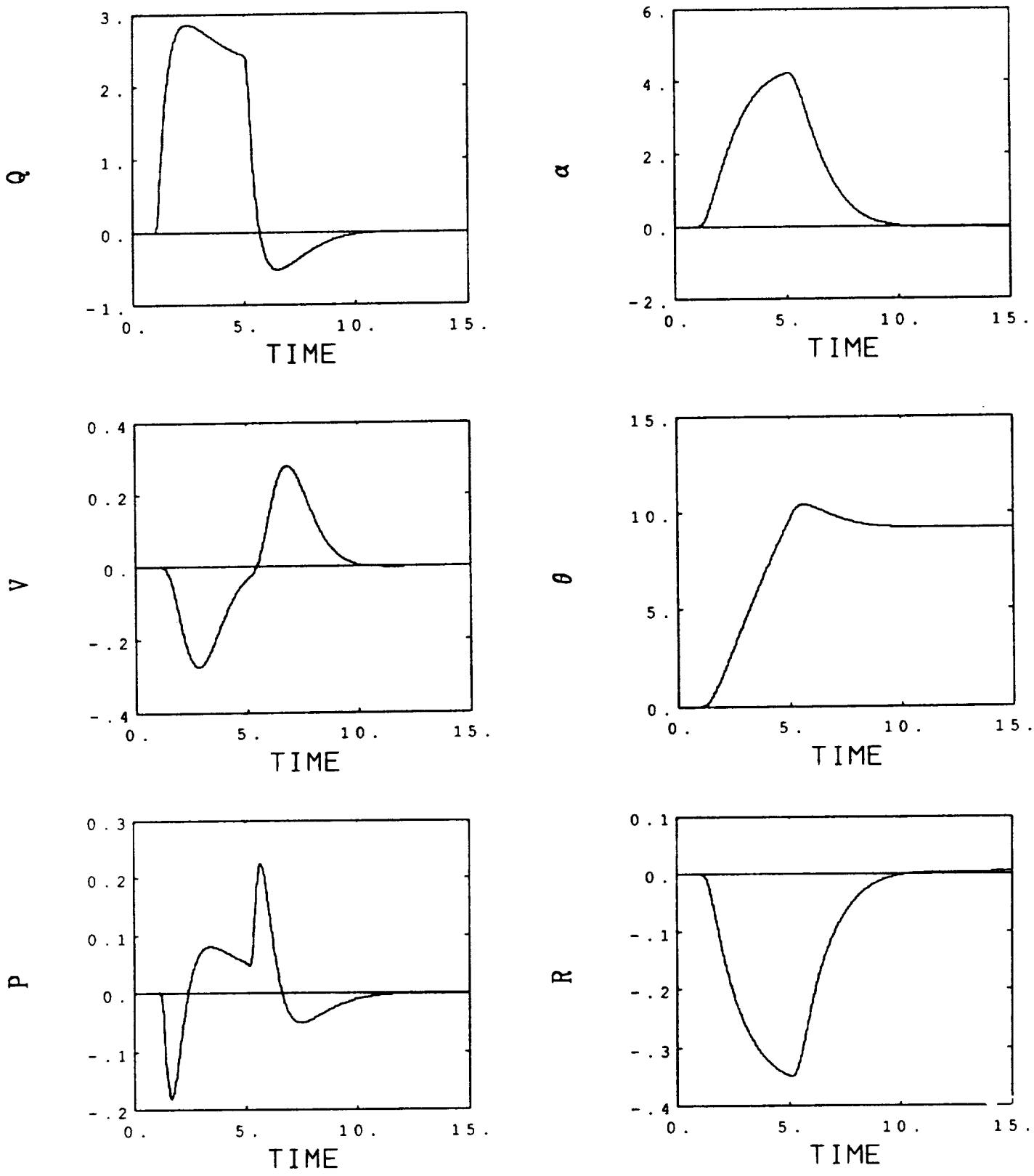

Figure 5-27a Longitudinal Stick Command: Case 4

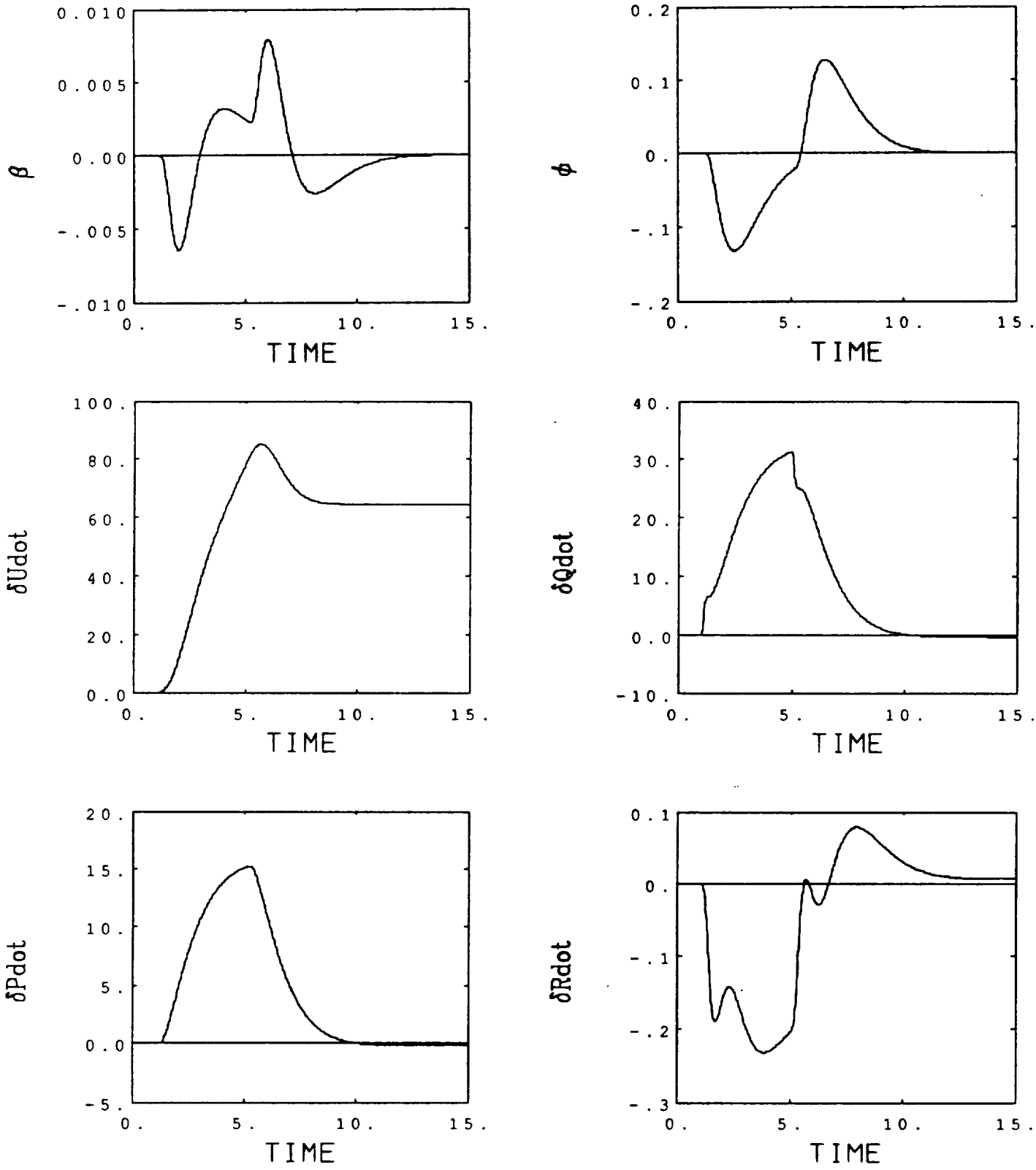

Figure 5-27b Longitudinal Stick Command: Case 4

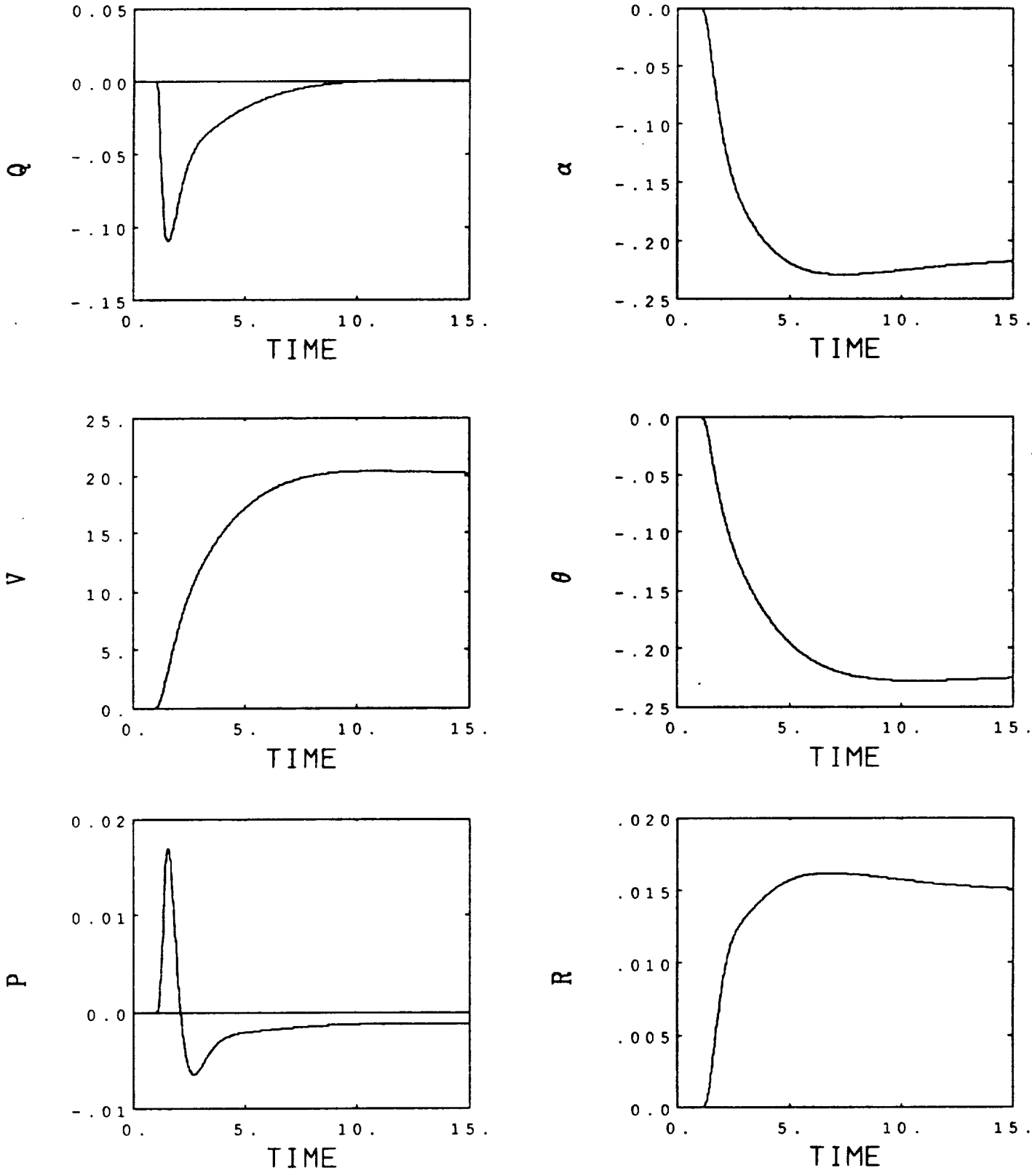

Figure 5-28a Airspeed Command: Case 4

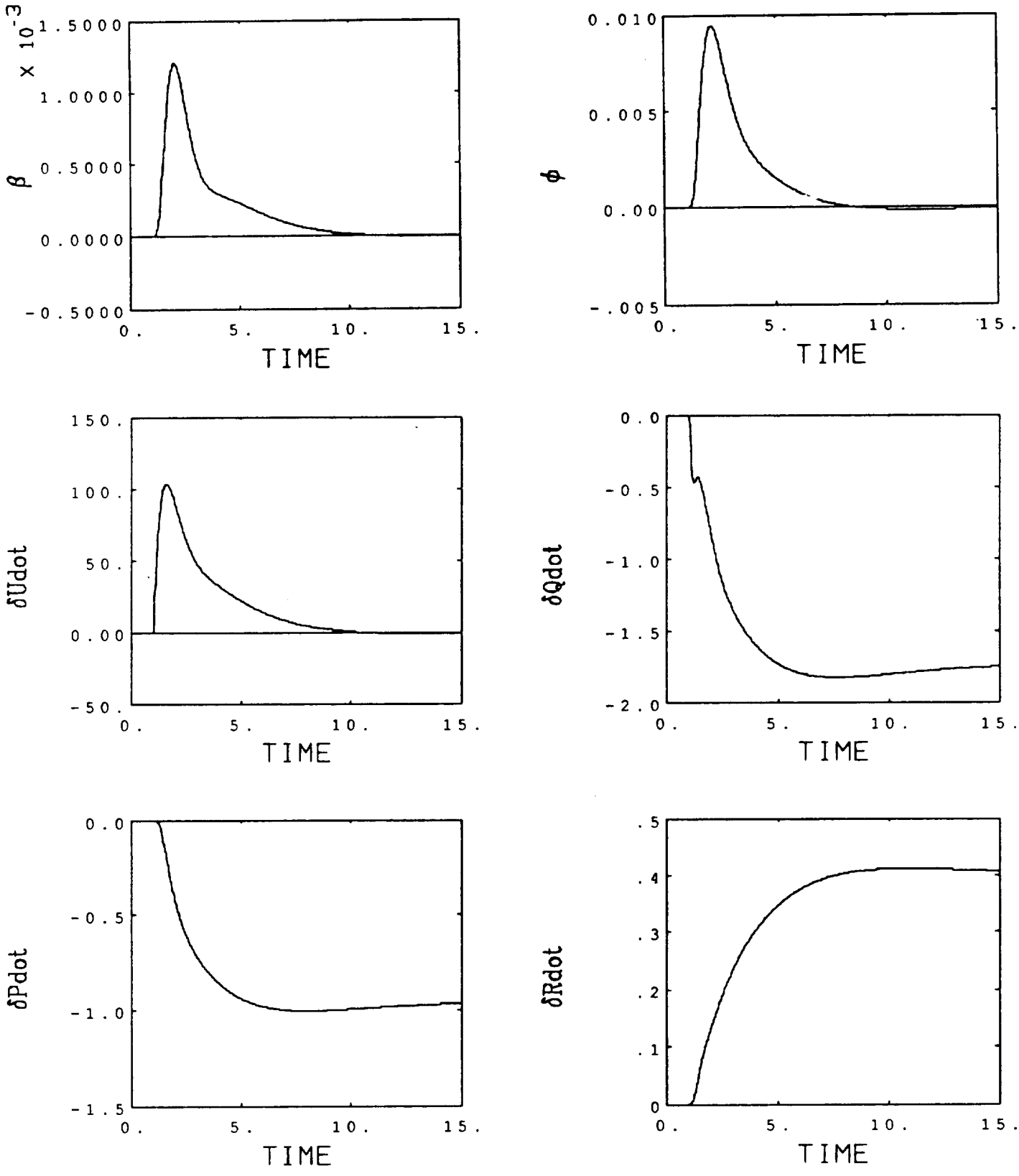

Figure 5-28b Airspeed Command: Case 4

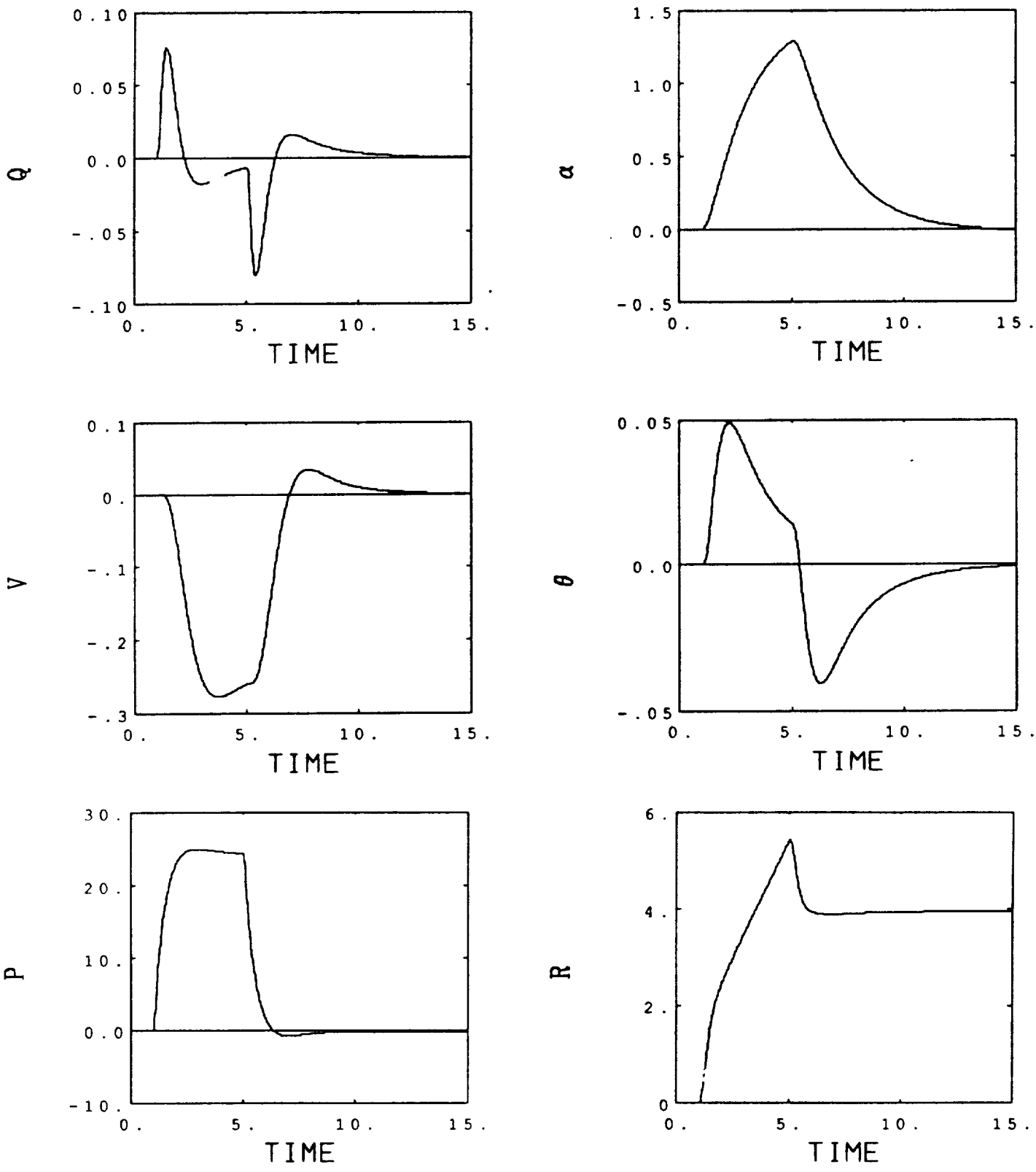

Figure 5-29a Lateral Stick Command: Case 4

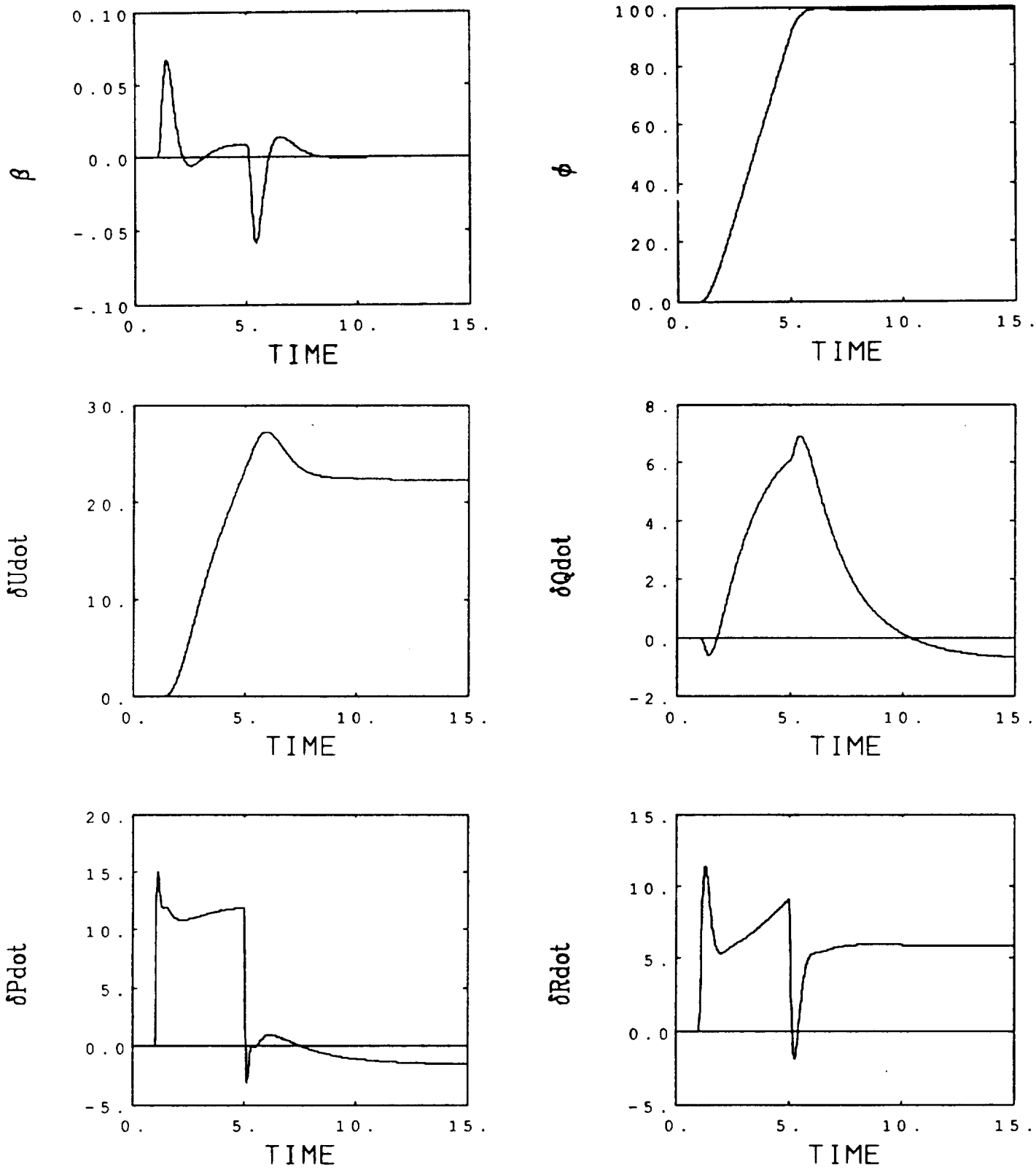

Figure 5-29b Lateral Stick Command: Case 4

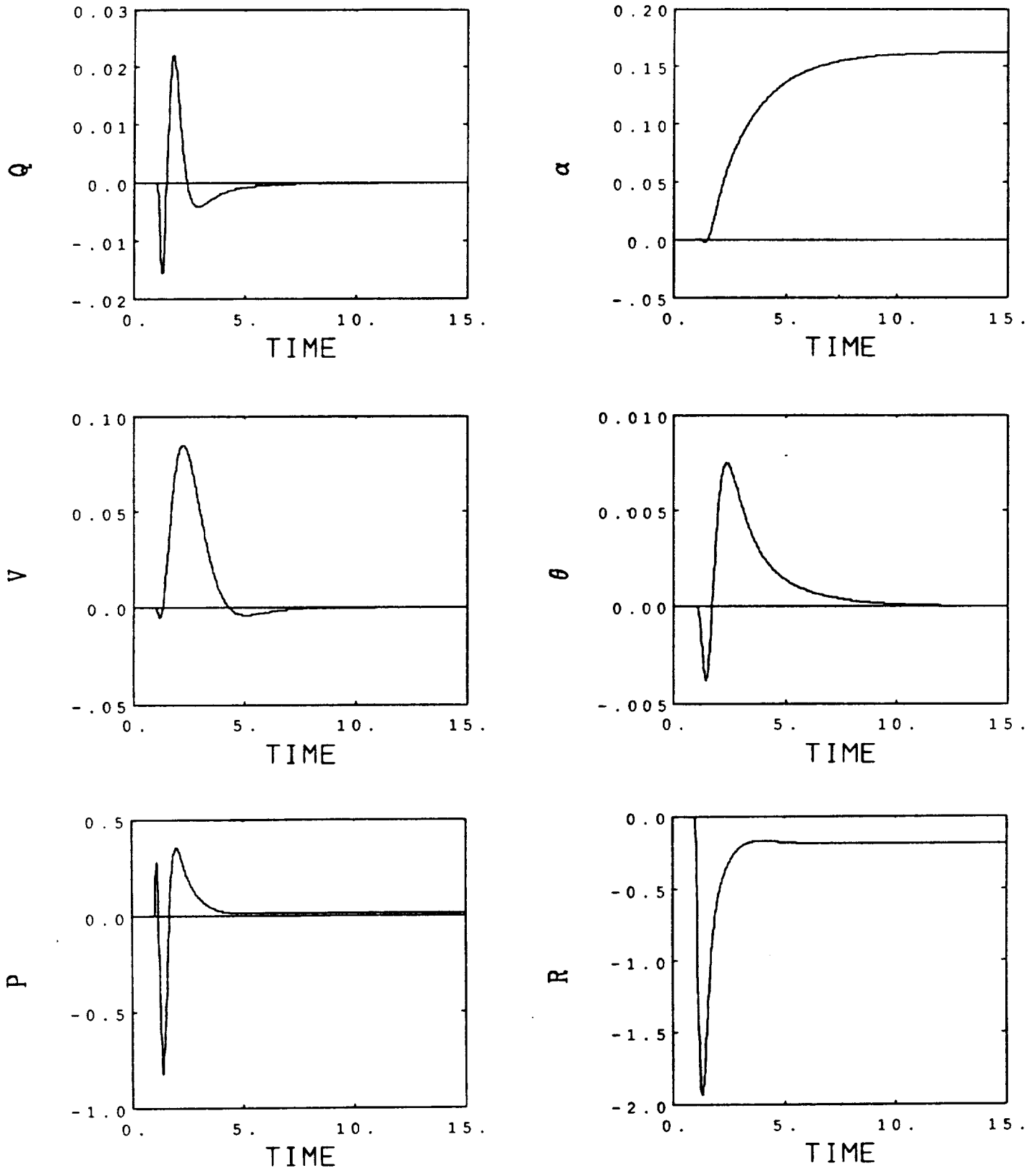

Figure 5-30a Pedal Command: Case 4

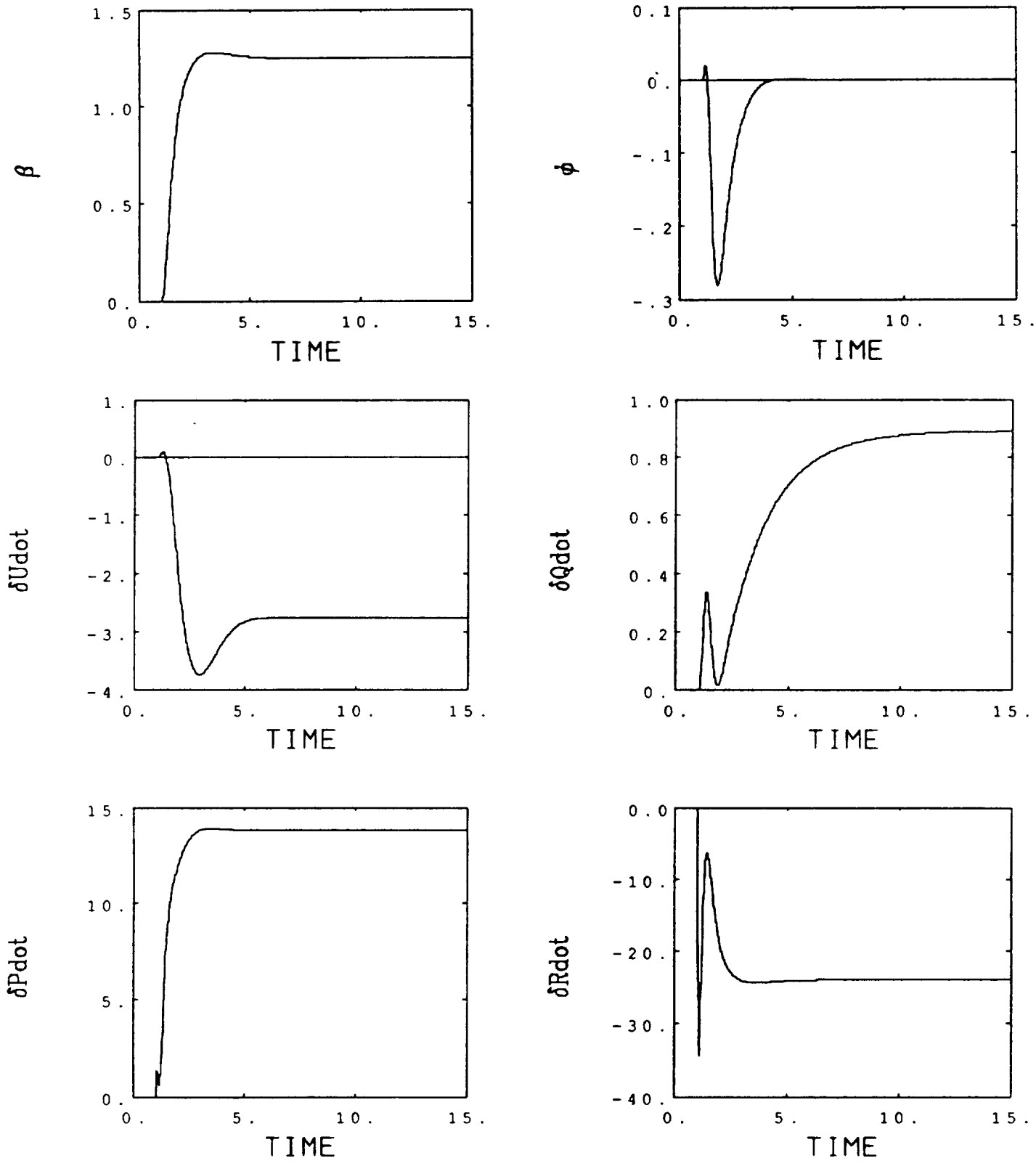

Figure 5-30b Pedal Command: Case 4

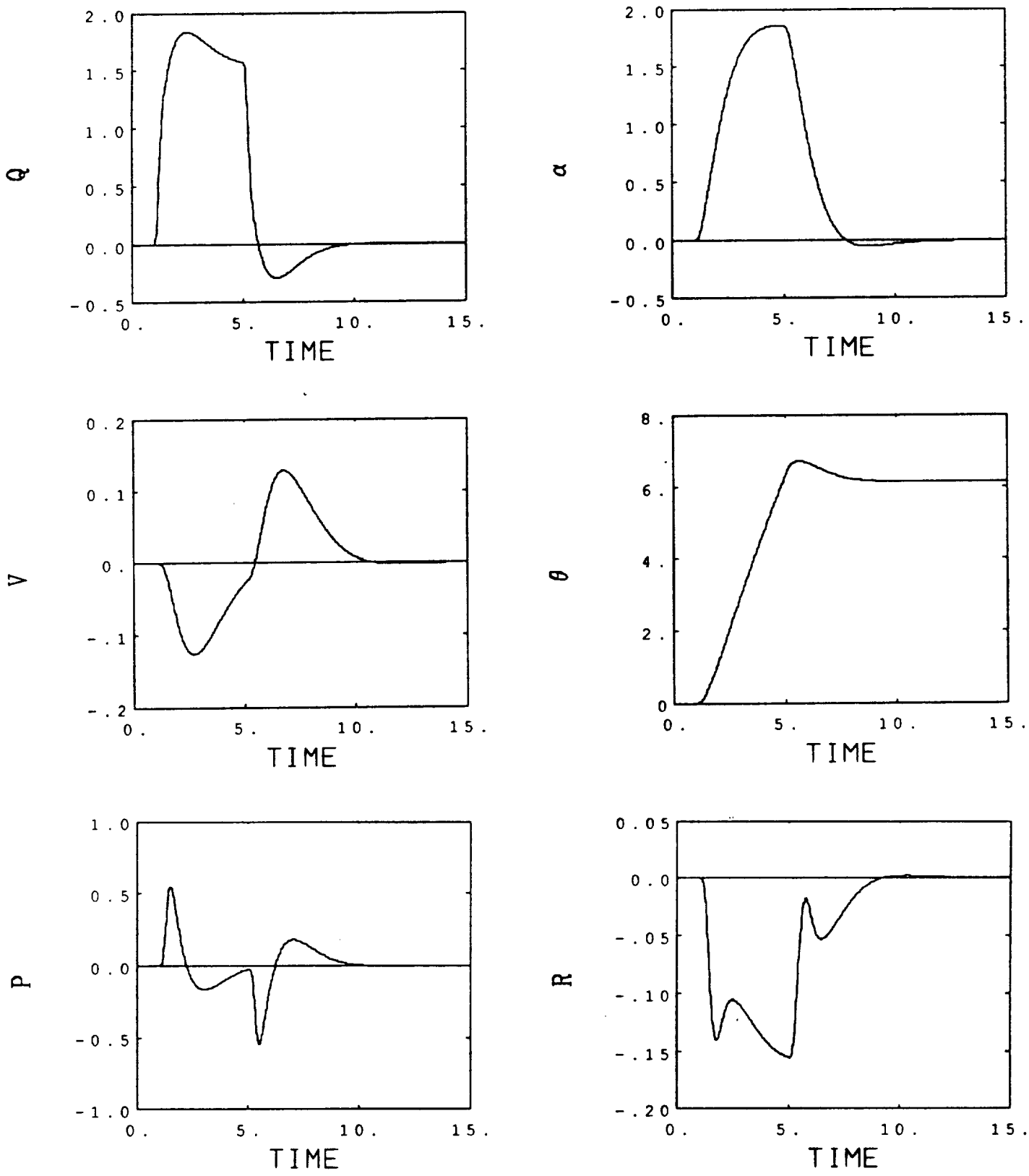

Figure 5-31a Longitudinal Stick Command: Case 5

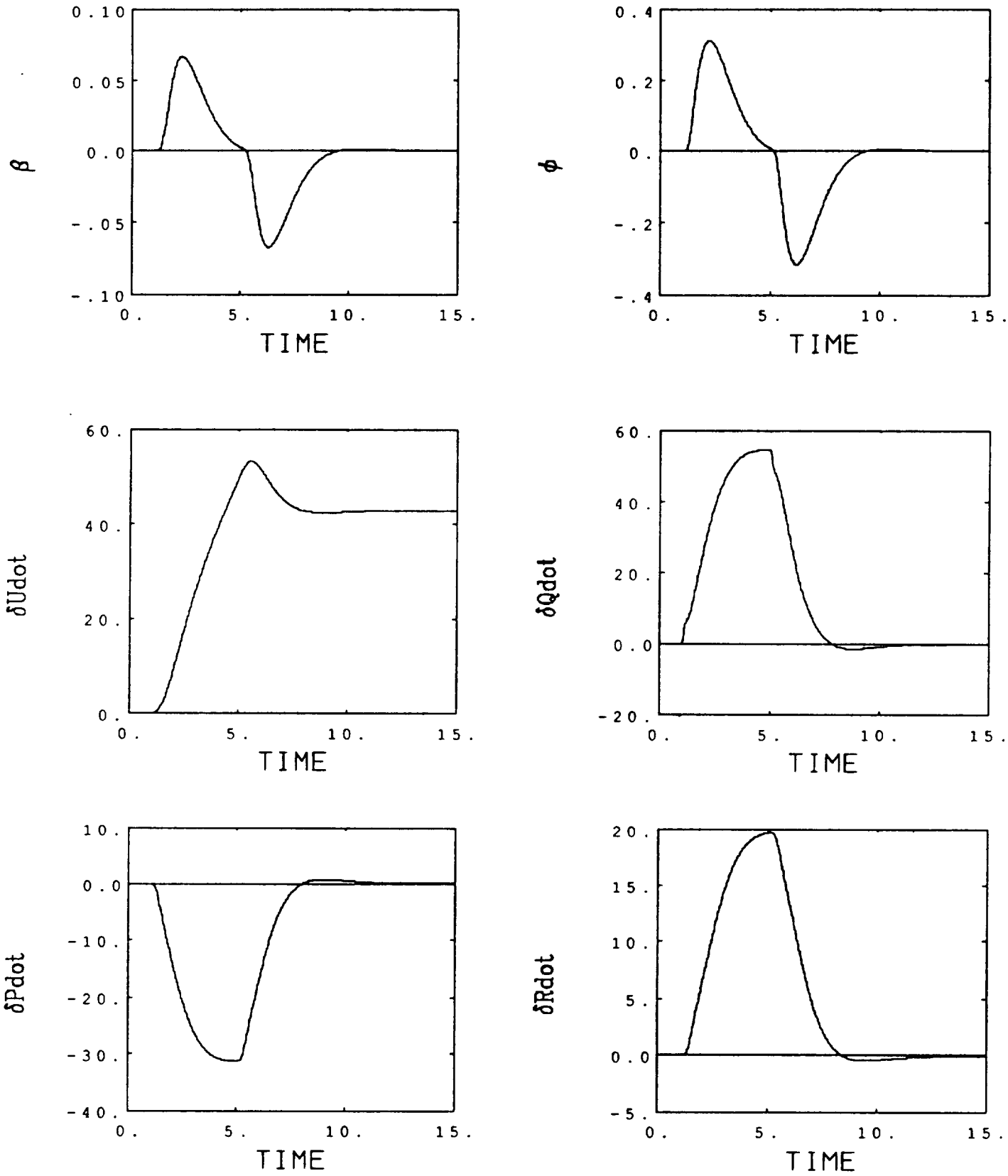

Figure 5-31b Longitudinal Stick Command: Case 5

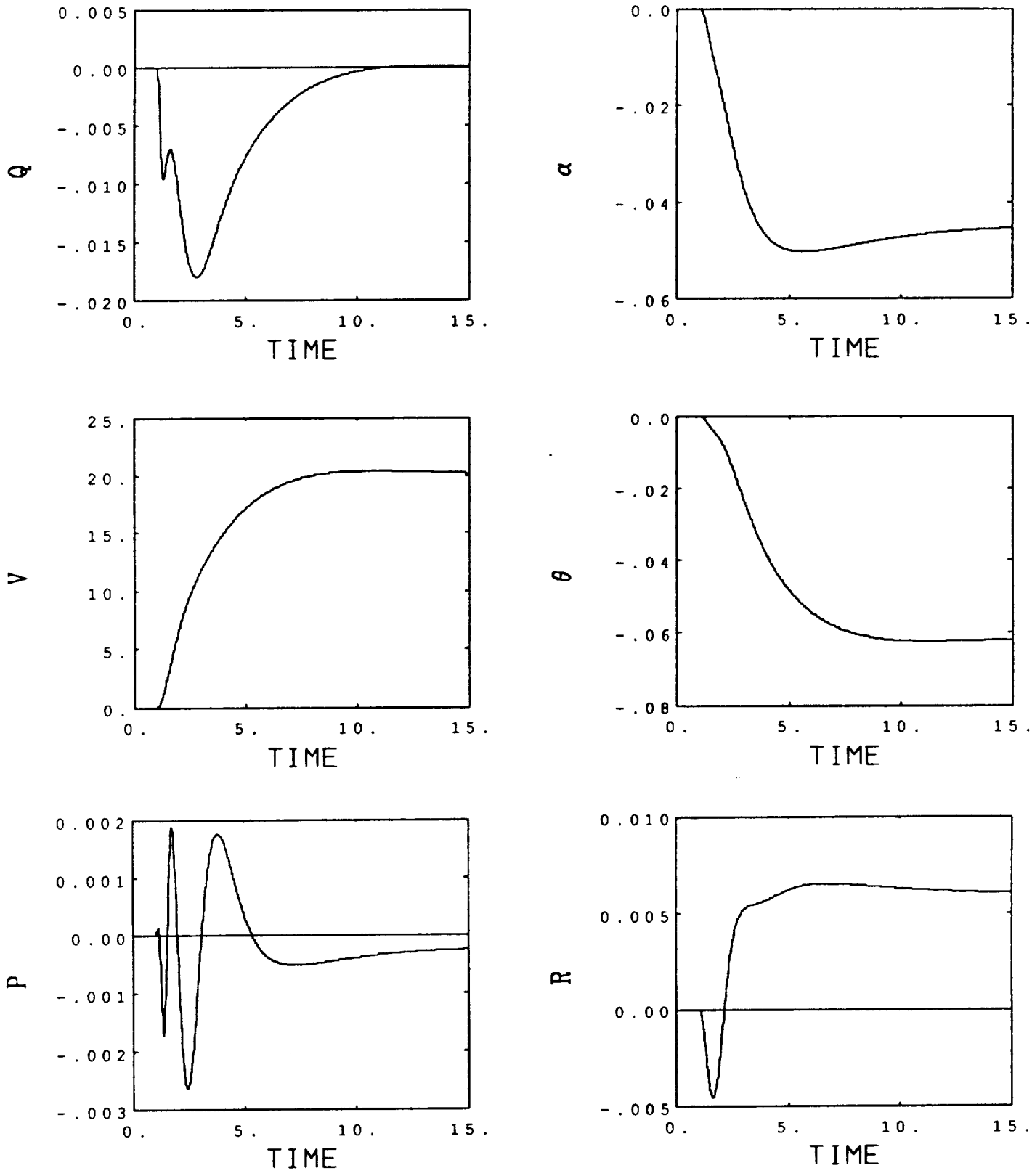

Figure 5-32a Airspeed Command: Case 5

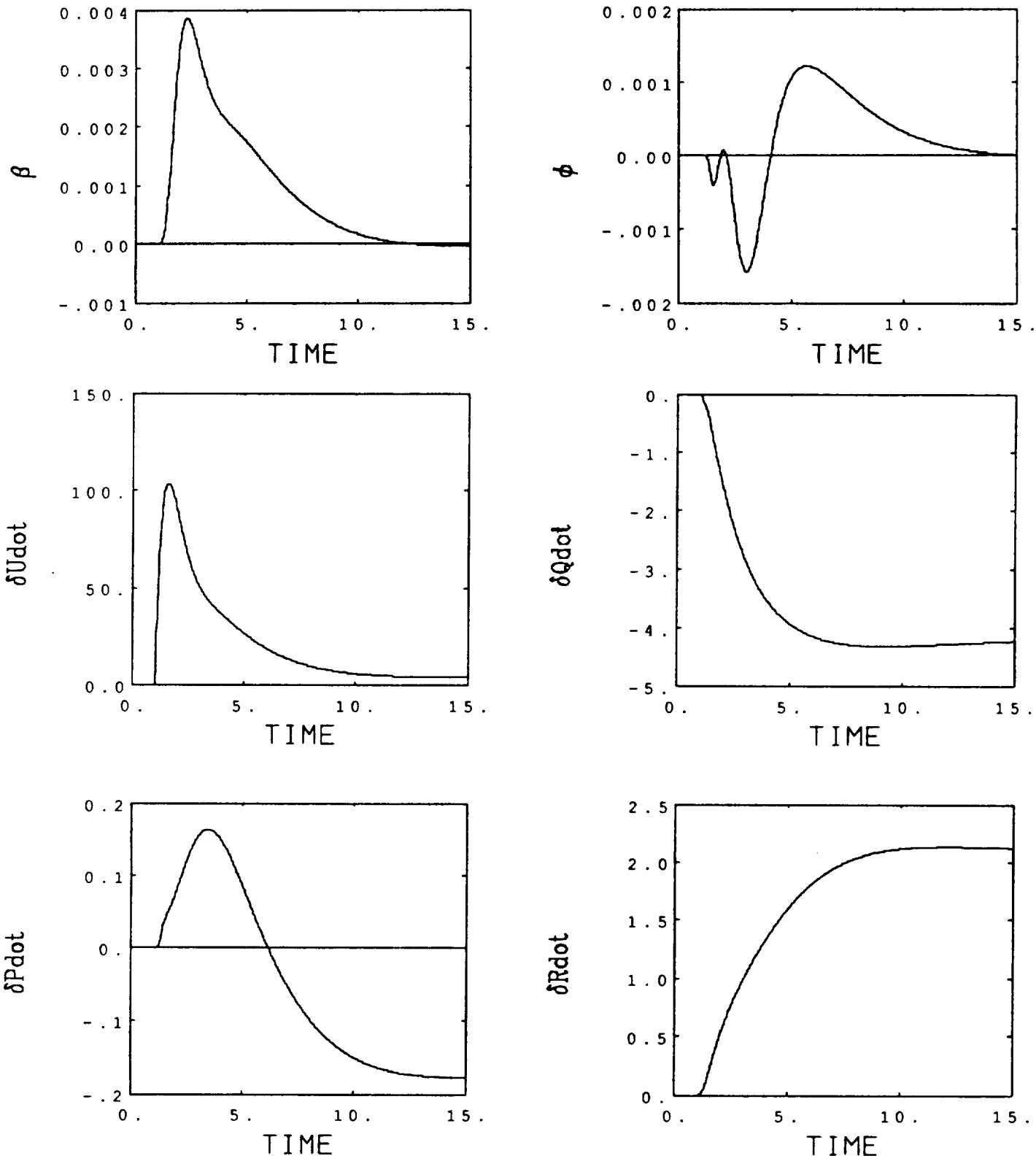

Figure 5-32b Airspeed Command: Case 5

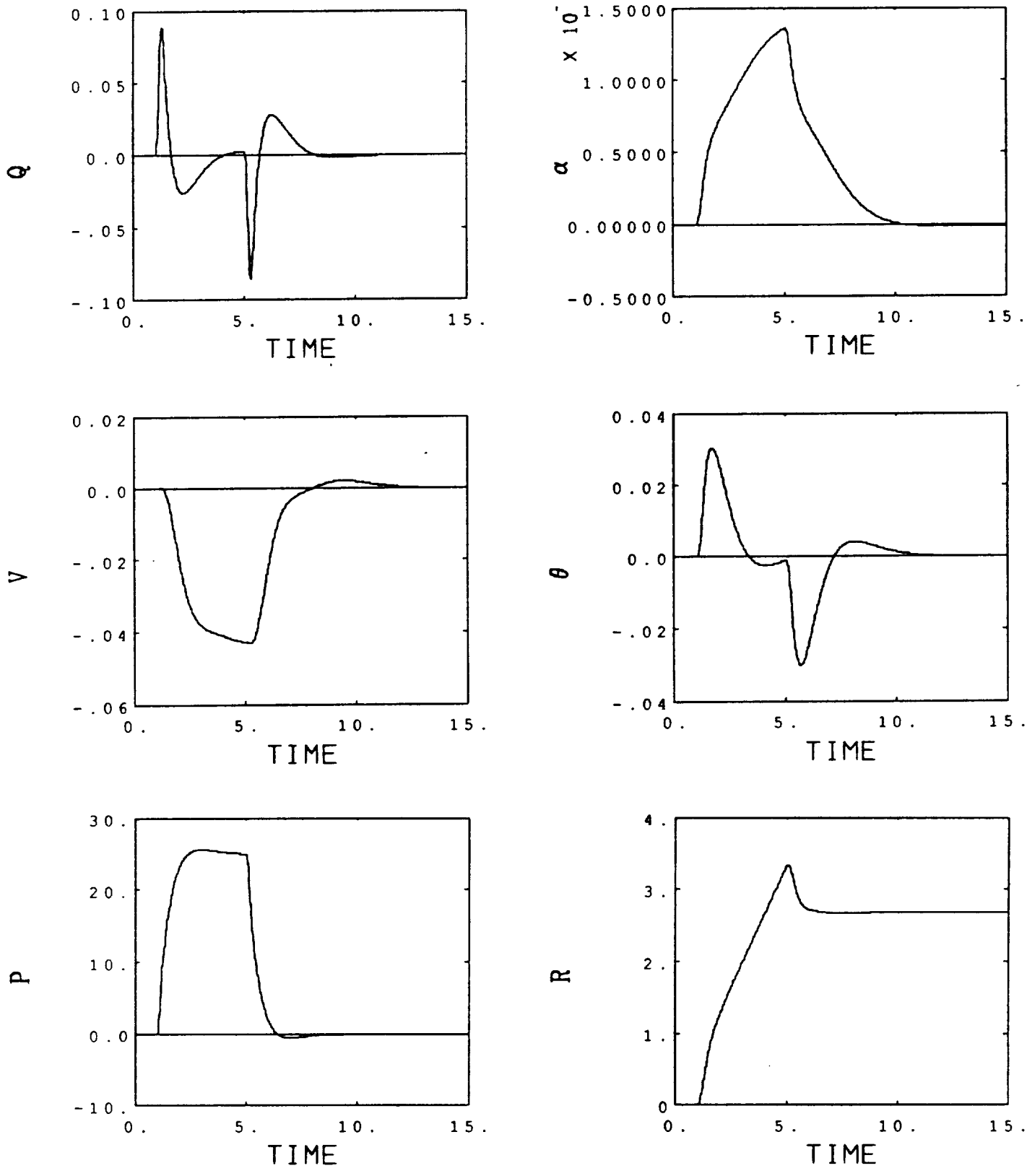

Figure 5-33a Lateral Stick Command: Case 5

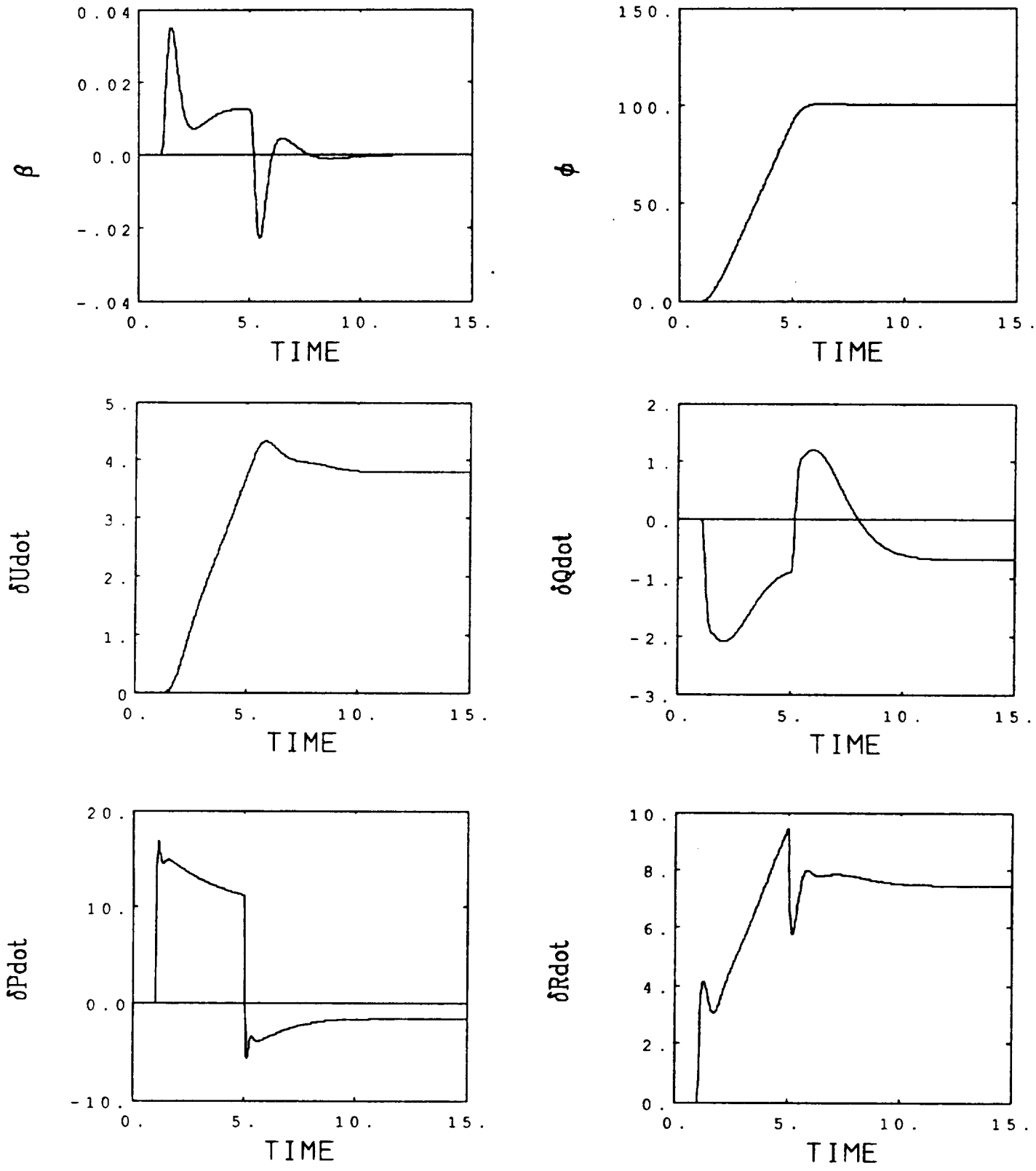

Figure 5-33b Lateral Stick Command: Case 5

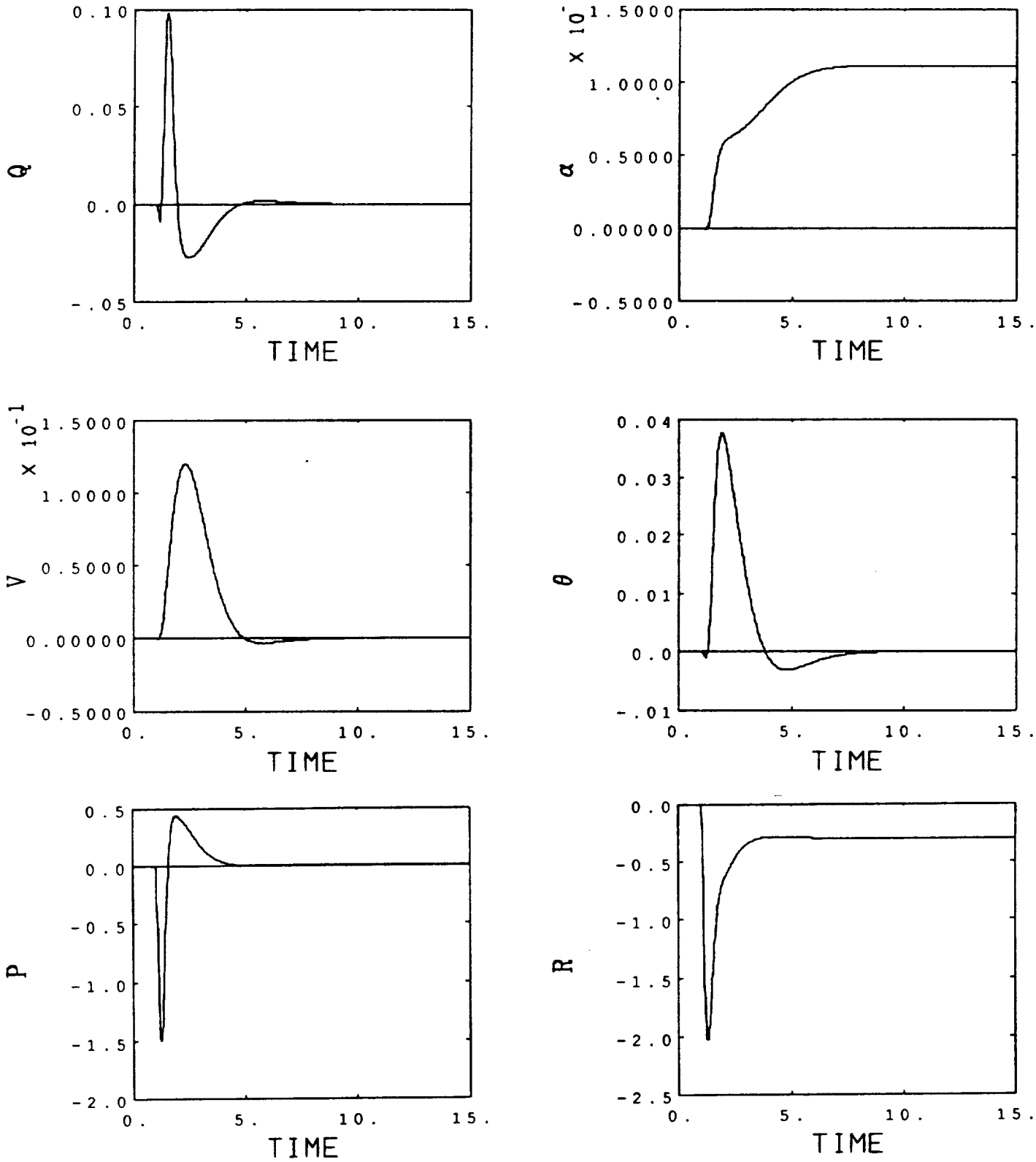

Figure 5-34a Pedal Command: Case 5

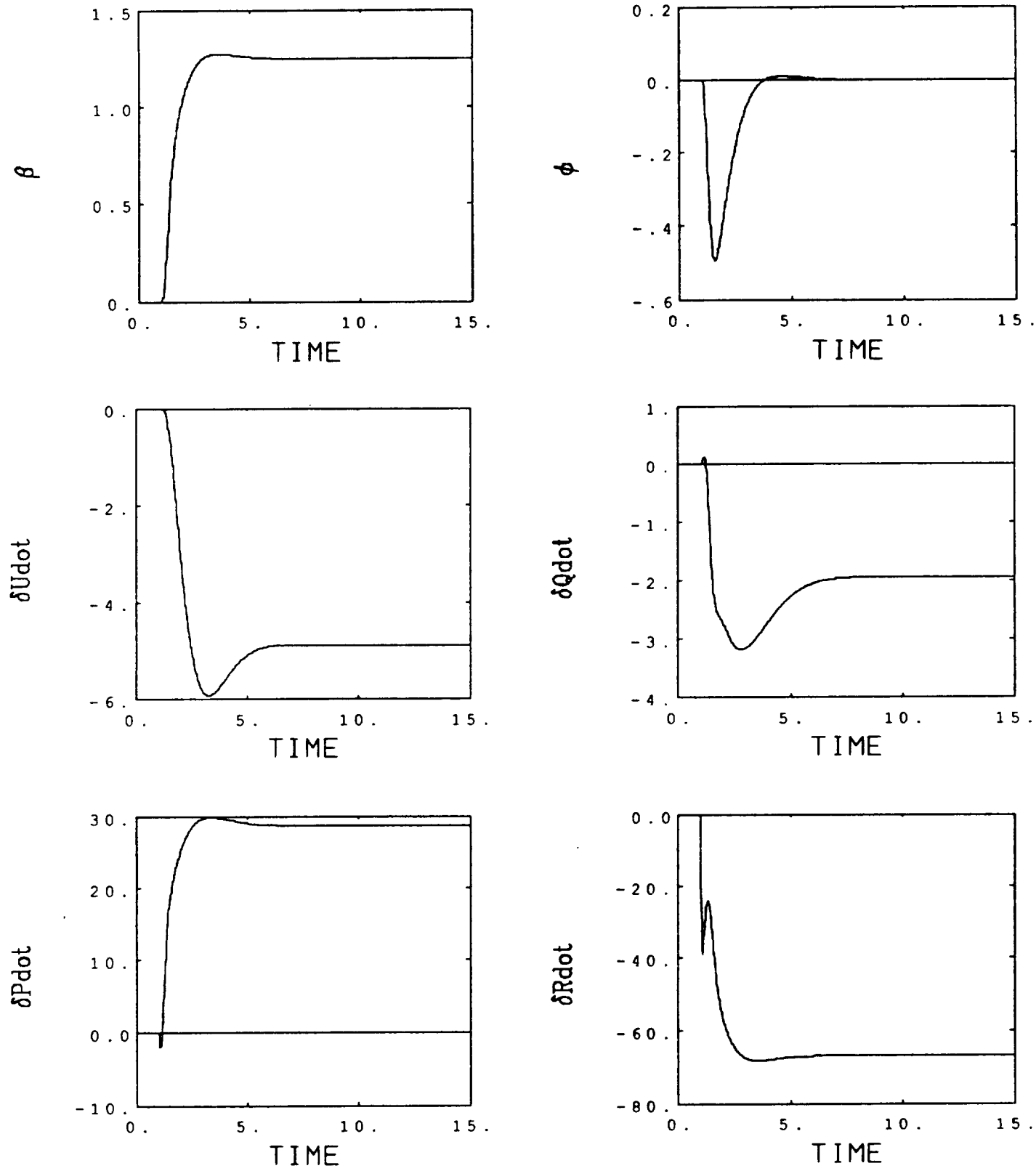

Figure 5-34b Pedal Command: Case 5

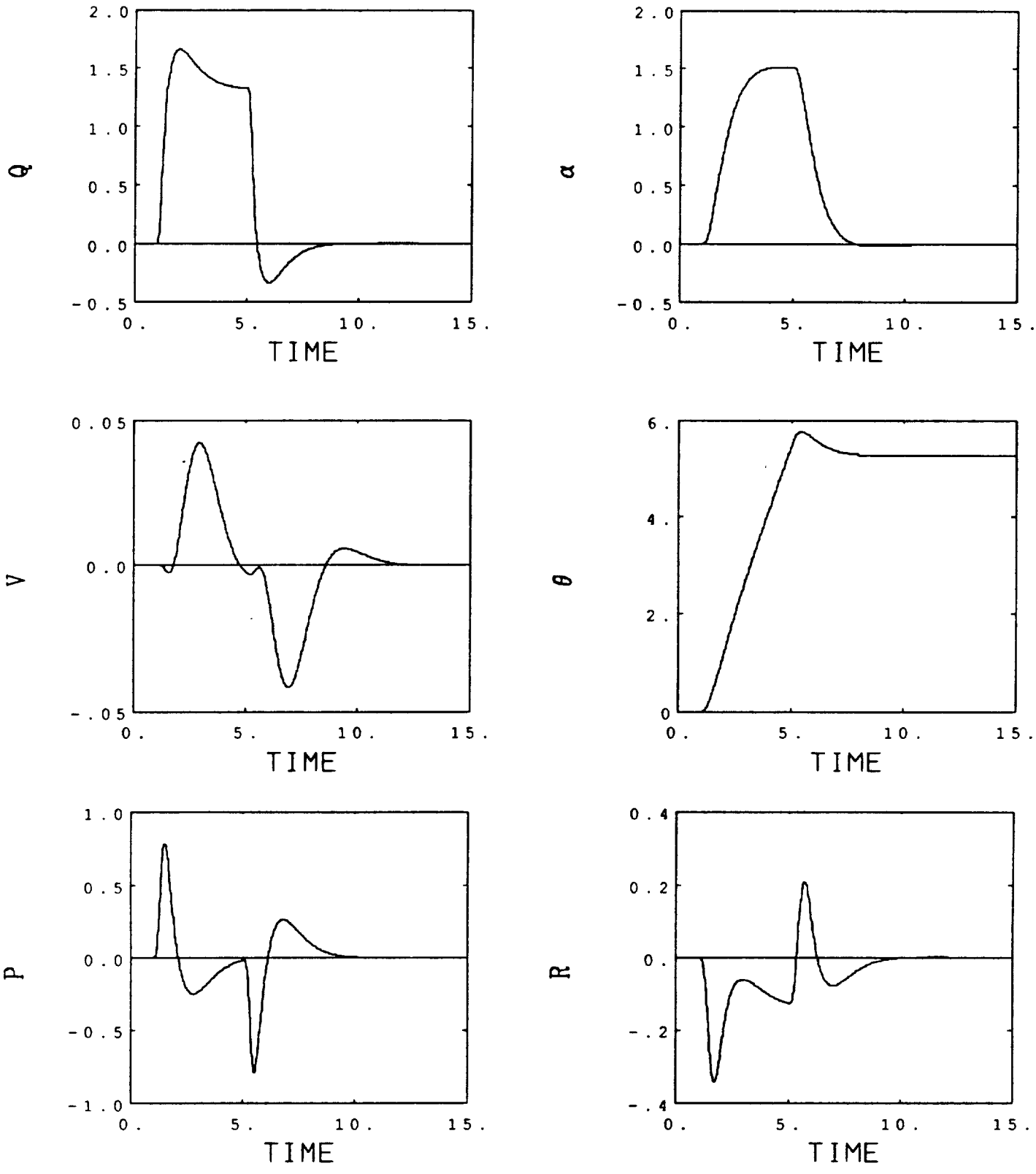

Figure 5-35a Longitudinal Stick Command: Case 6

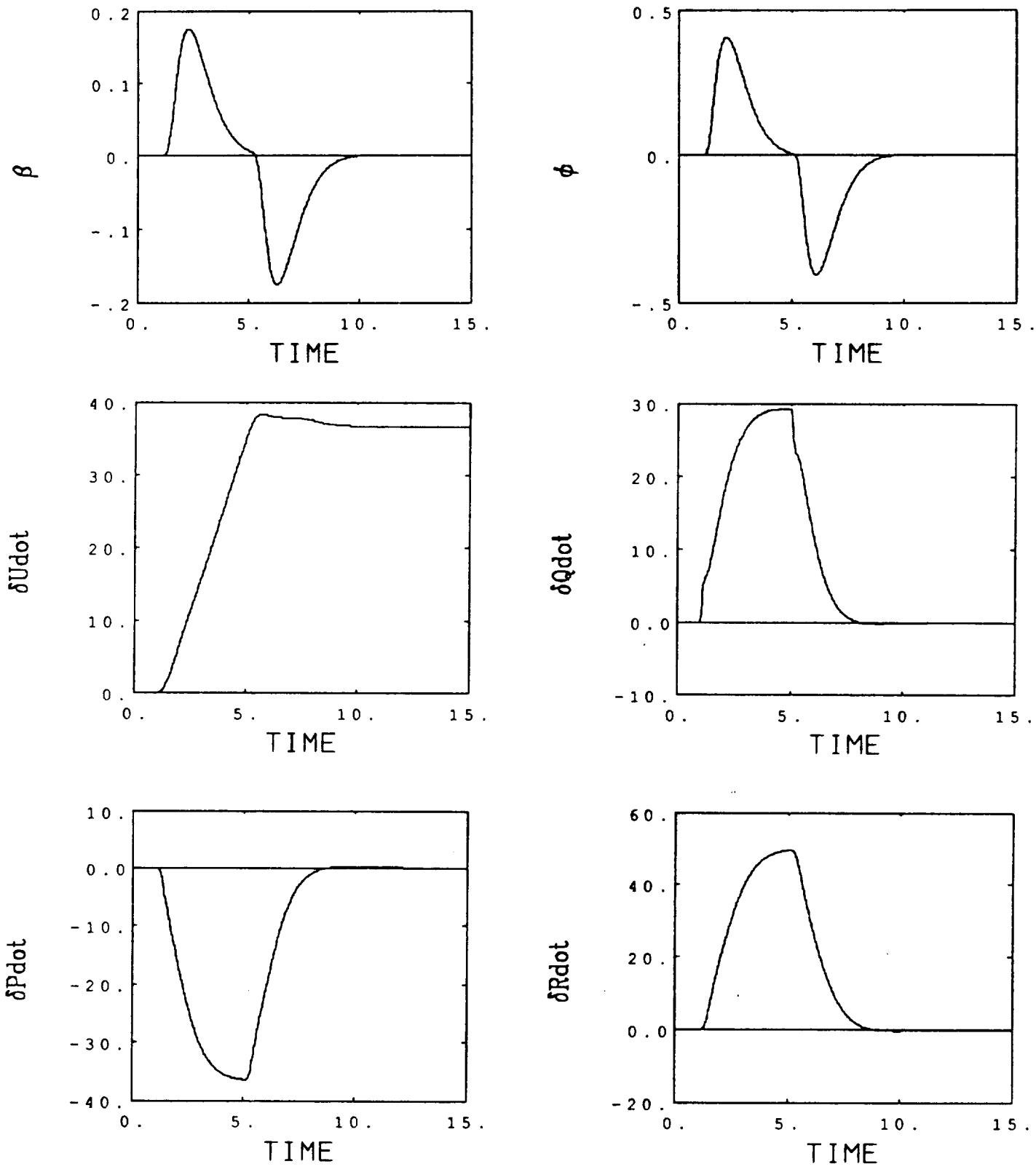

Figure 5-35b Longitudinal Stick Command: Case 6

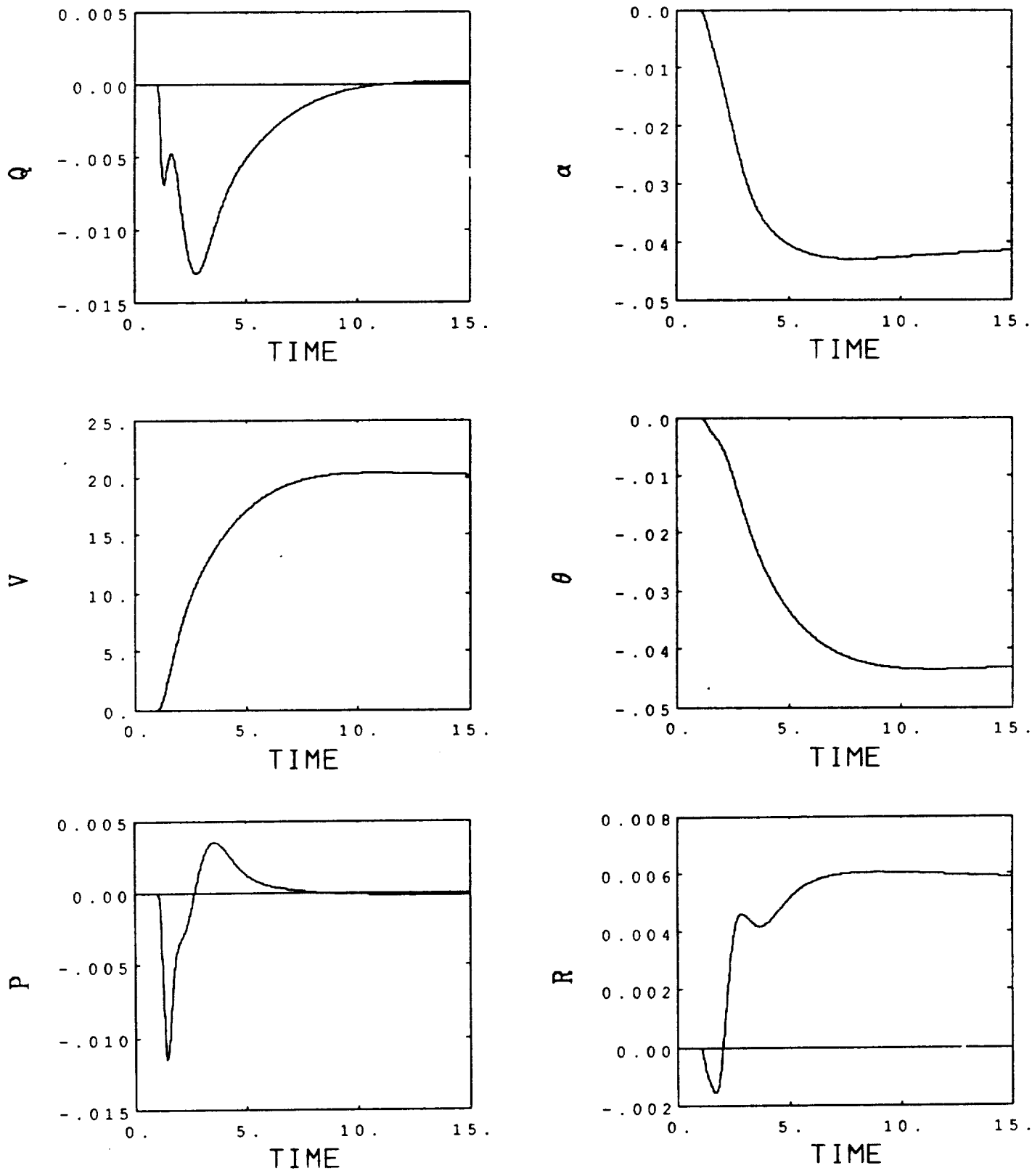

Figure 5-36a Airspeed Command: Case 6

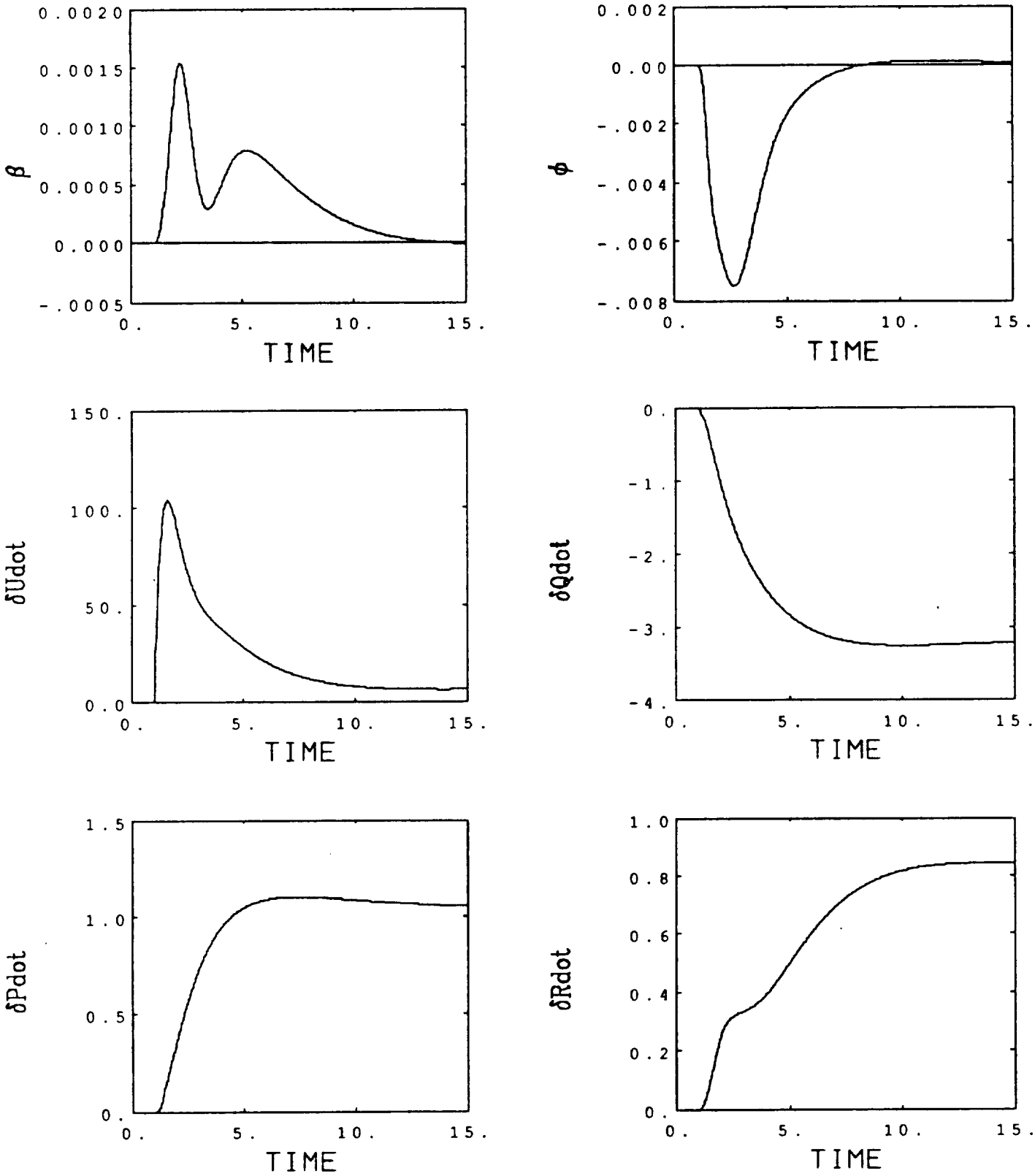

Figure 5-36b Airspeed Command: Case 6

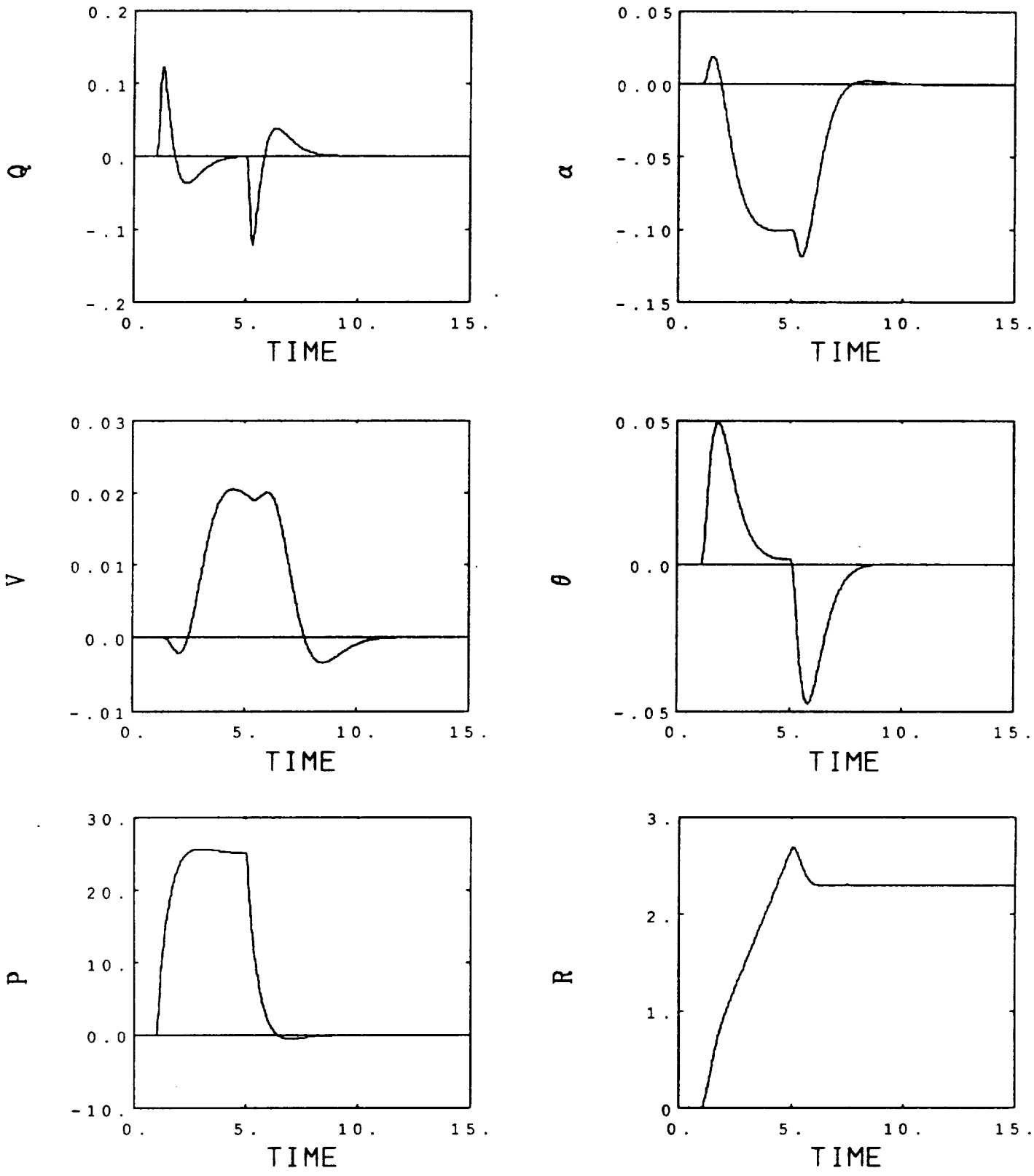

Figure 5-37a Lateral Stick Command: Case 6

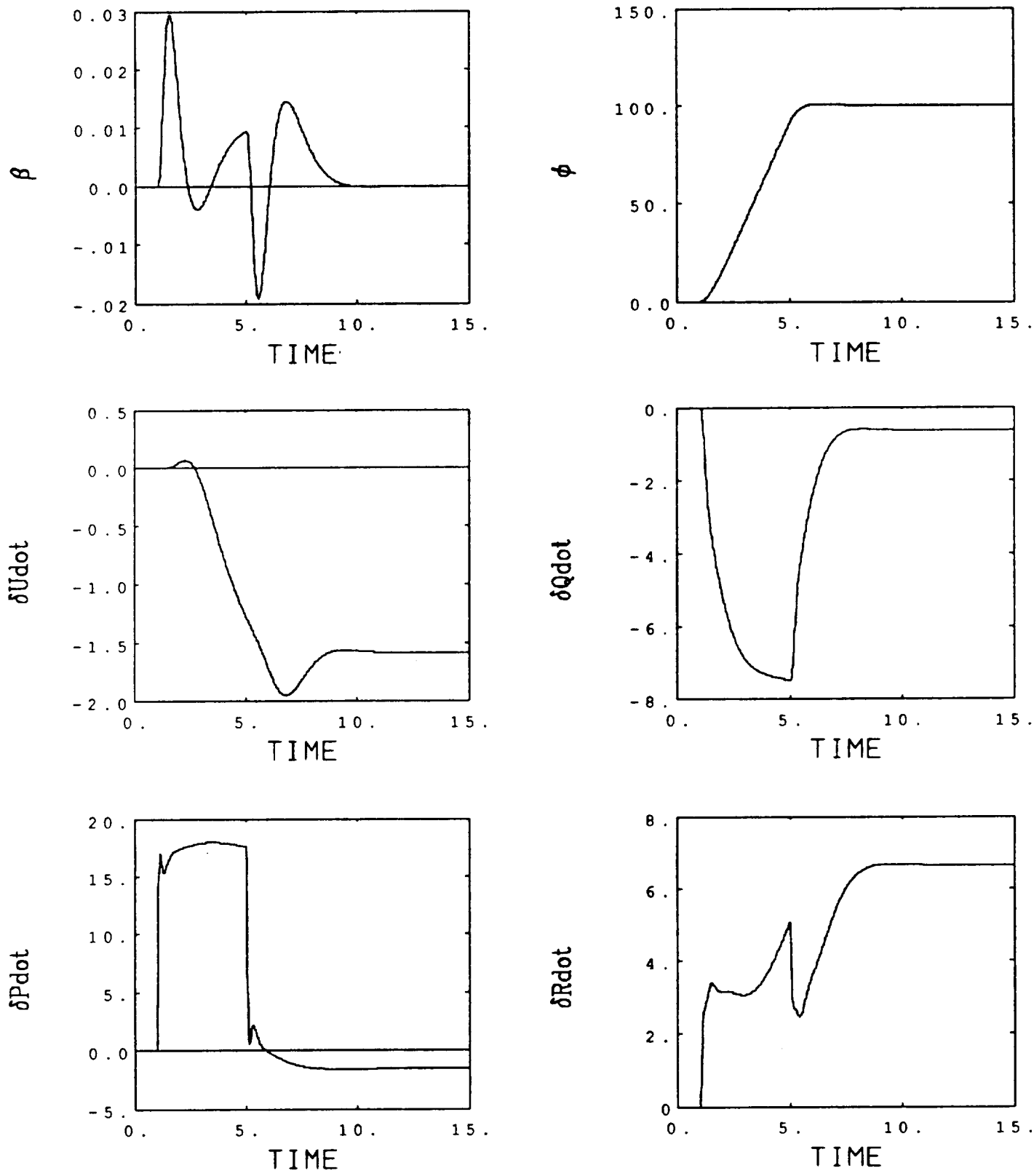

Figure 5-37b Lateral Stick Command: Case 6

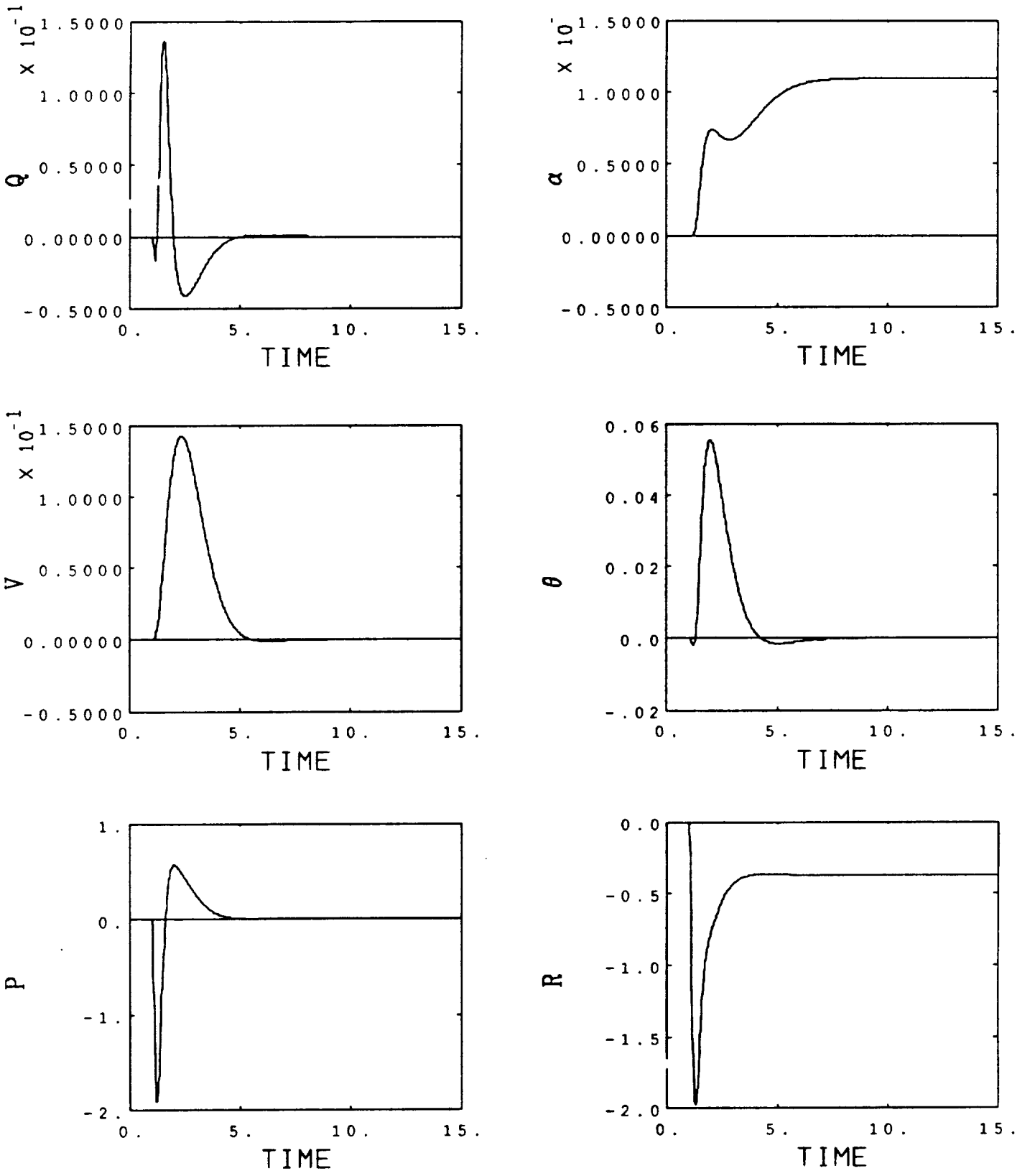

Figure 5-38a Pedal Command: Case 6

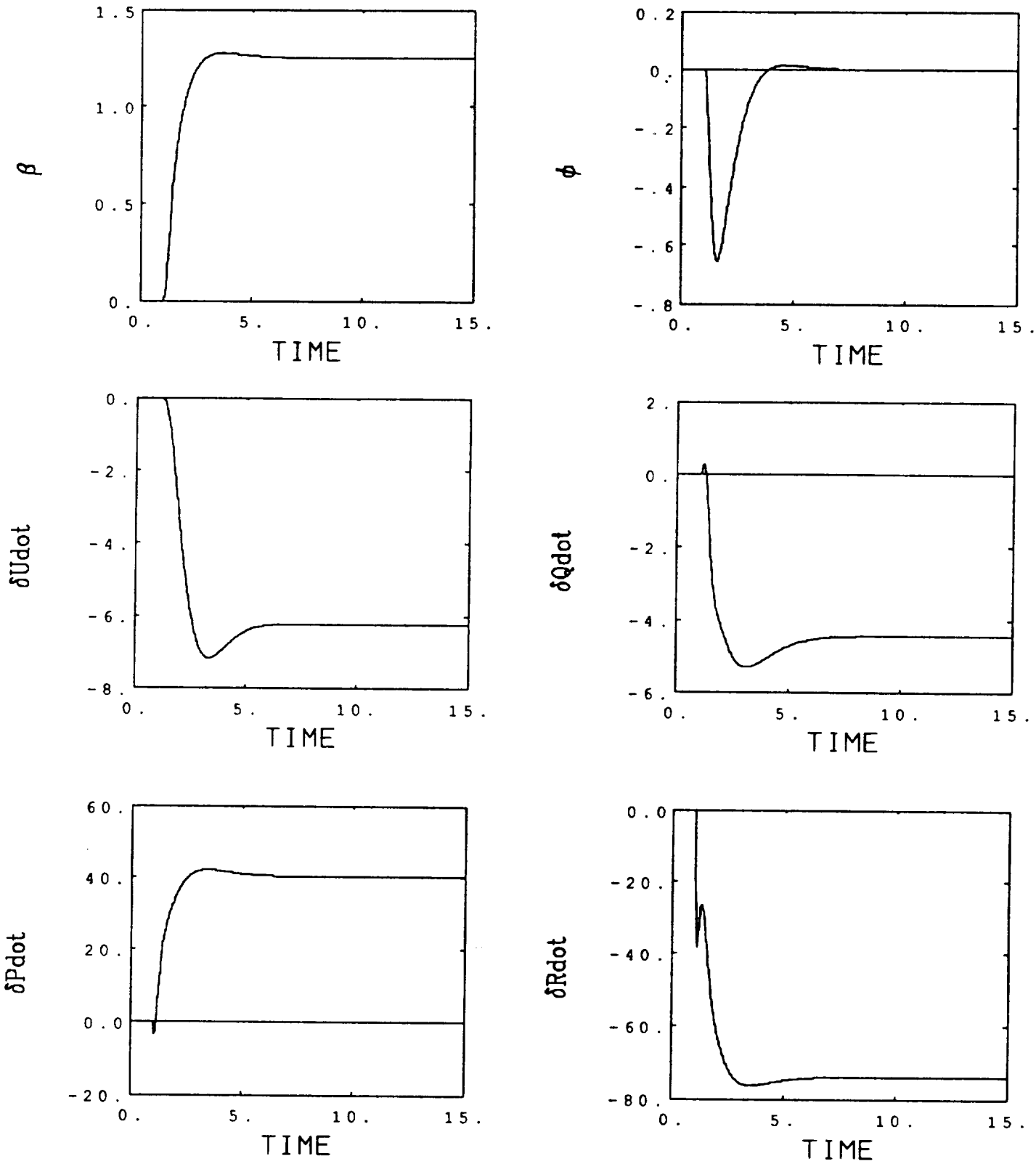

Figure 5-38b Pedal Command: Case 6

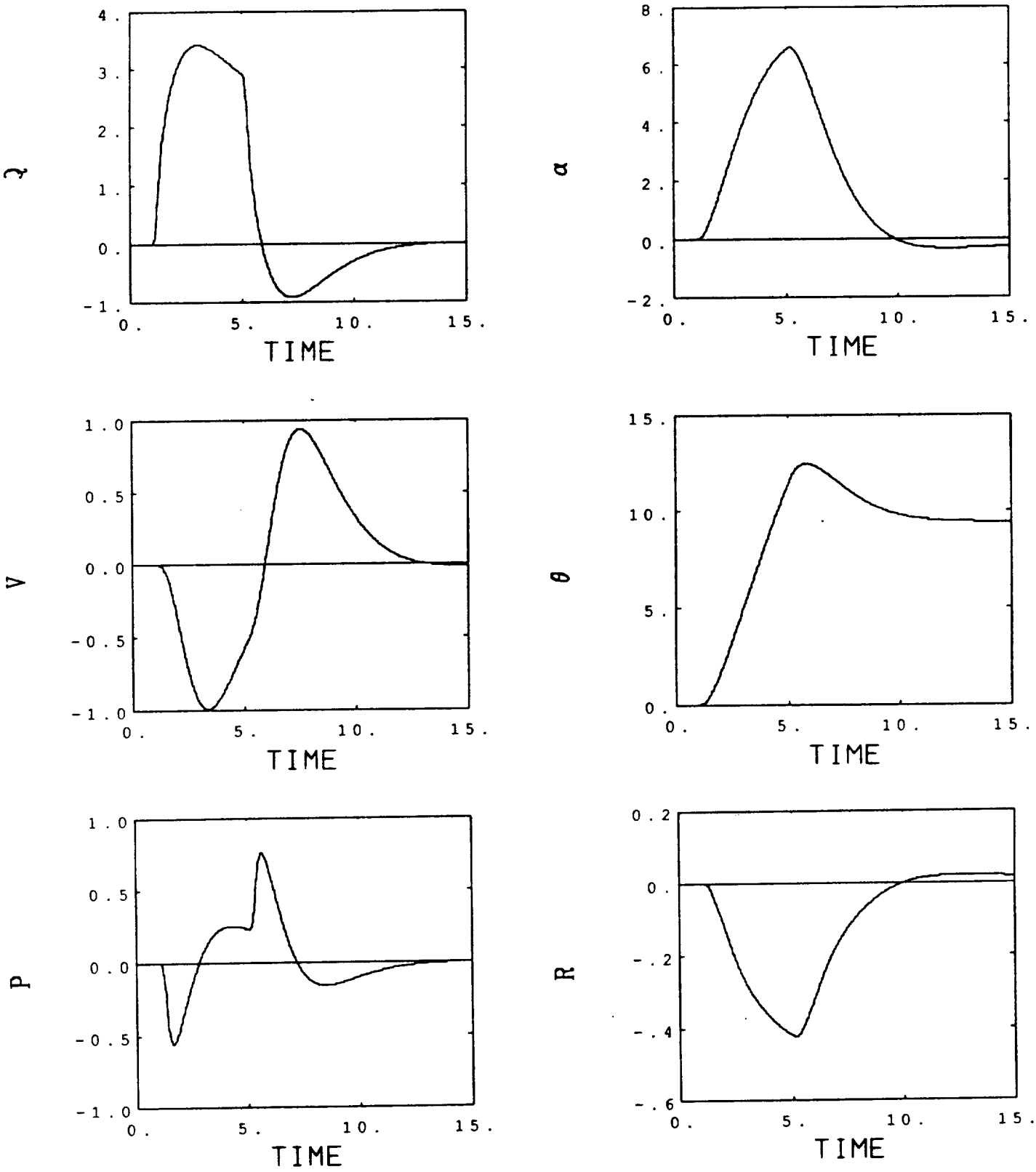

Figure 5-39a Longitudinal Stick Command: Case 7

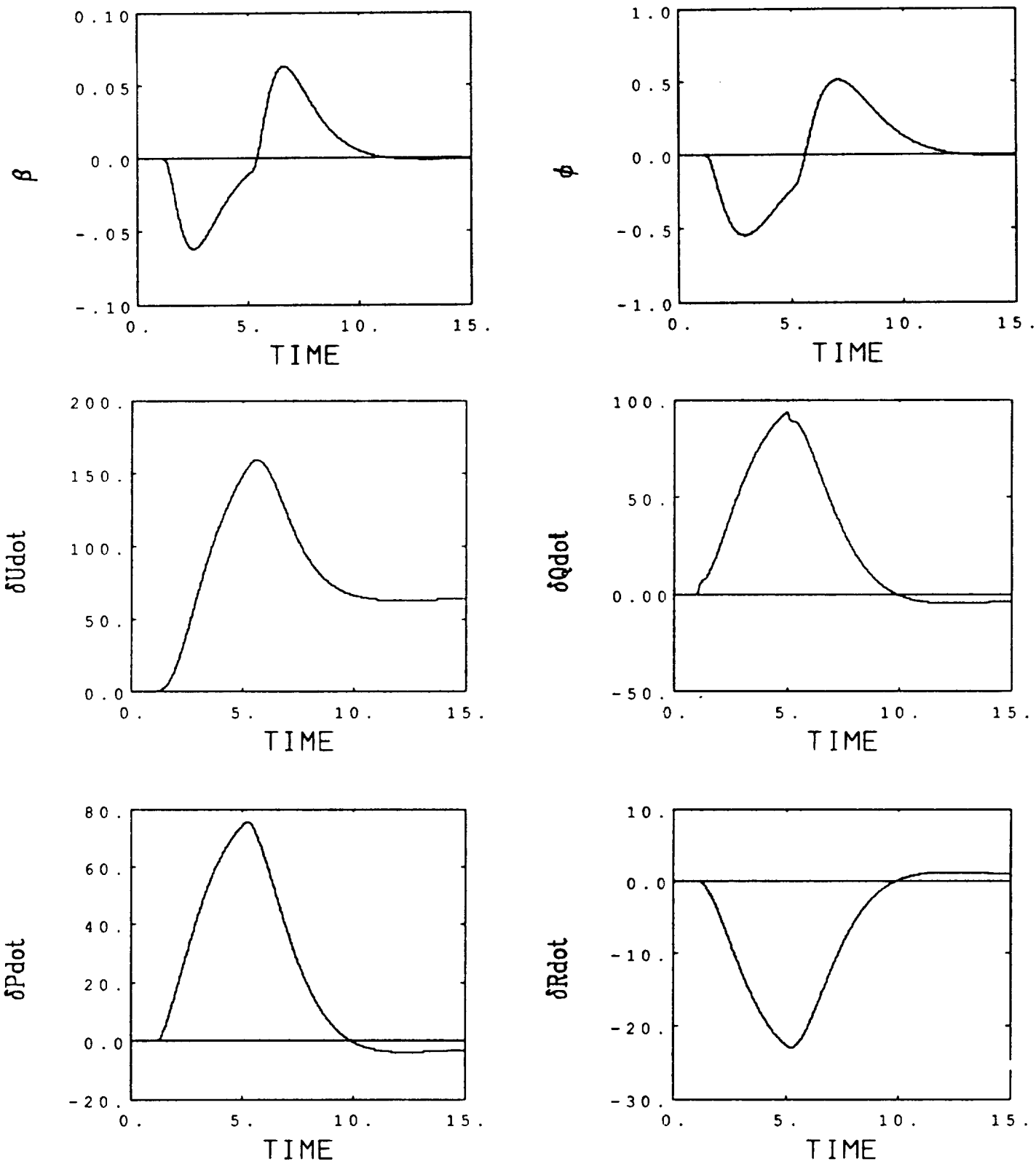

Figure 5-39b Longitudinal Stick Command: Case 7

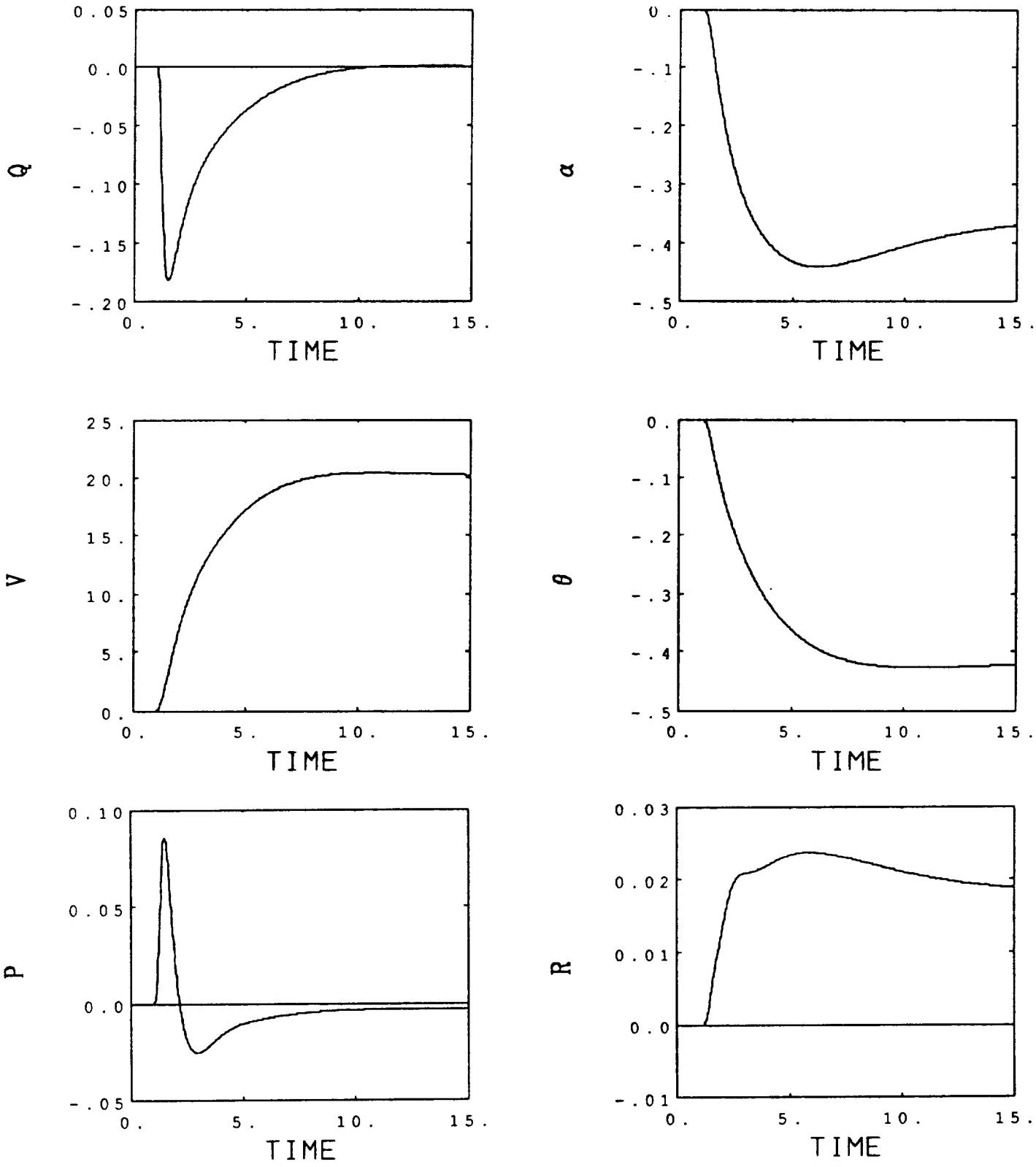

Figure 5-40a Airspeed Command: Case 7

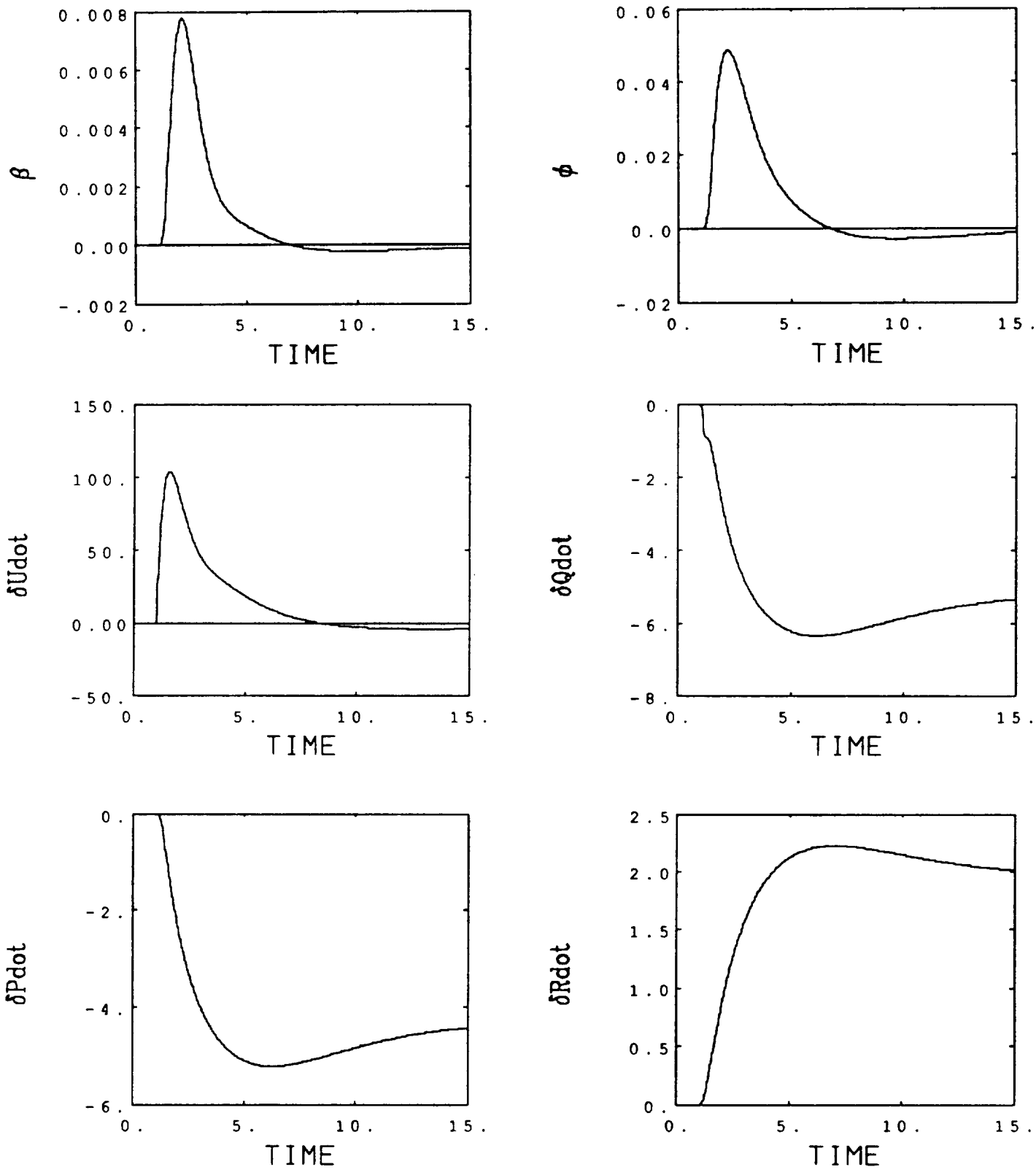

Figure 5-40b Airspeed Command: Case 7

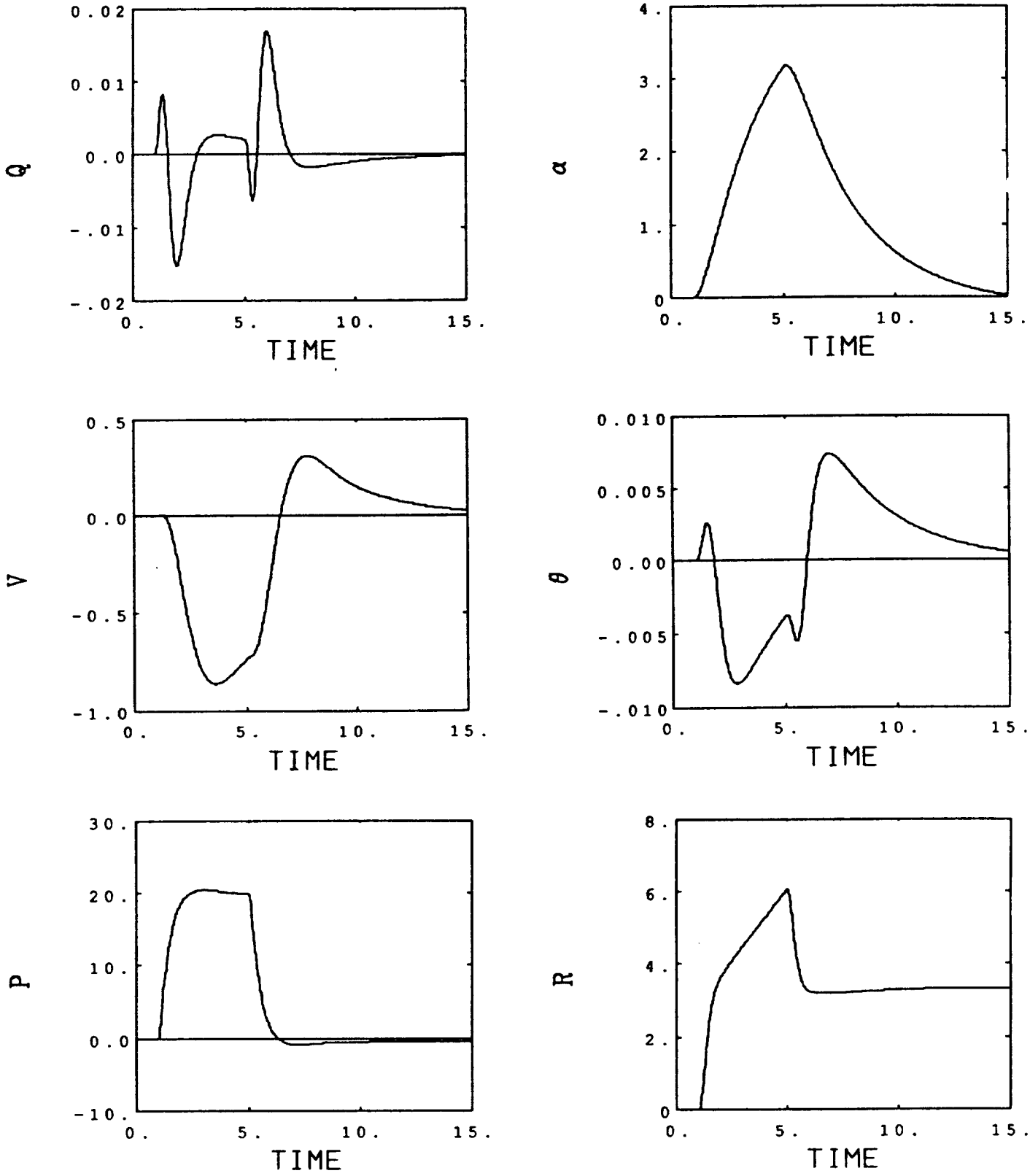

Figure 5-41a Lateral Stick Command: Case 7

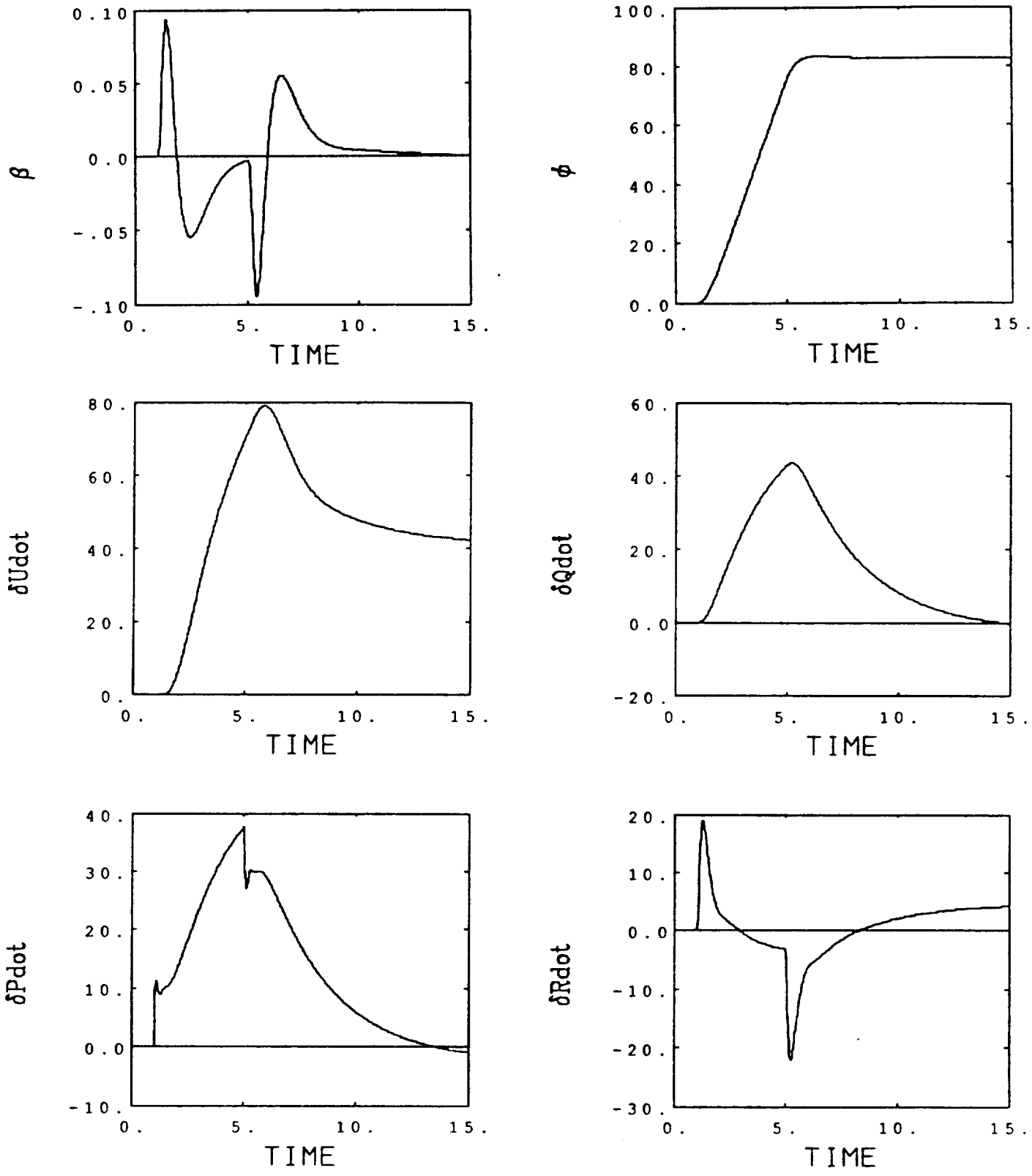

Figure 5-41b Lateral Stick Command: Case 7

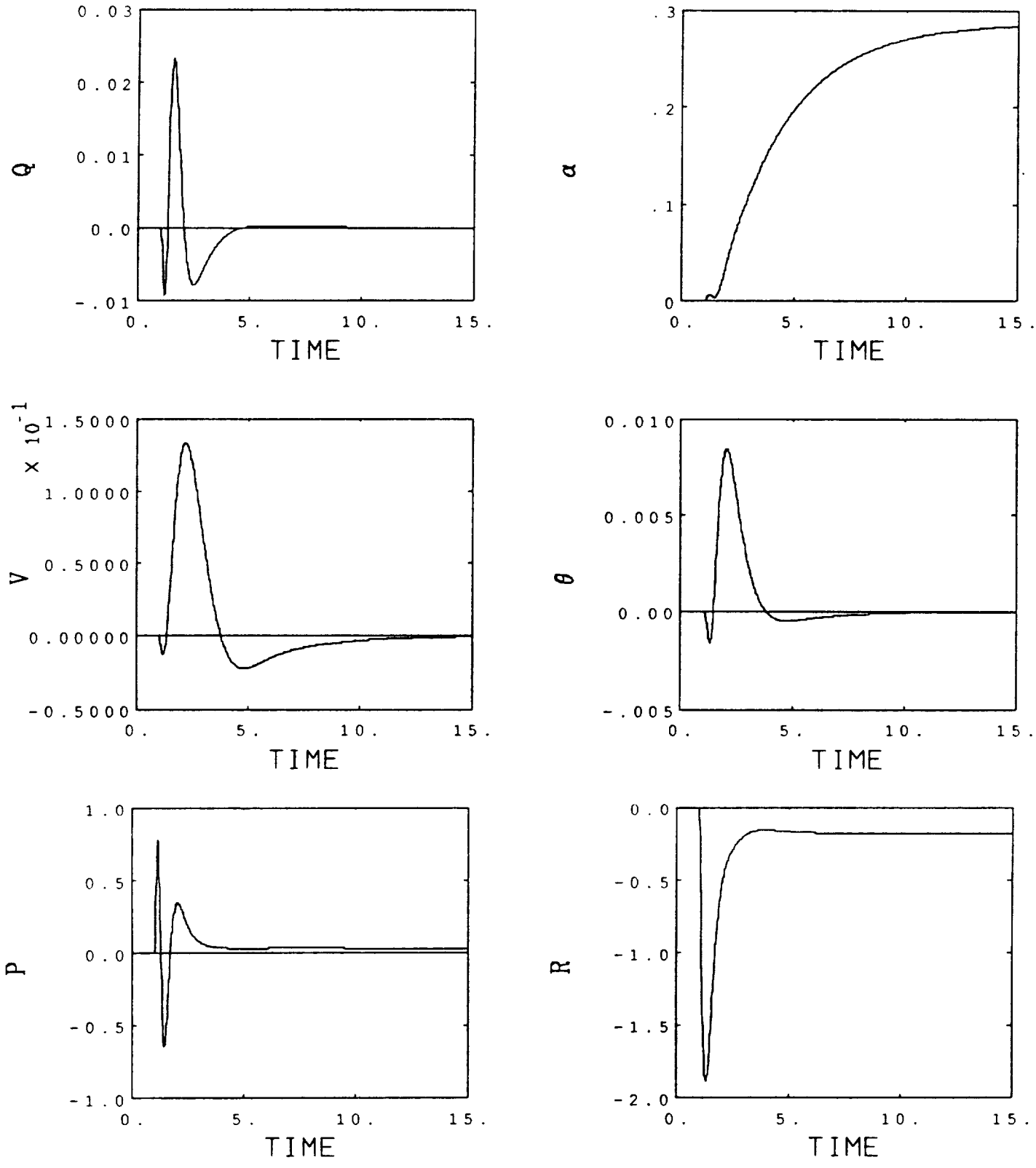

Figure 5-42a Pedal Command: Case 7

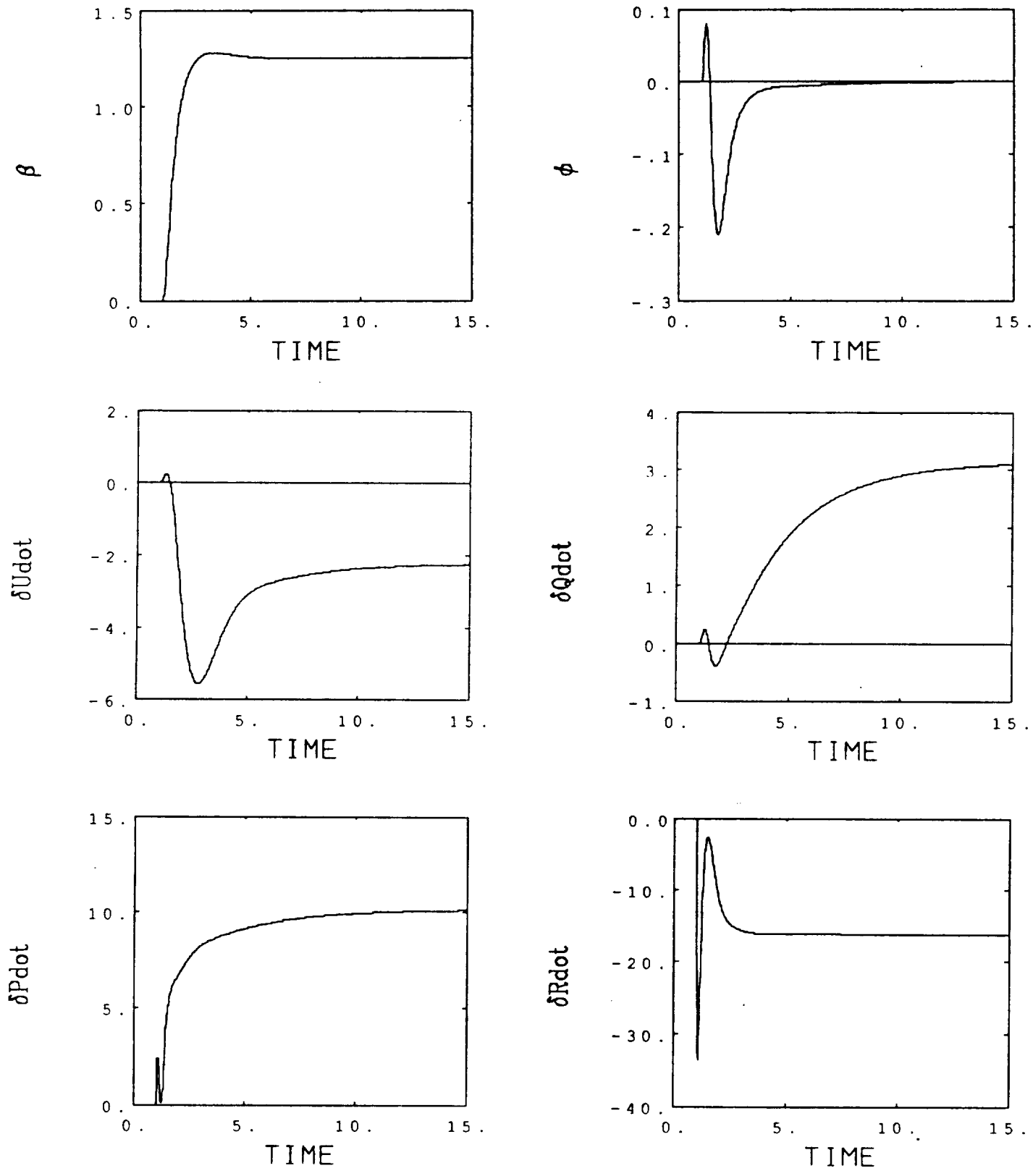

Figure 5-42b Pedal Command: Case 7

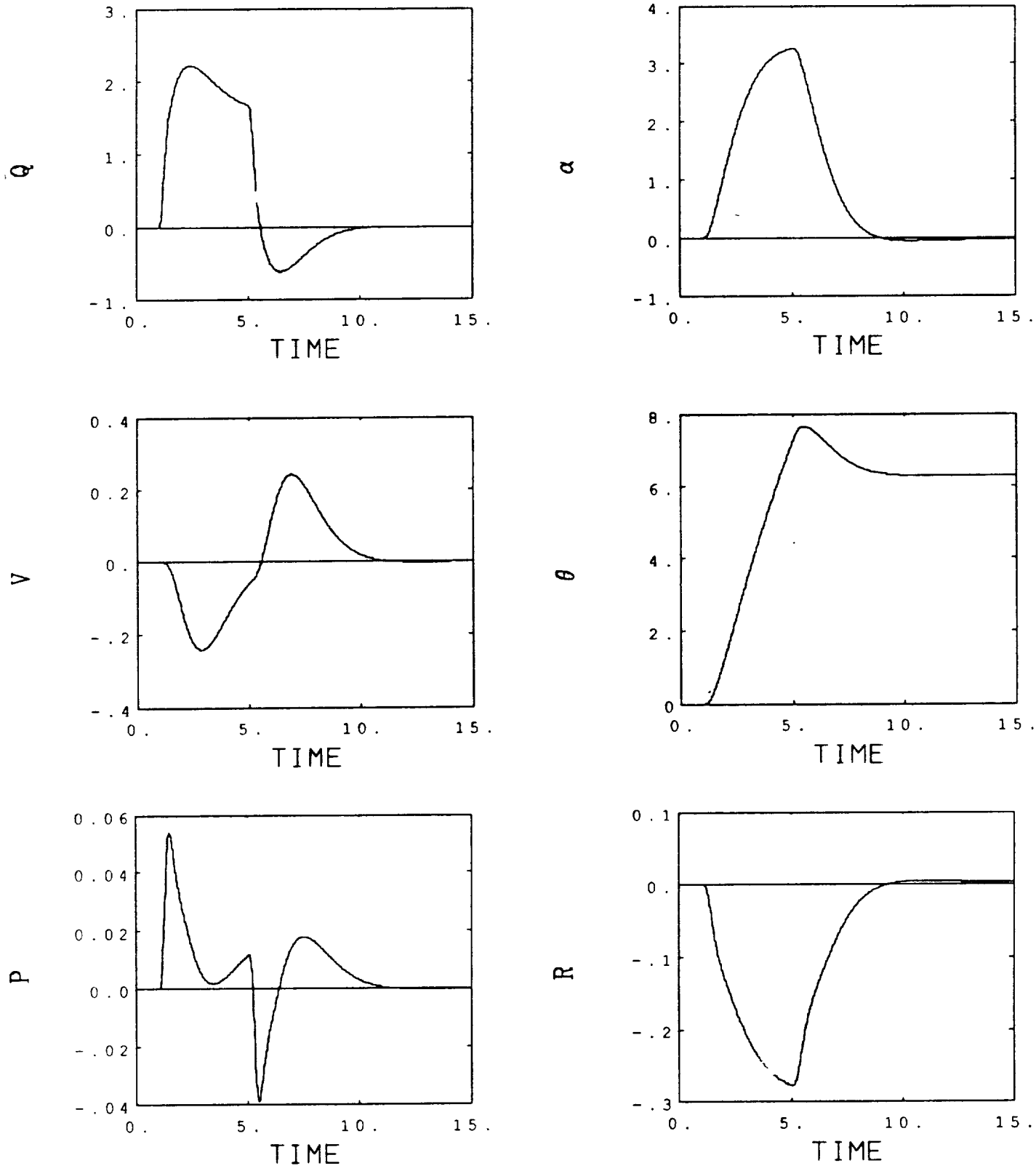

Figure 5-43a Longitudinal Stick Command: Case 8

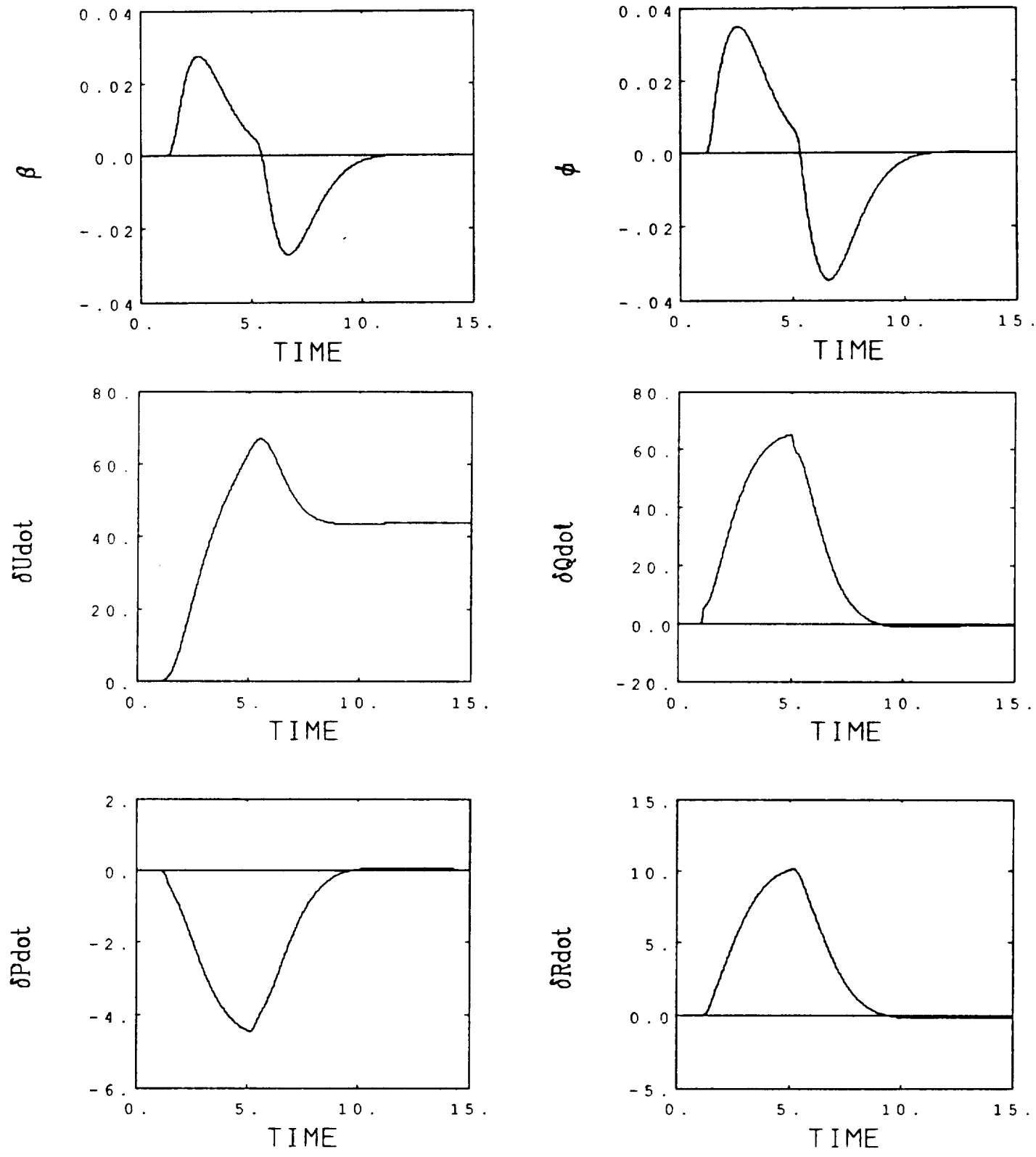

Figure 5-43b Longitudinal Stick Command: Case 8

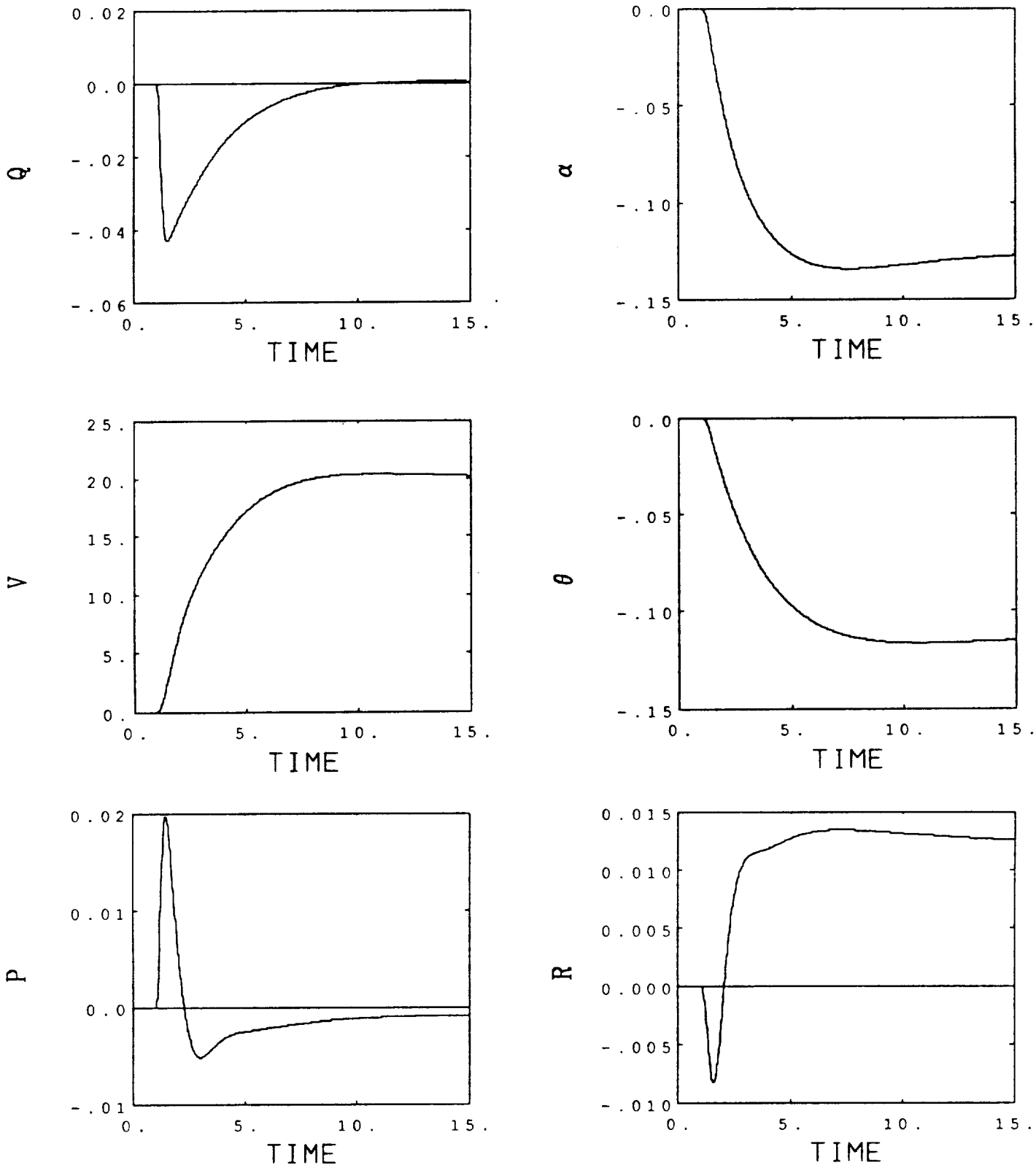

Figure 5-44a Airspeed Command: Case 8

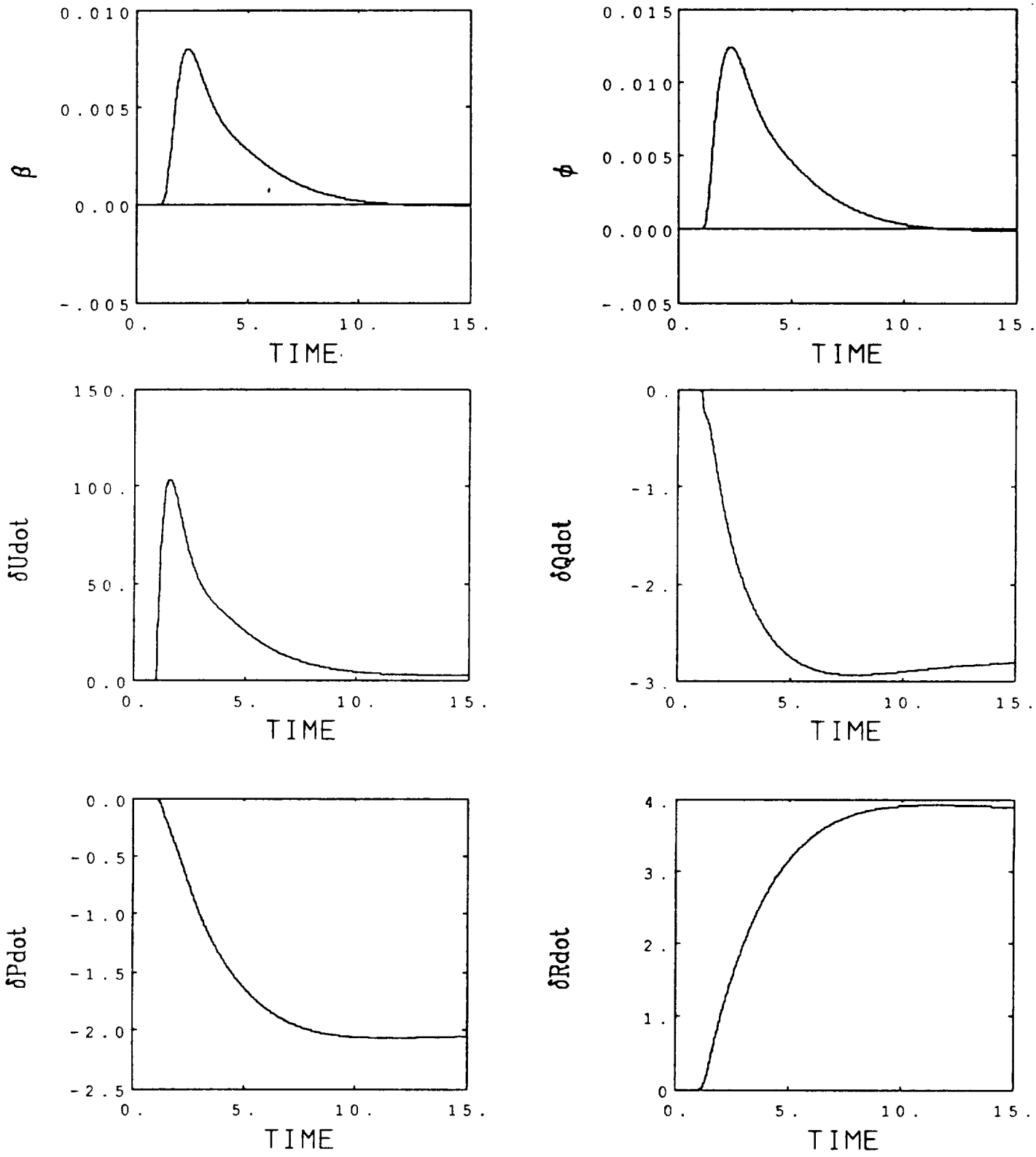

Figure 5-44b Airspeed Command: Case 8

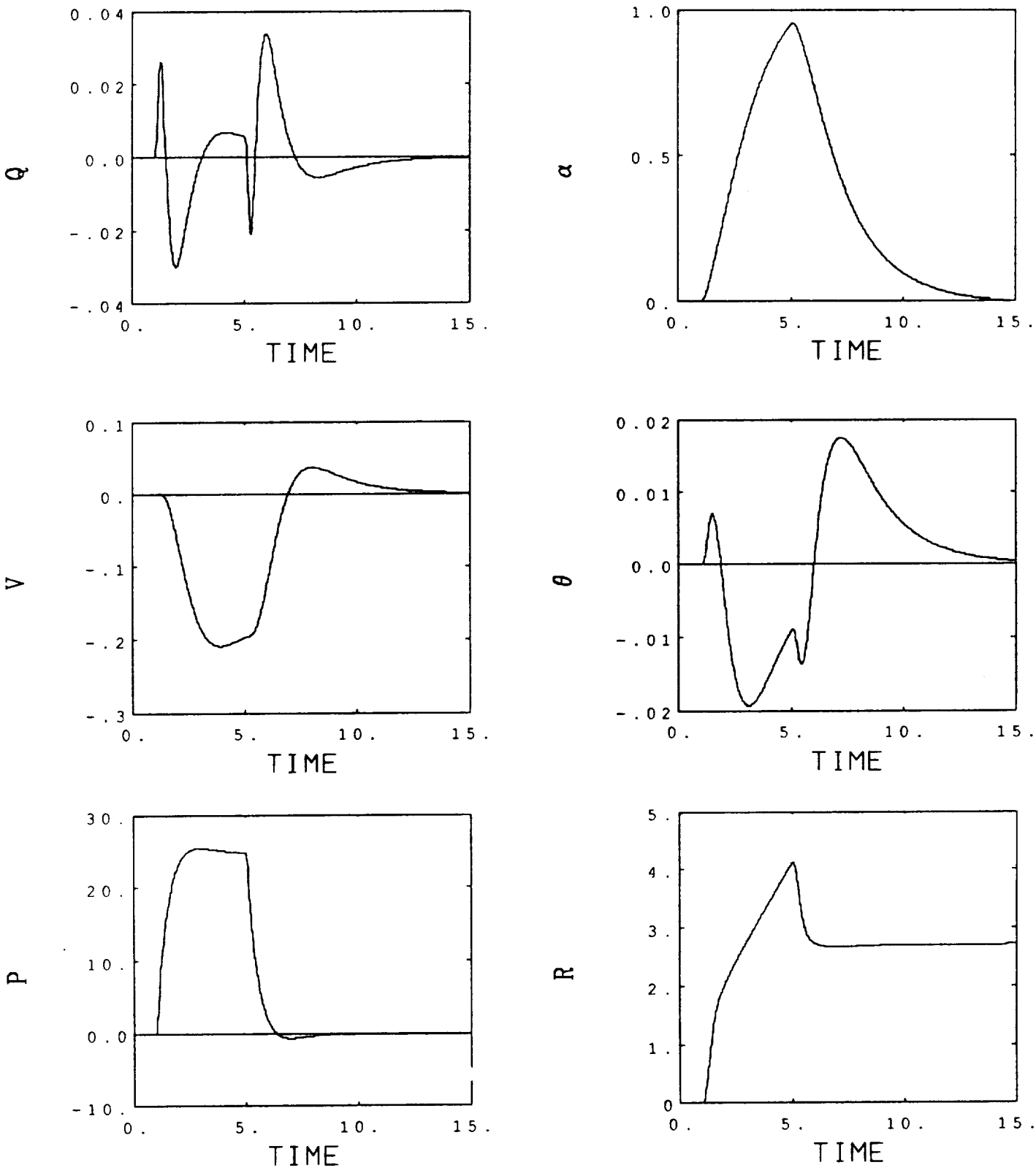

Figure 5-45a Lateral Stick Command: Case 8

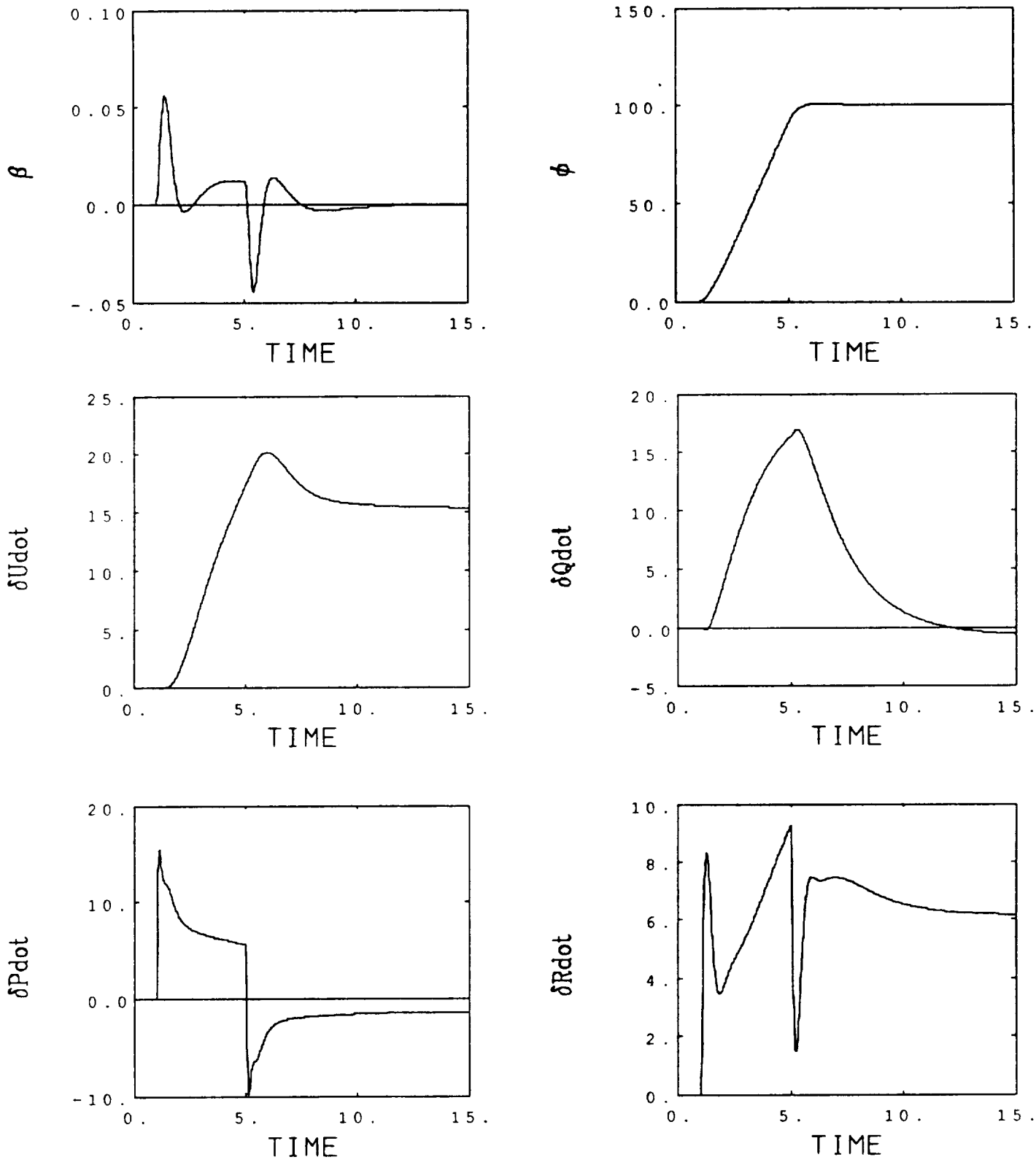

Figure 5-45b Lateral Stick Command: Case 8

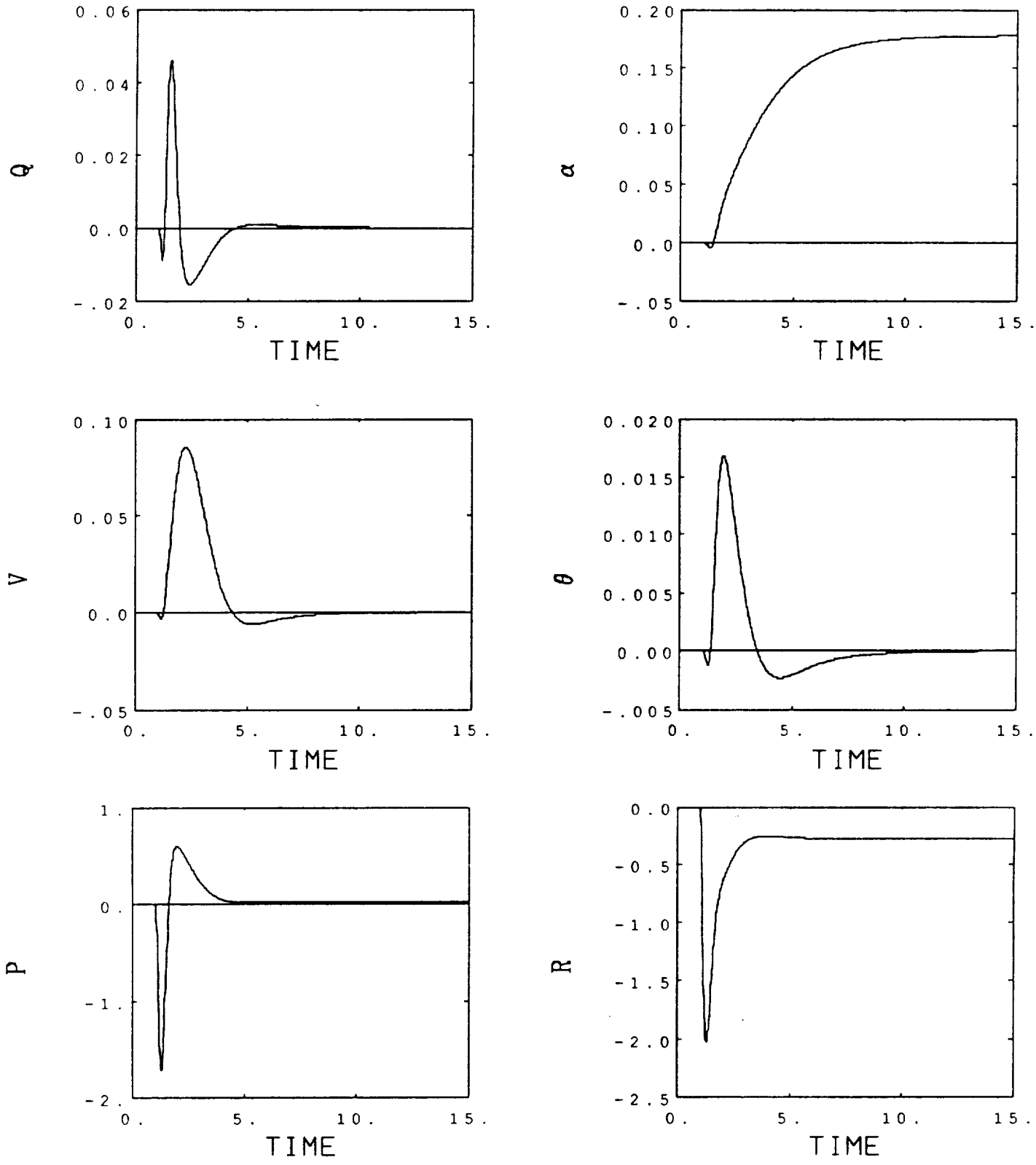

Figure 5-46. Pedal Command: Case 8

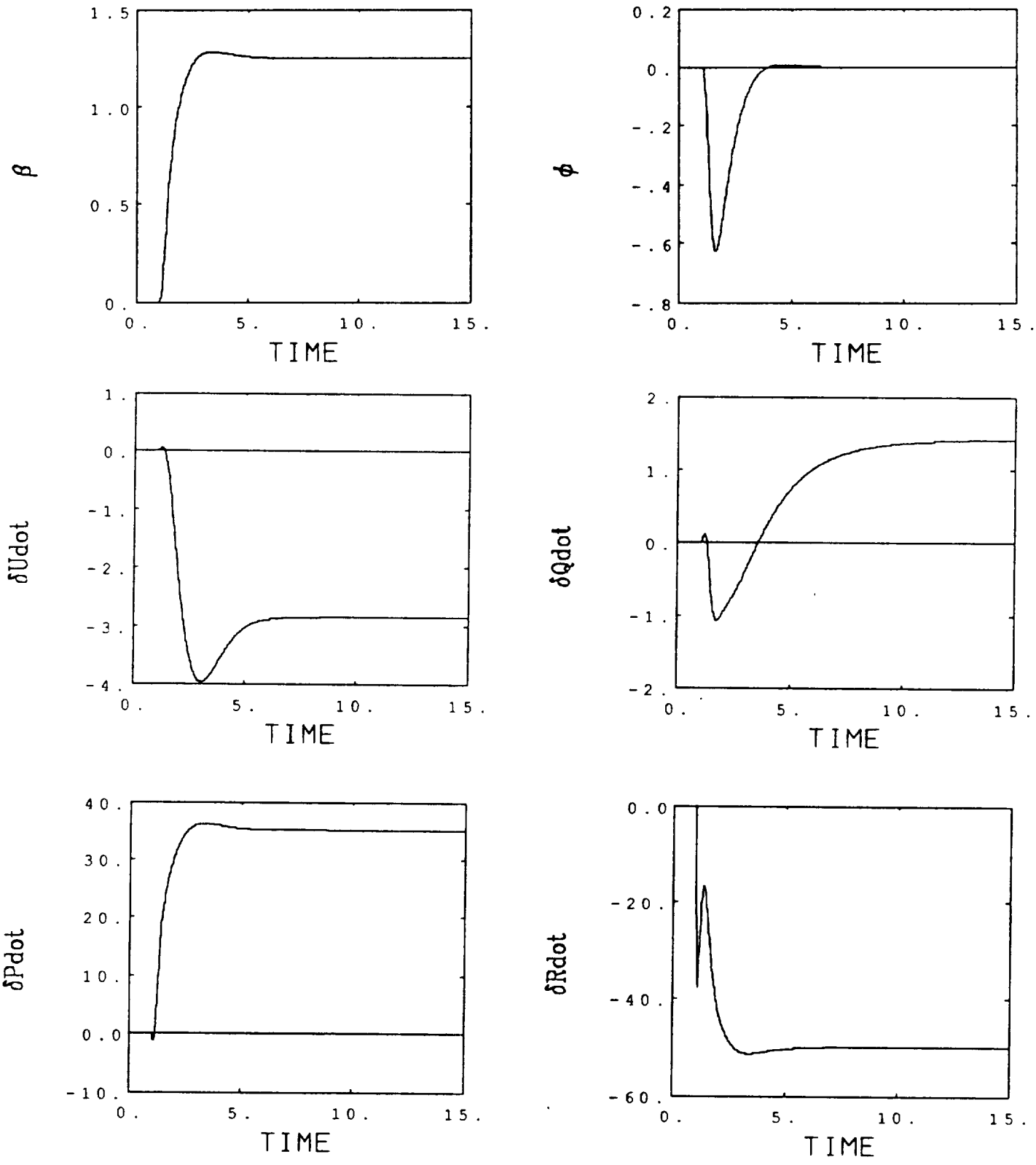

Figure 5-46b Pedal Command: Case 8

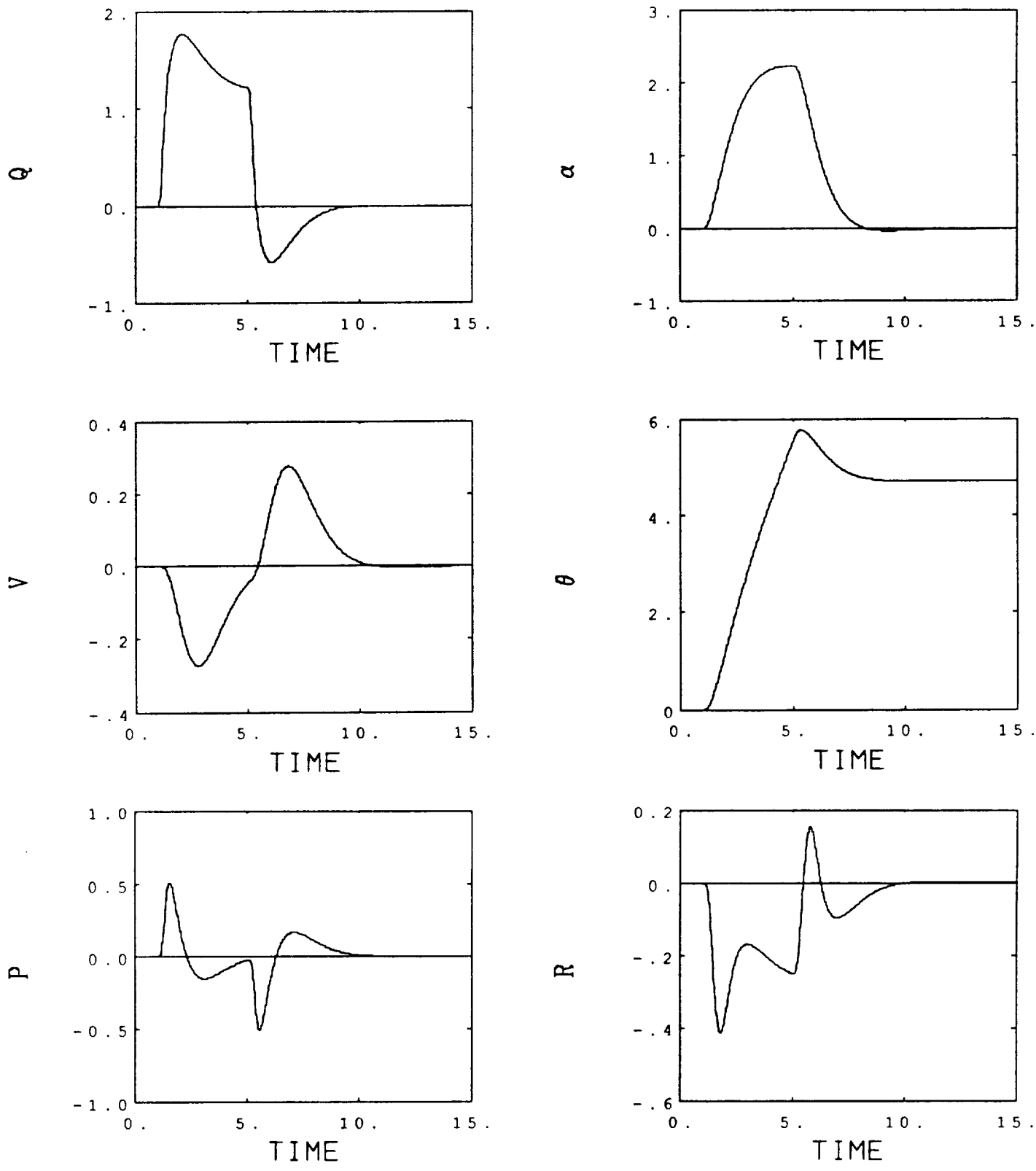

Figure 5-47a Longitudinal Stick Command: Case 9

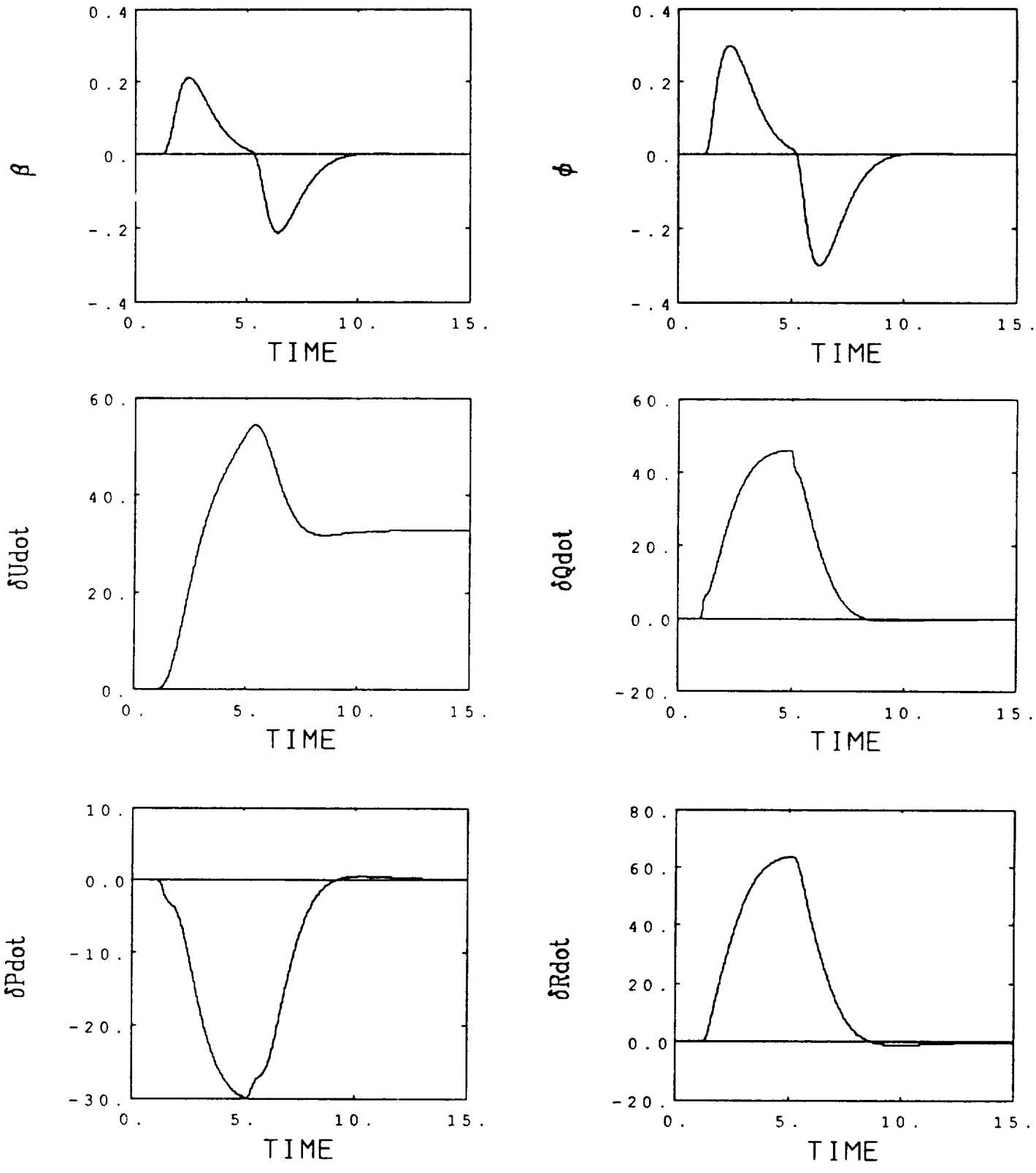

Figure 5-47b Longitudinal Stick Command: Case 9

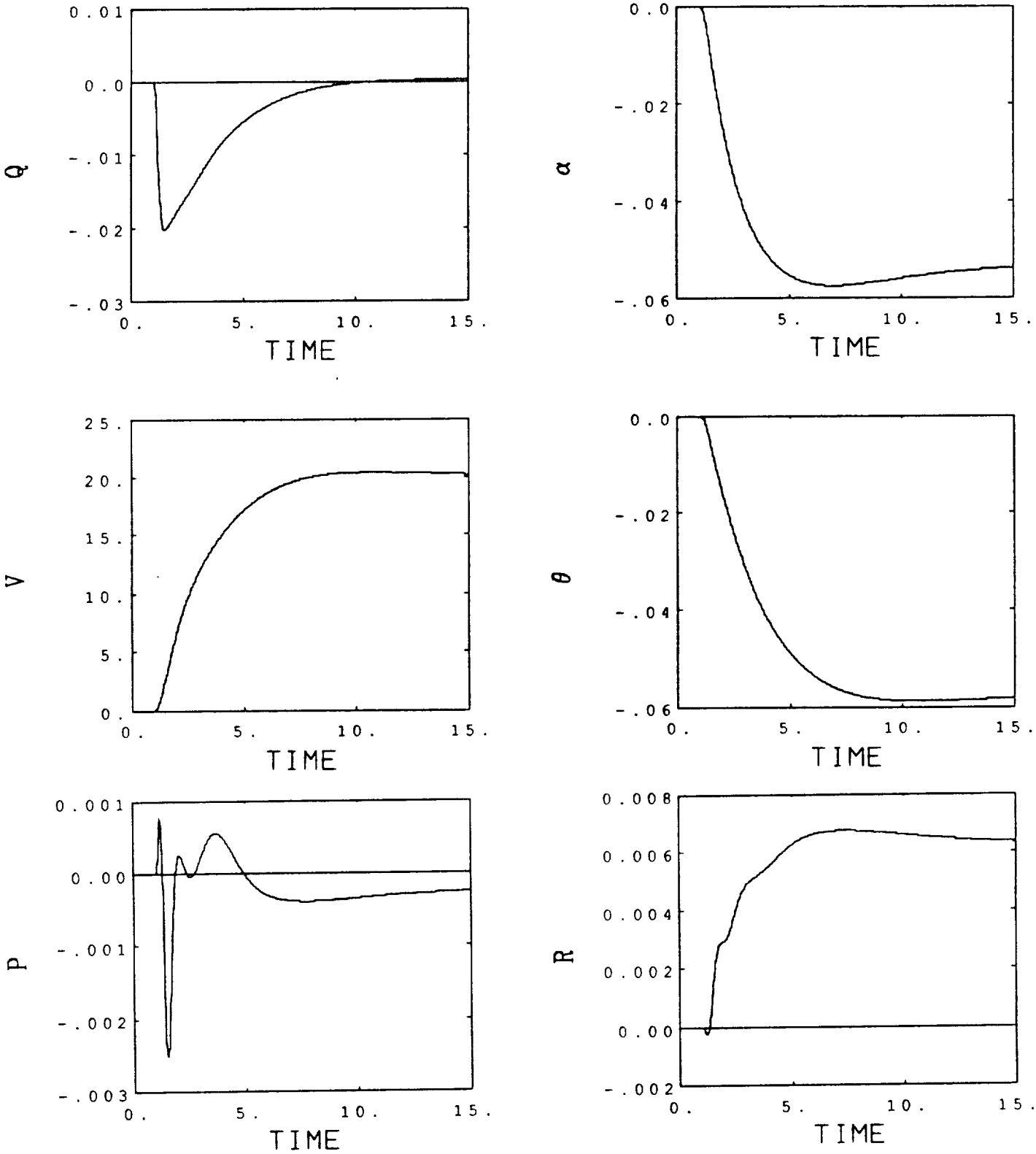

Figure 5-48a Airspeed Command: Case 9

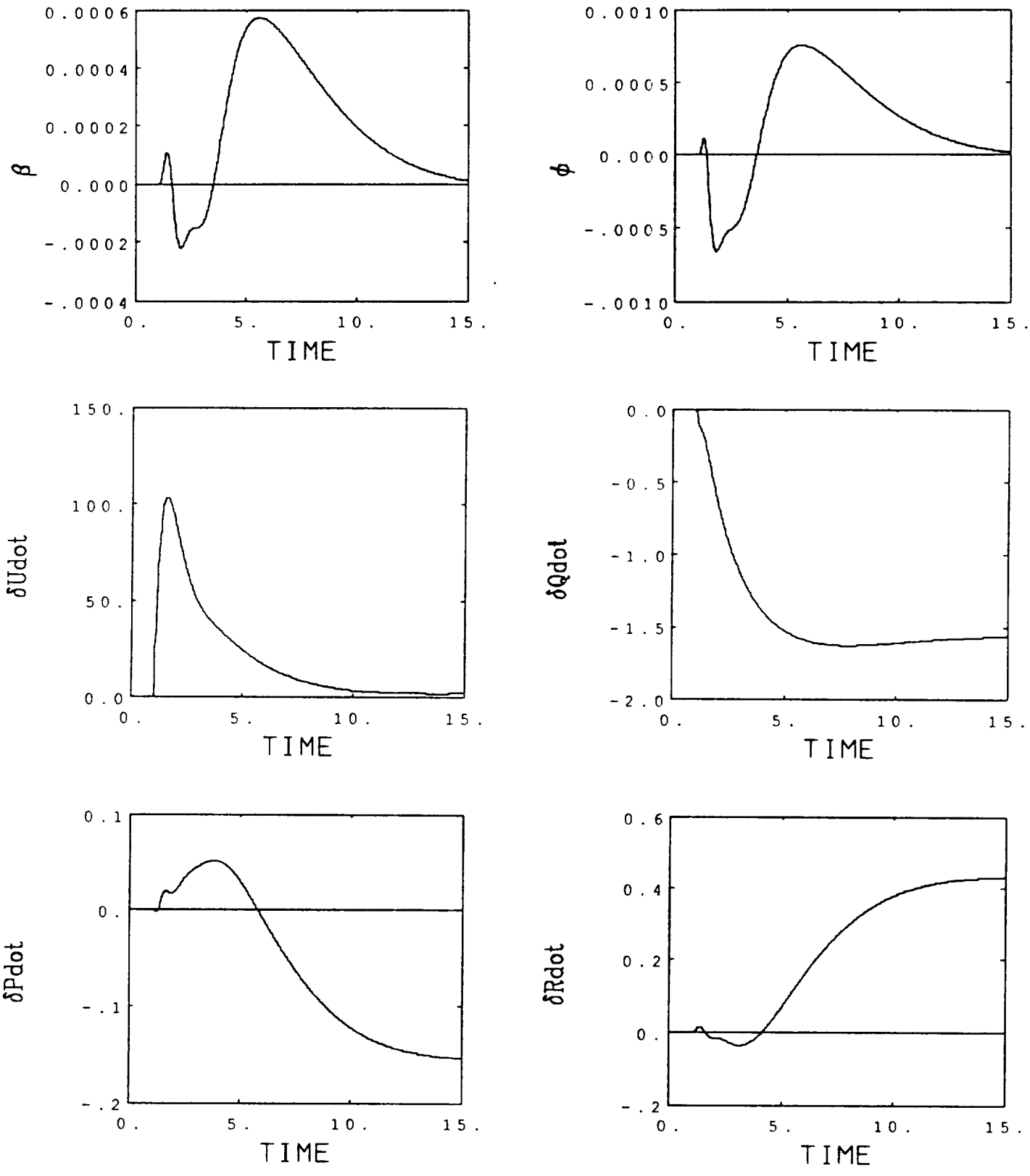

Figure 5-48b Airspeed Command: Case 9

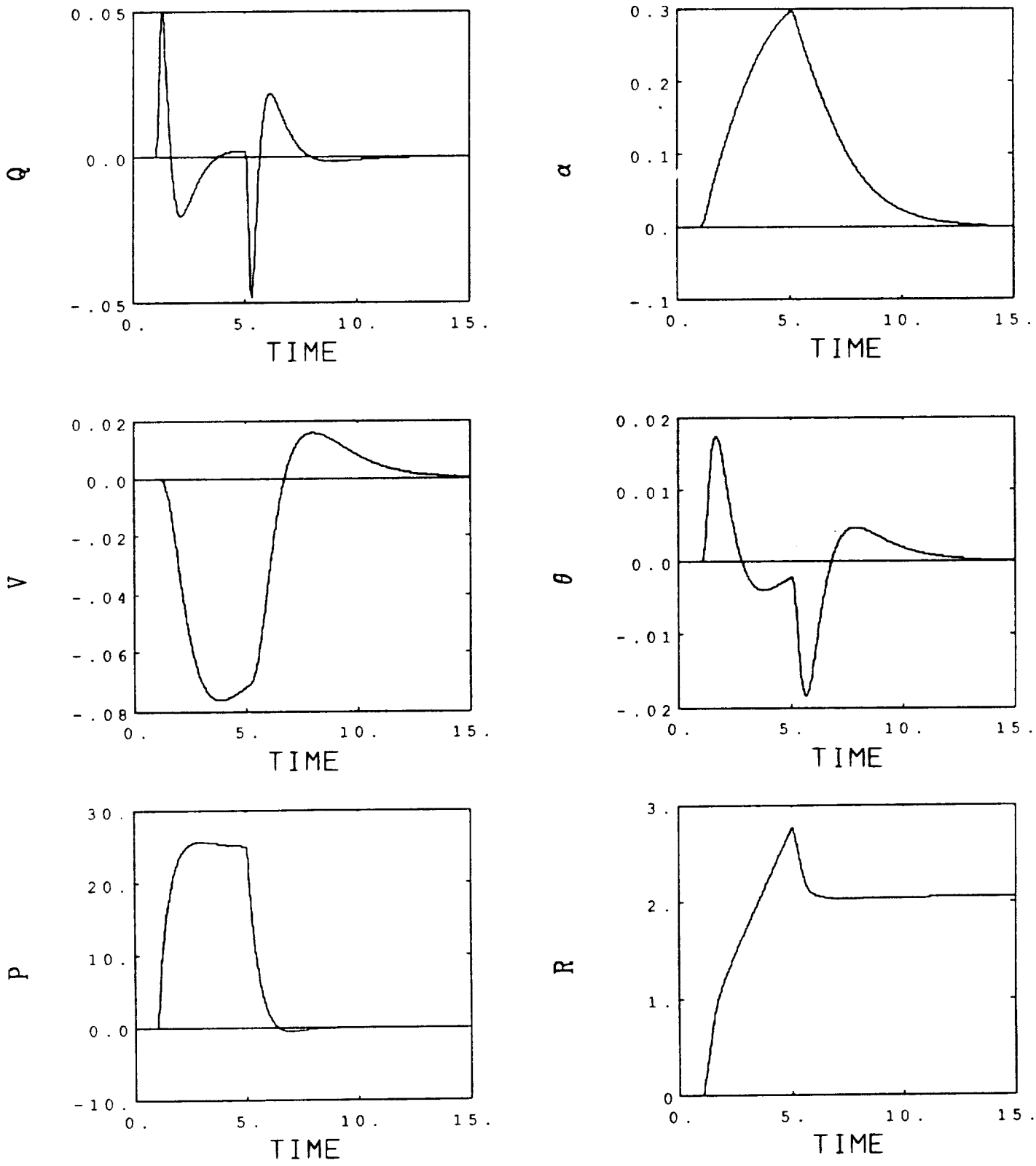

Figure 5-49a Lateral Stick Command: Case 9

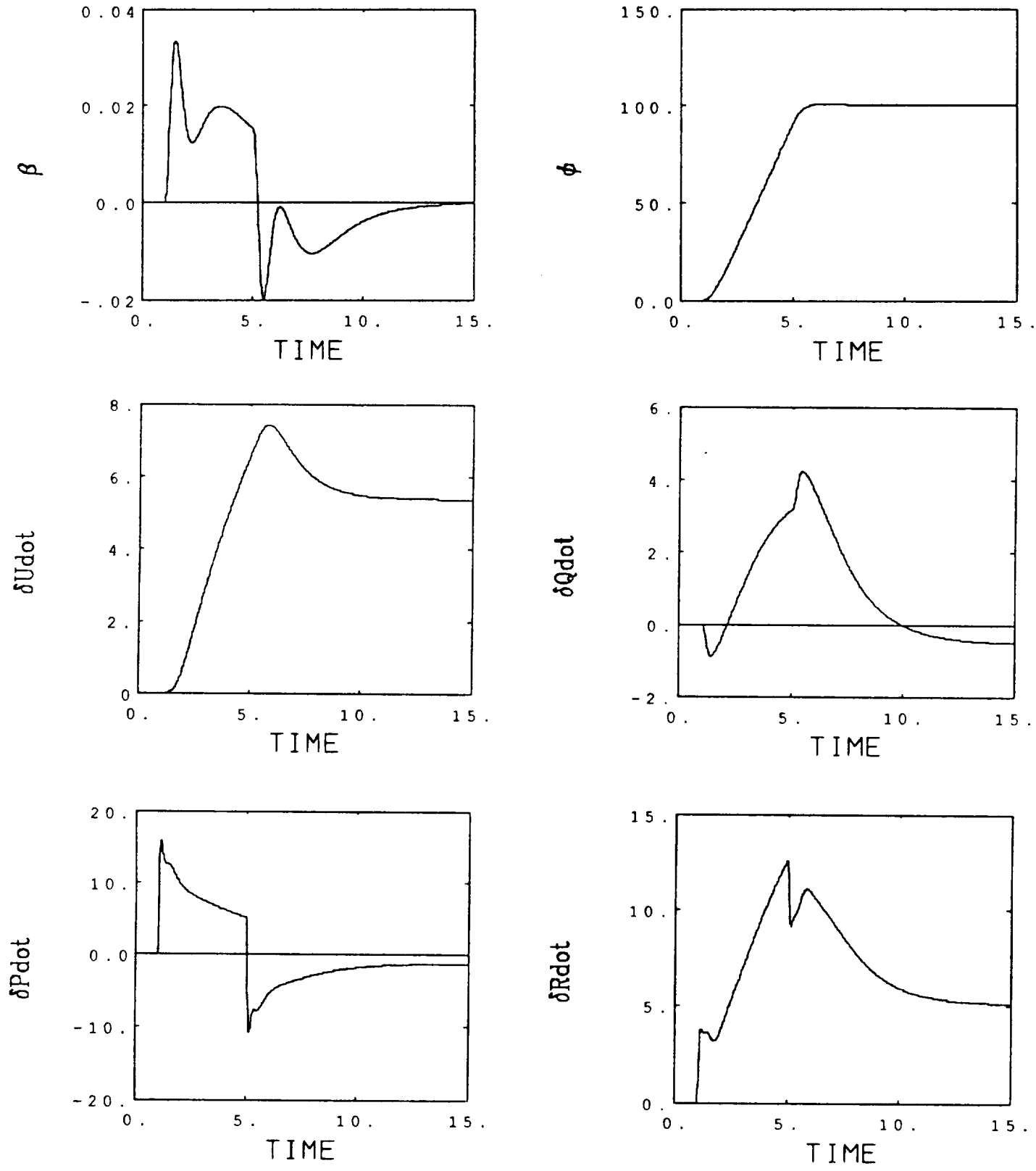

Figure 5-49b Lateral Stick Command: Case 9

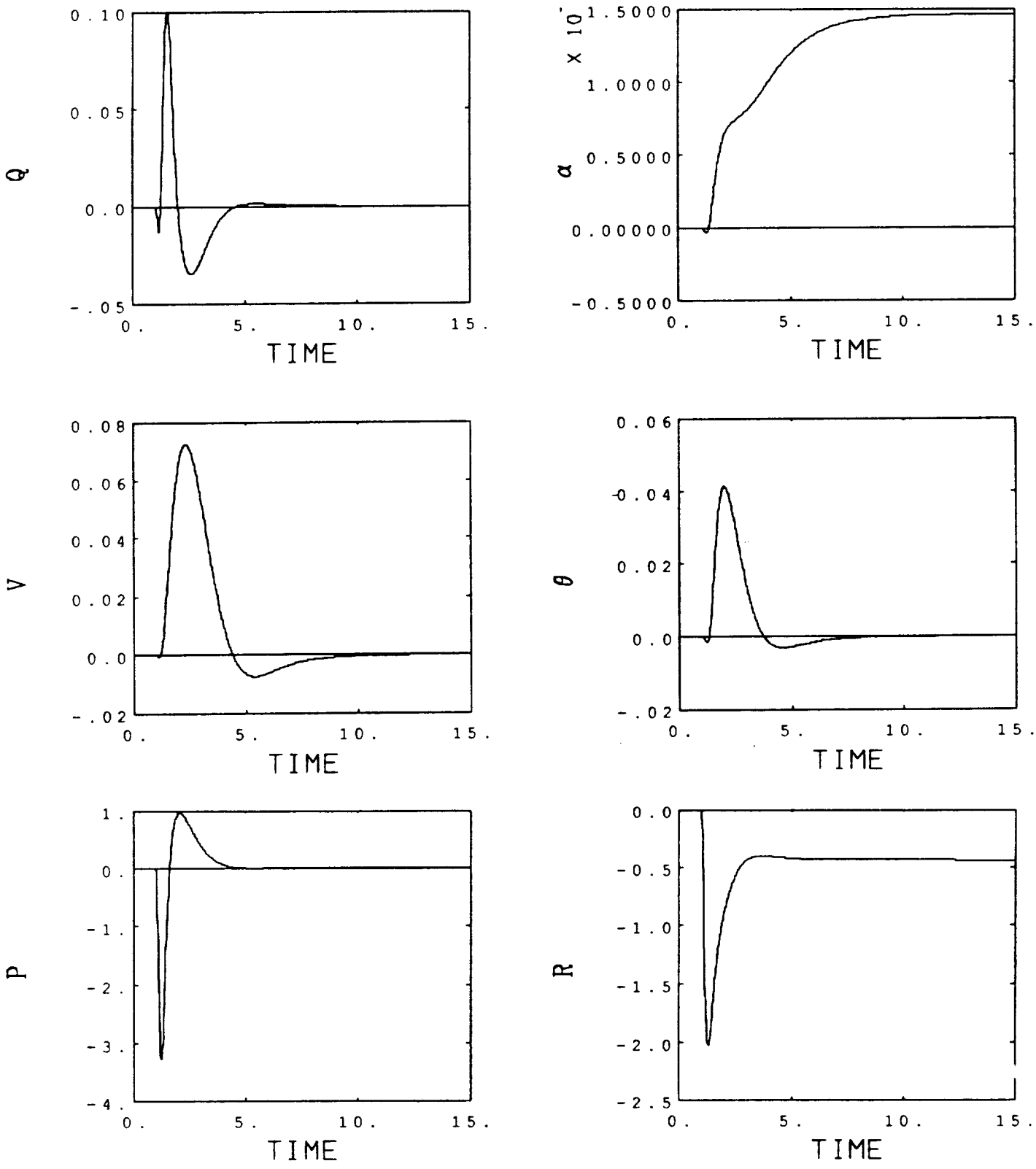

Figure 5-50a Pedal Command: Case 9

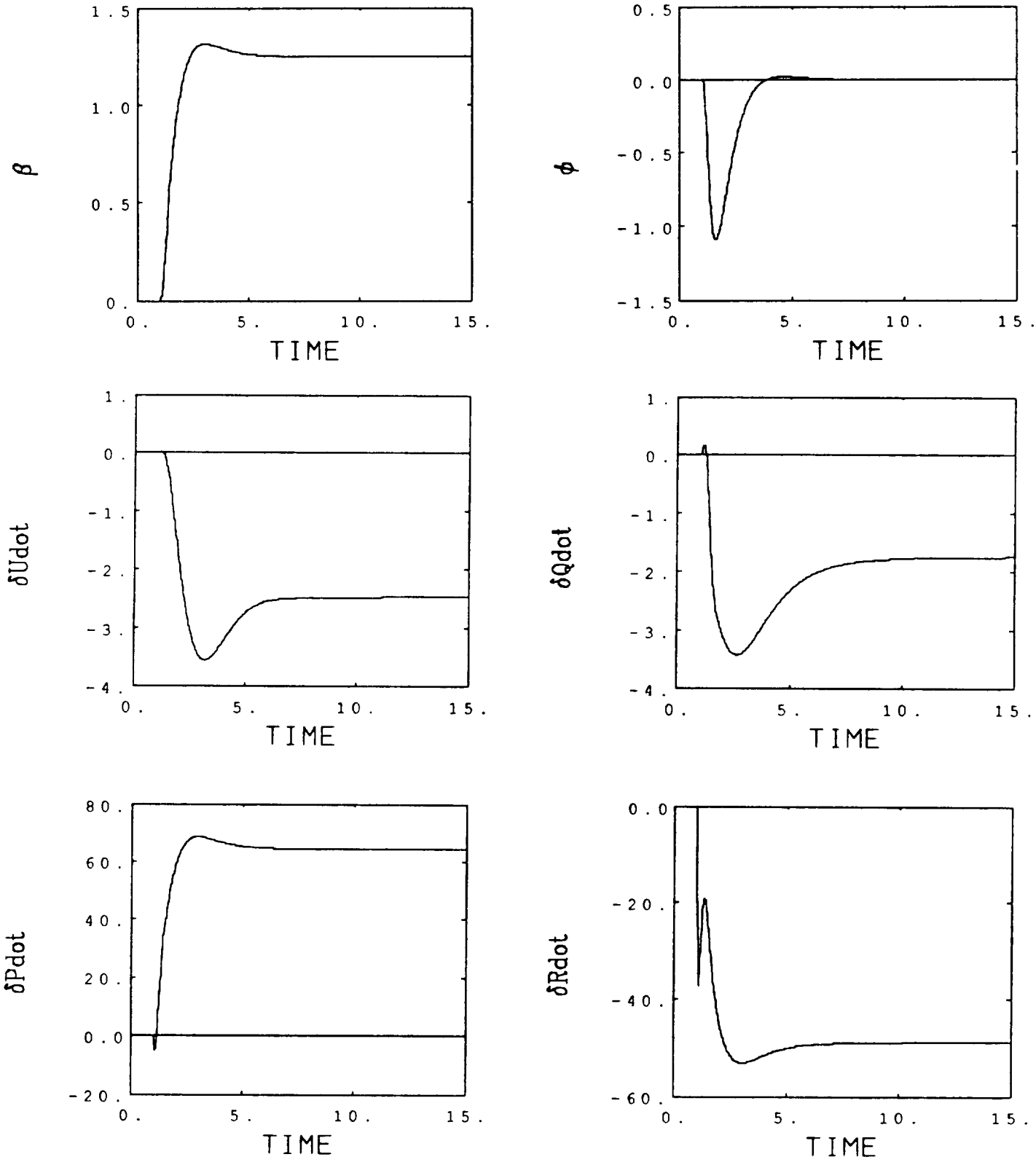

Figure 5-50b Pedal Command: Case 9

VI. CONCLUSIONS

A Linear Quadratic Regulator synthesis technique was used to design an explicit model-following control system for the Oblique Wing Research Aircraft. The forward path model (called the *Maneuver Command Generator*) was designed to incorporate the desired flying qualities and response decoupling. The LQR synthesis was based on the use of generalized controls, and it was structured to provide a proportional/integral error regulator with feedforward compensation. An unexpected consequence of this design approach was the ability to decouple the control synthesis into separate longitudinal and lateral-directional designs. This not only simplified the control law synthesis task, but it also removed all lateral-directional variables from the longitudinal control law and all longitudinal variables from the lateral-directional control law.

Longitudinal and lateral-directional control laws were generated for each of the nine design flight conditions (see Table 1.1), and gain scheduling requirements were addressed. The axial and pitch axis control laws did not require any gain scheduling. The roll and yaw axis control laws required gain scheduling to accommodate regulator gain variations with dynamic pressure and wing skew position.

A fully coupled 6-DOF open loop model of the OWRA along with the longitudinal and lateral-directional control laws was used to assess the closed loop performance of the design. Evaluations were performed for each of the nine design flight conditions. The explicit model-following control system provides excellent stability and performance robustness for the OWRA. Minimum closed loop damping ratios are all greater than $\zeta > .6$, and the model-following performance is excellent. Control activity to achieve the desired model-following accuracy is reasonable. Because of the control system's ability to closely track MCG commands, the aircraft responds to pilot commands as though it were a well behaved conventional (i.e., symmetric winged) aircraft.

REFERENCES

1. Kempel, Robert W., Walter E. McNeill, Glenn B. Gilyard, and Trindel A. Maine, "A Piloted Evaluation of an Oblique-Wing Research Aircraft Motion Simulation with Decoupling Control Laws," NASA Technical Paper 2874, 1988

2. Gregory, Tom, "Oblique Wing Ready for Research Aircraft," *Aerospace America*, pp.78-84, June 1985.

3. Holt, D.J., "Oblique Wing — New Approach to an Old Problem," *Aerospace Engineering*, Vol. 5, pp.26-29, October 1985.

4. Curry, R.E. and A.G. Sim, "Unique Flight Characteristics of the AD-1 Oblique-Wing Research Airplane," *AIAA J. of Aircraft*, Vol. 20, No. 6, pp.564-568, June 1983.

5. Curry, R.E. and A.G. Sim, "In Flight Total Forces, Moments, and Static Aeroelastic Characteristics of an Oblique-Wing Research Airplane," NASA TP-2224, 1984.

6. Sim, A.G. and R.E. Curry, "Flight-Determined Aerodynamic Derivatives of the AD-1 Oblique-Wing Research Airplane," NASA TP-2222, 1984.

7. Sim, A.G. and R.E. Curry, "Flight Characteristics of the AD-1 Oblique-Wing Research Aircraft," NASA TP-2223, 1985.

8. Alag, Gurbux S., Robert W. Kempel, and Joseph W. Pahle, "Decoupling Control Synthesis for an Oblique-Wing Aircraft, NASA Technical Memorandum 86801, June 1986.

9. Erzberger, H., "On the Use of Algebraic Methods in the Analysis and Design of Model-Following Control Systems," NASA TN D-4663, 1968.

10. Chan, Y.T., "Perfect Model Following with a Real Model," *14th Joint Auto. Ctrl. Conf. of the American Auto. Ctrl. Council*, Columbus, Ohio, Paper 10-5, pp.287-293, 1973.

11. Alag, Gurbux S., Robert W. Kempel, Joseph W. Pahle, John J. Bresina, and Febo Bartoli, "Model-Following Control for an Oblique-Wing Aircraft," presented at the *Aircraft Sys. Design and Tech. Meeting*, Dayton, Ohio, October 20-22, 1986.

12. Enns, D.F. D.J. Bugajski, and M. J. Klepl: "Flight Control for the F-8 Oblique-Wing Research Aircraft, *Proc. of the 1987 American Ctrl. Conf.*, p.1112, Minneapolis, 1987.

13. Enns, Dale, Gary Hartmann, and Kathryn Lenz, "Multivariable Control Designs for Advanced Vehicle Configurations" AIAA Paper No. 86-2714 presented at the *Aircraft Sys. Design and Tech. Meeting*, Dayton, Ohio, October 20-22, 1986.

14. Shaw, P. D., Haiges, K.R., Rock, S.R., Vincent, J.H., Emami, A., Anex, R., Fisk, W.S., Berg, D.F., Design Methods for Integrated Control Systems, AFWAL-TR-88-2061, Aero Propulsion Laboratory, AFWAL, Wright-Patterson Air Force Base, Ohio, June 1988.

15. Vincent, J.H., Oblique Wing Research Aircraft Flight Control Description, SCT Report No, 4520-280-2, February, 1989.

16. Vincent, J.H., Direct Incorporation of Flying Qualities Criteria into Multivariable Flight Control Design, Paper No. AIAA-84-1830, *AIAA Guidance, Nav., and Ctrl. Conf.*, Seattle, WA, August 1984.